ALI

UCRL-53363
Distribution Category UC-11

Health and Environmental Effects Document on Geothermal Energy—1982 Update

David W. Layton

Jeffrey I. Daniels

Lynn R. Anspaugh

Kerry D. O'Banion

Manuscript date: November 30, 1983

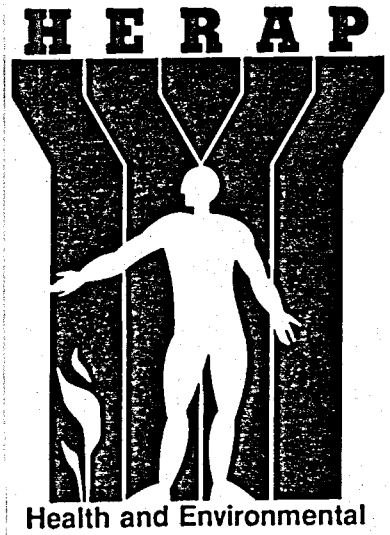

Health and Environmental
Risk Analysis Program

Prepared for:

Health and Environmental Risk Analysis Program
Human Health and Assessment Division
Office of Health and Environmental Research
Office of Energy Research
U.S. Department of Energy

LAWRENCE LIVERMORE NATIONAL LABORATORY
University of California • Livermore, California • 94550

Available from: National Technical Information Service • U.S. Department of Commerce
5285 Port Royal Road • Springfield, VA 22161 • per copy • (Microfiche $4.50)

DISCLAIMER

UCRL-53363

Health and Environmental Effects Document on Geothermal Energy—1982 Update

David W. Layton

Jeffrey I. Daniels

Lynn R. Anspaugh

Kerry D. O'Banion

November 30, 1983

CONTENTS

EXECUTIVE SUMMARY

The 1982 Update of the Health and Environmental Effects Document (HEED) on geothermal energy focuses on the effects of a reference industry that produces 21,000 MW_e for 30 y (i.e., 20 x 10^{18} J or 20 Quads of electrical energy). That level of development is equivalent to the estimated resource potential of identified, hot-water resources in the U.S. Hot-water resources can be processed by either flashed-steam or binary-fluid geothermal power plants to produce electricity. In this HEED, however, we are primarily concerned with operation of the flashed-steam facilities because they pose greater health and environmental risks due to atmospheric emissions of noncondensing gases.

The most important noncondensing gases from a health effects standpoint are hydrogen sulfide, particulate sulfate from the atmospheric oxidation of hydrogen sulfide, benzene, mercury, and radon. We calculated the population exposures resulting from atmospheric dispersion near geothermal facilities (<80 km) and long-range transport. Dose-response functions were used to quantify the health risks of the predicted exposures. We also examined the potential health risks of arsenic contained in cooling tower emissions and solid wastes. The occupational health risks were estimated for 21,000 MW_e of development to conclude the analysis of human health effects. In our ecological analysis, we examined the potential effects of hydrogen sulfide and carbon dioxide emissions on crops and forest plants, the occurrence of accidental spills of geothermal fluids that would damage soils and vegetation adjacent to power plants, and the phytotoxic effects of boron emitted from cooling towers. Finally, we addressed the nonpollutant effects of land subsidence and induced seismicity.

PUBLIC HEALTH EFFECTS

We summarize here the health effects associated with exposure to hydrogen sulfide, sulfur oxides, benzene, mercury, and radon in air and arsenic in food.

- Atmospheric releases of hydrogen sulfide constitute the most significant public health issue of geothermal energy production. It is a toxic gas, causing death at concentrations above 1000 parts per million by volume (ppmv) and eye damage at concentrations as low as 50 ppmv. However, the primary concern is its annoying odor, which can be detected by 20% of the population at a

concentration of just 0.002 ppmv. According to our analyses, at least 29 of the 51 geothermal resource areas are likely to have one or more power plants that emit enough hydrogen sulfide (without abatement) to cause odor-related problems.

- Hydrogen sulfide in the atmosphere oxidizes to particulate sulfate. According to our analyses, the mean population risk of exposure to sulfate is 66 premature deaths per 10^{18} J of electrical energy production, with an uncertainty range of 0 to about 360. These risks would be reduced in proportion to the fraction of energy that is produced by binary-fluid power plants, which do not release noncondensing gases. The primary source of uncertainty is the "surrogate" damage function for sulfate in which concentrations of that pollutant are used to estimate premature deaths from sulfate aerosols plus other correlated air contaminants. A second source of uncertainty is our estimation of far-field population exposures using an emission rate of sulfur dioxide rather than hydrogen sulfide because of the inability of the transport model to simulate the chemical kinetics of two species.

- Benzene has been identified as a leukemogen, and it is also found in some geothermal fluids, particularly those that are extracted from geothermal reservoirs composed of sedimentary rocks such as those in California's Imperial Valley. The mean population risk of incurring leukemia from exposure to benzene released from geothermal facilities in the Imperial Valley was calculated to be 0.15 leukemias per 10^{18} J. The approximate uncertainty bounds are 0 and 0.51.

- Mercury is frequently found in geothermal waters and gases. Prolonged exposure to elemental mercury released from geothermal facilities may induce neurologic disorders. To assess this risk, we derived an estimate of the lifetime probability of muscle tremors based on four epidemiological studies. The mean number of cases of tremors was calculated to be 14 per 10^{18} J of electrical energy. The uncertainty range is from 0 to 39. The principal source of uncertainty is the nature of the dose-response function. We used a linear, no-threshold function, but because of the body's clearance mechanism for mercury, a threshold may indeed exist.

- Exposure to radon and its short-lived daughters poses a risk of lung cancer. We calculated the probability of lung cancer from 30 y of exposure to ^{222}Rn (in equilibrium with its daughters) to be 8×10^{-6} m^3/pCi, using a basic risk factor of 5×10^{-4} cases of lung cancer per working-level month. The mean population risk was predicted to be 0.68 lung cancers per 10^{18} J of electrical energy with an approximate uncertainty range of 0 to 1.8.

- The ingestion of leafy vegetables that have accumulated arsenic as a result of emissions from flashed-steam facilities in the Imperial Valley could cause skin cancers. Our best estimate of this risk is 0.15 fatal skin cancers for 6.1×10^{18} J of development in the Valley (a third of the capacity of the reference industry). Upper and lower bounds on this estimate are 1.5 and 0. Arsenic will also accumulate on the land surface as part of solid wastes and cooling tower emissions. The health risk of this ingestion is calculated as the result of the transfer of arsenic to the general population over geologic time ($\sim$100,000 y), and it was predicted to be 41 fatal skin cancers per 10^{18} J, with an uncertainty range of 0 to 205/10^{18} J.

OCCUPATIONAL HEALTH

We used occupational health statistics from a number of different industries to estimate the occupational health effects of a mature geothermal industry. Based on data from surrogate industries, our best estimate of accidental deaths is 8 per 10^{18} J, with lower and upper bounds of 1.5 and 24, respectively. We estimate that 300 cases of occupational diseases will occur per 10^{18} J, with a range from 43 to 1600. Our best estimate for occupational injuries is 3,400 per 10^{18} J, with a range from 700 to 10,000.

ECOSYSTEM EFFECTS

We examined the potential effects of emissions of hydrogen sulfide and carbon dioxide on forest plants and crops and concluded that no negative effects on vegetation would occur. In fact, growth enhancement of plants is more likely than stress. We also analyzed the potential consequences of accidental releases of geothermal fluids onto vegetation and soils adjacent to power plants. Our calculations show that less than 5 ha of land will be affected by inadvertent releases--assuming that berms and sumps are not

used to contain the spilled fluids. Boron emitted from cooling towers using condensed steam as cooling water could injure crops grown adjacent to geothermal power plants in the Imperial Valley. To assess the potential magnitude of such emissions, we calculated the boron doses to crops via foliar deposition and root uptake. We found that none of the primary crops in the Valley will suffer adverse effects from boron emitted from state-of-the-art cooling towers operating with 100-MW_e flashed-steam power plants. Salt emitted from cooling towers using brackish surface waters will add a negligible amount of salt ($\sim$0.15% of the current salt loading from irrigation water) to crop lands that are now under salinity stress.

NONPOLLUTANT EFFECTS

The two nonpollutant effects we considered were land subsidence and induced seismicity. Effects from both will vary from resource area to resource area. We prepared a bounding analysis of the levels of ultimate land subsidence averaged over all geothermal reservoirs. Our upper bound estimate is 1.8 m per 100-m decline in hydrostatic head, while our lower bound estimate is 0.2 m per 100-m decline. The effects of land subsidence associated with the reference industry are not expected to be significant because most of the surface land uses are insensitive to changes in elevation. We could not directly quantify the risks of induced earthquakes, but we note that the induced events that have occurred to date have been nondestructive. Nevertheless, we believe that additional research is needed on the mechanisms that could cause earthquakes in or near geothermal reservoirs.

HEALTH AND ENVIRONMENTAL EFFECTS DOCUMENT ON GEOTHERMAL ENERGY--1982 UPDATE

ABSTRACT

We assess several of the important health and environmental risks associated with a reference geothermal industry that produces 21,000 MW_e for 30 y (equivalent to 20 x 10^{18} J). The analyses of health effects focus on the risks associated with exposure to hydrogen sulfide, particulate sulfate, benzene, mercury, and radon in air and arsenic in food. Results indicate that emissions of hydrogen sulfide are likely to cause odor-related problems in 29 of 51 geothermal resources areas, assuming that no pollution controls are employed. Our best estimates and ranges of uncertainty for the health risks of chronic population exposures to atmospheric pollutants are as follows (risks expressed per 10^{18} J of electricity): particulate sulfate, 44 premature deaths (uncertainty range of 0 to 360); benzene, 0.15 leukemias (range of 0 to 0.51); elemental mercury, 14 muscle tremors (range of 0 to 39); and radon, 0.68 lung cancers (range of 0 to 1.8). The ultimate risk of fatal skin cancers as the result of the transfer of waste arsenic to the general population over geologic time ($\sim$ 100,000 y) was calculated as 41 per 10^{18} J. We based our estimates of occupational health effects on rates of accidental deaths together with data on occupational diseases and injuries in surrogate industries. According to our best estimates, there would be 8 accidental deaths per 10^{18} J of electricity, 300 cases of occupational diseases per 10^{18} J, and 3400 occupational injuries per 10^{18} J.

The analysis of the effects of noncondensing gases on vegetation showed that ambient concentrations of hydrogen sulfide and carbon dioxide are more likely to enhance rather than inhibit the growth of plants. We also studied the possible consequences of accidental releases of geothermal fluids and concluded that probably less than 5 ha of land would be affected by such releases during the production of 20 x 10^{18} J of electricity. Boron emitted from cooling towers in the Imperial Valley was identified as a potential source of crop damage. Our analyses, however, showed that such damage is unlikely.

Finally, we examined the nonpollutant effects of land subsidence and induced seismicity. Land subsidence is possible around some facilities, but surface-related damage is not expected to be great. Induced seismic events that have occurred to date at geothermal resource areas have been nondestructive. It is not possible to predict accurately the risk of potentially destructive events, and more research is needed in this area.

INTRODUCTION

Geothermal resources usually exist as either convective or conductive heat flow systems within the earth's crust. In both systems most of the heat is stored in the rock matrix. Heat transfer within convective systems is primarily through the circulation of water or steam in porous or fractured geologic media. The heat source for these so-called hydrothermal-convection systems is often a shallow, magmatic intrusion.[1] Hydrothermal systems are subcategorized as vapor-dominated (steam) or hot-water systems. Vapor-dominated systems such as The Geysers in northern California are the easiest to utilize for the production of electricity as the tapped steam can be sent directly to a low-pressure turbine. The installed electric generating capacity there is now over 1200 MW_e, and additional units under construction will produce another 600 MW_e.[2] Hot-water systems with temperatures greater than 150°C can be used to generate electricity with currently available technology; however, the conversion process is more complex because the geothermal liquid must be flashed to produce steam.[3] At the present time less than 20 MW_e of electricity are generated from hot water resources in the U.S., but the growth potential of those resources remains strong. Lower temperature systems (~90 to 150°C) are usable for other purposes such as space heating and other nonelectric or direct uses.

Two examples of conductive geothermal systems are geopressured and hot dry rock resources. Geopresssured resources exist as deep sedimentary formations containing hot, saline liquid at pressures considerably higher than normal hydrostatic. The value of these resources is enhanced by the presence of natural gas dissolved in the fluids. The extraction of geopressured energy is not a demonstrated technology at this time. Most of the development activities associated with this resource have focused on characterization of the resource in the Gulf Coast region. Hot dry rock resources refer to low permeability, high-temperature granitic, metamorphic, or cemented sedimentary formations that are usually in contact with a young magmatic intrusion. Heat transfer from the intrusion is strictly by conduction. To exploit hot dry rock resources, fractures are artificially created in the formation by hydraulic fracturing, and then water is circulated through the fracture zone, heated, and returned to the surface where the heat is extracted for electricity production or direct uses.[4] This method of resource extraction is under active research and development, but it is not considered a near-term technology.

OVERVIEW OF POTENTIAL HEALTH AND ENVIRONMENTAL EFFECTS

There are several health and environmental issues connected with the extraction of hot water or steam from geothermal reservoirs and the subsequent processing to generate electricity. Based on measurements and experience at existing geothermal facilities and wells, the most serious concerns for both types of resources relate to emissions of gases that are not condensed at operating temperatures and pressures. The chemical composition of these gases varies widely from reservoir to reservoir; however, the major constituent is typically carbon dioxide, and significant amounts of methane and hydrogen sulfide are nearly always present along with trace amounts of benzene, radon, and mercury. Exposure to atmospheric concentrations of hydrogen sulfide, benzene, radon, and mercury pose potential hazards to public and occupational health. In addition, exposure to hydrogen sulfide and toxic chemicals used in hydrogen sulfide abatement systems has been identified as an occupational health hazard.[5] Environmentally, noise emissions have been a problem at The Geysers due to venting of high-pressure steam at wellheads and generating units.[6] Issues more applicable to the development of hot-water resources include the disposal of large volumes of spent geothermal liquids, accidental spills of fluids, land subsidence caused by the withdrawal of fluids, and enhanced seismicity from fluid injection or reservoir cooling. In addition, phytotoxic effects to vegetation in the vicinity of power plants can be caused by cooling tower emissions of water droplets (i.e., drift) containing toxic substances derived from steam condensate used as cooling water.[7]

METHODOLOGY

The basic methodology we use to assess the risks of geothermal power production is outlined in Fig. 1. To begin with, we define the basic attributes of the reference energy industry including the level of energy production to be assessed; the relevant characteristics of energy conversion technologies; and importantly, the potential releases of pollutants from geothermal facilities. Next, the transport and fate of the pollutants released into the environment are simulated by media-specific (i.e., air and water) models. Estimates of the environmental concentrations of contaminants are then used in dose-response models to determine effects on vegetation, animals, and man. The occupational health effects associated with geothermal energy are evaluated using occupational health data along with exposure estimates and effects models. Finally, special models or analytical techniques are used to simulate nonpollutant effects

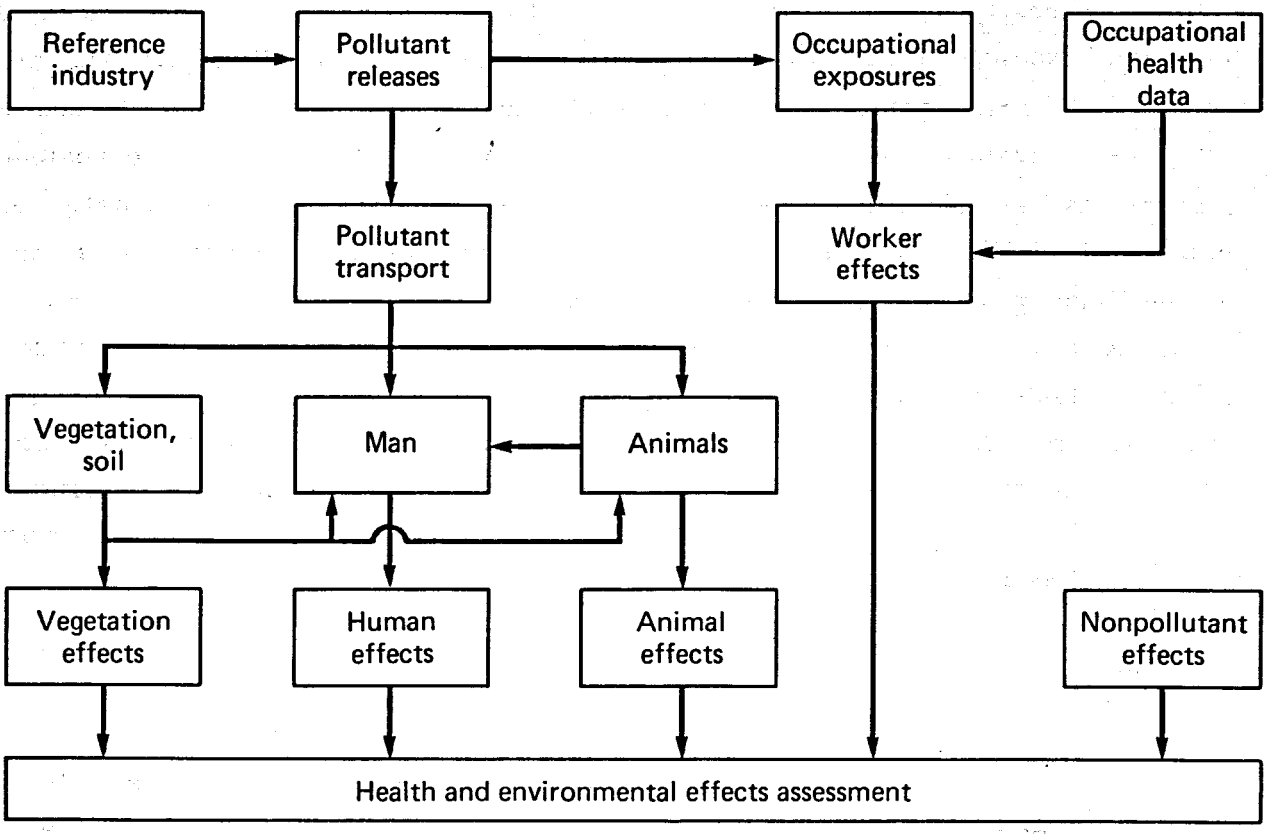

Figure 1. Conceptual diagram of the methodological approach of performing the health and environmental effects assessment of geothermal energy.

associated with noise emissions, subsidence, and seismicity. Another component of the assessment methodology is the quantification of the uncertainty or the accuracy of our estimates of health and environmental effects.

THE REFERENCE GEOTHERMAL POWER INDUSTRY

Geothermal power production is projected to grow steadily in the years ahead. Most of the new generating facilities will rely on the proven, vapor-dominated resources of The Geysers, but substantial development is also expected to occur at the more prevalent hot-water resource areas. The energy potential of the discovered hot-water resources is estimated to be 21,000 MW_e for 30 y (equivalent to 20 x 10^{18} J or 20 Quads of electrical energy), compared with an estimated undiscovered resource base of over 72,000 MW_e for 30 y.[8] For the purposes of our analyses, the reference industry consists of power plants with an installed capacity equivalent to the 30-y power potential of the discovered resources (i.e., 21,000 MW_e). There are currently 51 identified resource areas in 11 western states, with estimated energy potentials ranging from 23 to 3400 MW_e for 30 y. The locations of all the resource areas, except those in Hawaii and Alaska, are shown in Fig. 2. Over 99% of the resources are found in the eight states shown in Fig. 3. Emission rates of pollutants from the power plants that comprise the reference industry will vary according to the chemical and physical characteristics of the 51 resource areas as well as the types of power plants installed. The mix of binary and flashed-steam power plants making up the reference industry will directly affect the magnitude of public health impacts. As the proportion of flashed-steam facilities increases, the quantity of noncondensing gases released to the atmosphere also increases and so do health risks (e.g., lifetime risk of incurring cancer due to the inhalation of radon). At the present time it is not possible to estimate accurately the technology mix of a mature industry. It is clear that binary facilities offer increased conversion efficiencies with low to moderate temperature resources, which make up the bulk of the known geothermal resource areas. However, because binary facilities require external sources of cooling water, the siting of such plants could be constrained by the lack of sufficient water supplies.[10] From a public health standpoint, the worst case would occur if the reference industry was comprised solely of flashed-steam facilities. To bound our estimates of health risk for the geothermal power industry, we will assume that all of the plants installed are flashed steam. The ensuing discussion, therefore, begins with a brief review of the geothermal energy technologies addressed in the risk assessment followed by analyses of potential emissions of noncondensing gases.

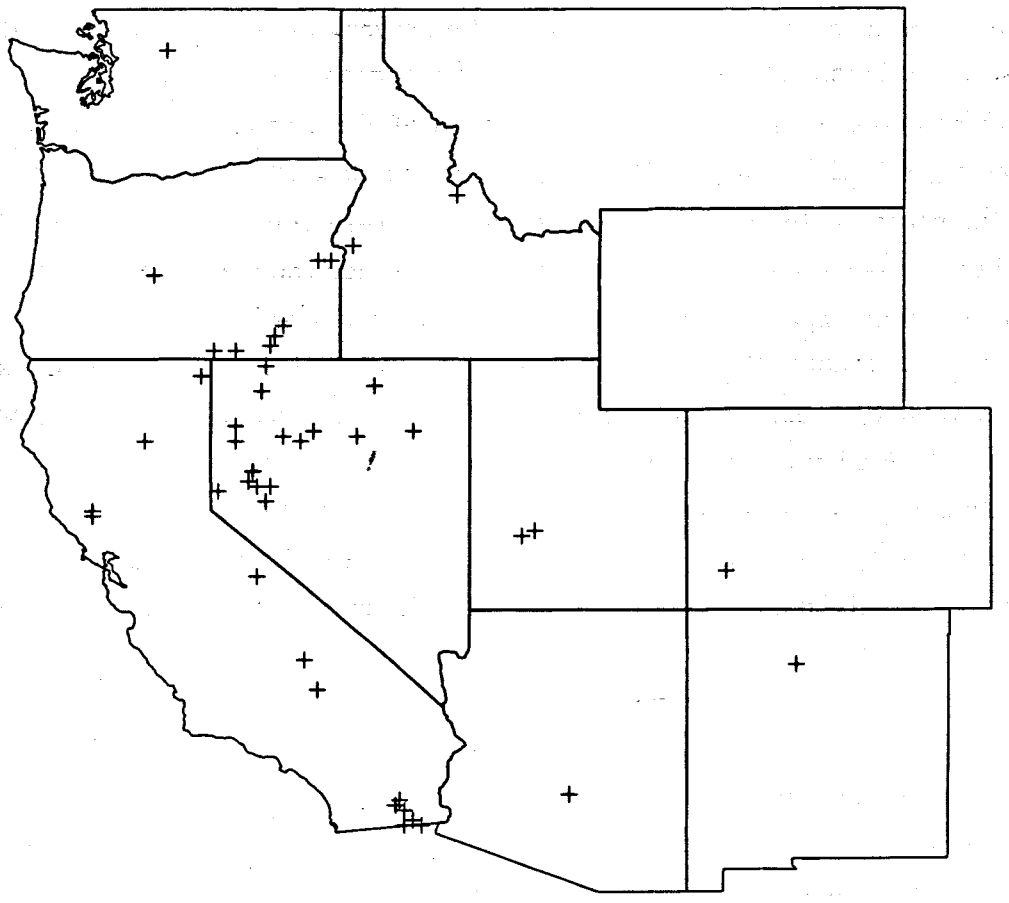

Figure 2. Locations of geothermal resource areas in nine western states.

GEOTHERMAL POWER TECHNOLOGIES

The two basic types of geothermal power cycles that are being developed for commercial applications are flashed-steam and binary-fluid. A simple flashed-steam system is depicted in Fig. 4. Geothermal fluid is withdrawn from a well and afterwards steam is separated (i.e., flashed) from the extracted fluid by pressure reduction. The residual geothermal liquids are disposed of (usually by subsurface injection) while the separated steam is sent to a turbine. Steam exhausted from the turbine is condensed, creating enough water to meet the cooling water needs of the facility. Noncondensing gases are normally ejected from the condenser and if necessary piped to an abatement system. At The Geysers, steam is extracted from a geothermal reservoir by wells and

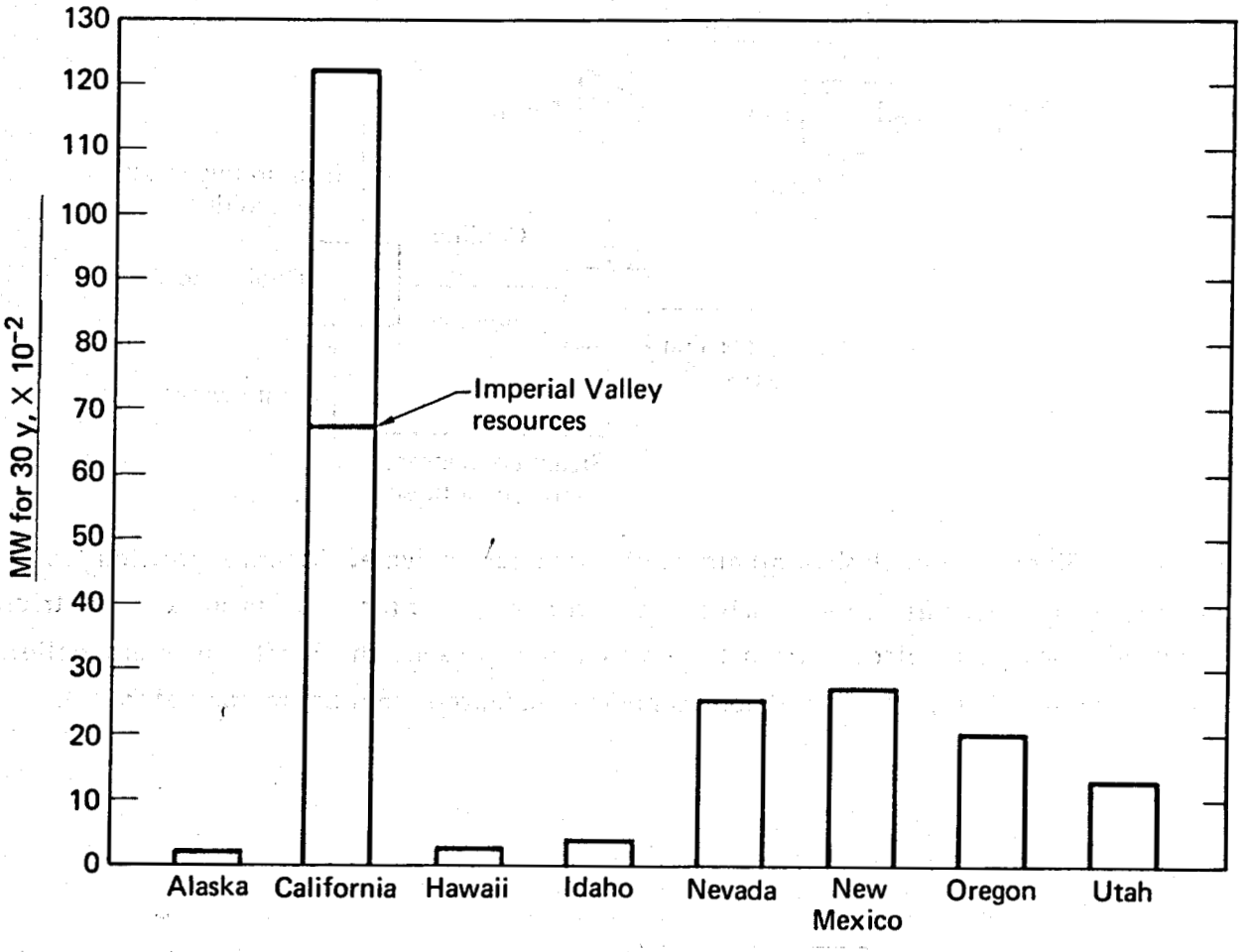

Figure 3. Electrical energy potentials for identified hot-water geothermal resources in eight western states.[8,9] Nearly a third of the total energy potential of the discovered resource base is associated with the resource of the Imperial Valley.

then sent directly to a turbine. Thus, power plants at The Geysers are essentially the same as flashed-steam facilities except for equipment needed to separate steam from geothermal fluids and the extra injection wells required to dispose of the waste fluids. The binary-fluid cycle (Fig. 5) does not use steam to drive a turbine; instead, down-hole pumps withdraw geothermal fluid from production wells and then the pressurized fluids are sent through a heat exchanger that heats and vaporizes a secondary working fluid (e.g., isobutane). The working fluid is subsequently expanded through a turbine, condensed, and reheated for another cycle. Spent geothermal fluids are disposed of by subsurface injection. One advantage of this type of power system is the absence of gaseous emissions as long as the geothermal fluids are kept at pressures high enough to

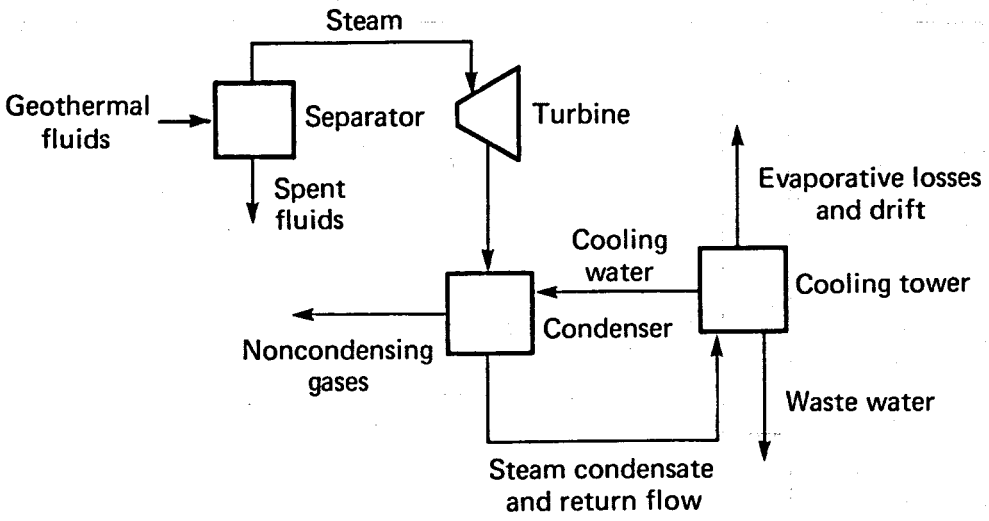

Figure 4. Single-stage, flashed-steam geothermal power cycle. Steam separated from the extracted geothermal fluids drives a turbine-generator to produce electricity. Noncondensing gases ejected from the condenser represent the most important pollutant released from this type of conversion technology (adapted from Layton and Morris[7]).

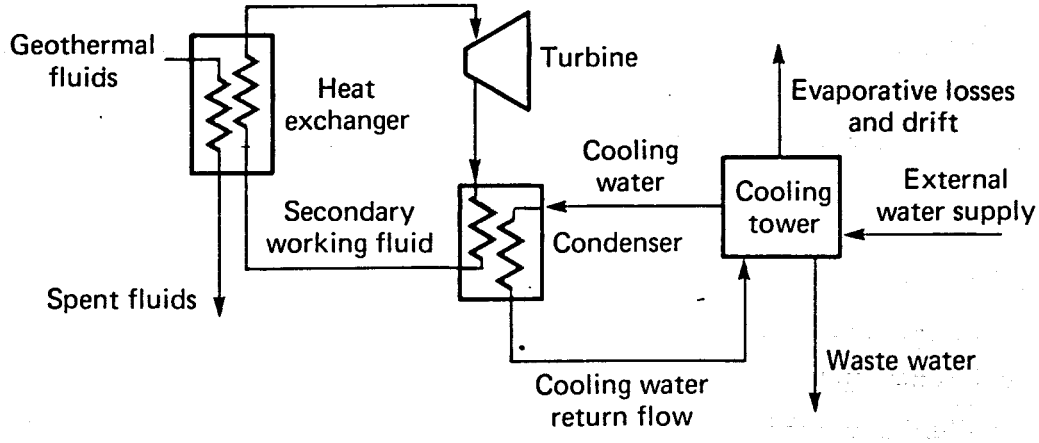

Figure 5. Binary-fluid power cycle. Geothermal fluids are sent through a heat exchanger that vaporizes a secondary working fluid, which in turn expands through a turbine-generator to produce electricity. Atmospheric emissions are not expected from this conversion technology as long as the extracted fluids are kept at pressures that prevent the dissolution of gases (adapted from Layton and Morris[7]).

prevent the volatilization of gases.[11] Moreover, binary-systems are capable of higher conversion efficiencies than flashed-steam facilities and consequently, smaller amounts of geothermal fluids are required per net unit of electricity generated. On the other hand, binary-fluid facilities must rely on external sources of cooling water because of the lack of steam condensate.

Aside from the design differences between the two conversion cycles, the primary determinant of resource requirements at a constant heat-rejection temperature is the temperature of the geothermal fluid. More precisely, as the temperature of a geothermal resource increases, the efficiency of converting the associated heat energy to electrical energy also increases, thereby reducing the demand for fluid. This relationship is important because the gaseous emissions from flashed-steam power plants are primarily a function of the fluid extraction rate and the concentration of noncondensing gases in the geothermal fluid. Therefore, the lowest gaseous emission rates would be from power plants utilizing high temperature resources containing low concentrations of dissolved gases. To estimate the fluid requirements of two-stage, flashed-steam power plants,* we use the following equation, which represents a power function fit of a curve presented in a simulation study by Pope et al.[12]

$$E = 2.618 \times 10^{8} T^{-2.82} , \quad (1)$$

where

E = fluid extraction rate, kg/net kW_e • h and
T = down-hole resource temperature, °C.

Appendix A contains the temperature data on the 51 geothermal resource areas. Using the temperature data as input to eq. (1), we calculated the extraction rate for each resource. The weighted-average extraction rate was 68.4 kg/kW_e • h, with individual values ranging from 35 to 184 kg/kW_e • h. Geothermal fluids from a well field are not usually transported more than a mile in order to minimize losses in temperature and pressure. Consequently, power plants will always be situated within the immediate vicinity of geothermal resource areas. This restriction is significant because it means

* In a two-stage facility geothermal fluids discharged from the first steam separator are flashed a second time and the resulting steam is expanded through a low-pressure turbine.

that the environmental and health-related risks of an expanding geothermal power industry will depend heavily on the site-specific characteristics of the various resource areas (e.g., population density, fluid characteristics, etc.).

Subsurface injection of residual geothermal fluids is the final step in the relatively short geothermal fuel cycle. Injection is used to maintain reservoir pressures (which also provide some protection against subsurface compaction of sediments), to recover heat contained in reservoir rocks, and to dispose of waste fluids. The injection of waste fluids is actually a crucial pollution-control technology--for without it, geothermal power plants in the U.S. using hot-water resources would not be able to operate because of stringent water-quality regulations prohibiting the surface discharge of fluids containing toxic substances or having elevated temperatures.

EMISSIONS OF NONCONDENSING GASES

Geothermal fluids at depth are complex mixtures of dissolved gases and solids. As these fluids are withdrawn from a reservoir and processed to produce electricity in flashed-steam facilities, reductions in temperature and pressure cause the volatilization and subsequent release of various gases that do not condense at atmospheric temperatures and pressures. The major gases in the noncondensing gas phase normally consist of carbon dioxide (at around 90 mole %), methane, hydrogen sulfide, ammonia, nitrogen, and hydrogen. Concentrations of these major gases as well as minor gases like benzene, mercury, and radon will vary among wells in the same geothermal resource area and they will also vary in time.[13] In the following analyses we review data on concentrations and emissions of hydrogen sulfide, benzene, mercury, and radon--the most important gases from a health effects standpoint.

Hydrogen Sulfide

Hydrogen sulfide is found in nearly all high-temperature geothermal fluids (i.e., >150°C). It is probably formed by one or more of the following mechanisms: reaction of sulfur that is present in reservoir rocks with hot water, magmatic exhalation, or thermal metamorphism of marine sedimentary rocks.[13,14] Concentrations of this gas sampled from geothermal fluids in the U.S. range from 0.18 to 60.7 mg/kg. Table 1 presents data on concentrations and emission rates of hydrogen sulfide from several water-dominated resource areas. Where published values were unavailable, the emission rates were determined by multiplying the concentrations of hydrogen sulfide in fluids by the fluid

Table 1. Concentrations of hydrogen sulfide in geothermal fluids and uncontrolled emission rates estimated for hot-water and vapor-dominated geothermal reservoirs in the U.S. and elsewhere.

Resource area	Concentration	Estimated emissions ($g/MW_e \cdot h$)	Reference
	in liquids (mg/kg)		
Salton Sea, California	3.2	128[a]	15
Brawley, California	55.1	2,424	16
Heber, California	0.18	20	16
East Mesa, California	0.54	60	15
Baca, New Mexico	60.7	2,125	16
Roosevelt Hot Springs, Utah	8	304	17
Long Valley, California	14	826	18
Beowawe Hot Springs, Nevada	6	348	19
Wairakei, New Zealand	--[b]	570	20
Ahuachapan, El Salvador	48	1,580	21
Otake, Japan	--[b]	542	21
Matsukawa, Japan	--[b]	5,050 - 20,800	21
Cerro Prieto, Mexico	--[b]	32,000	20
	in steam (wt %)		
Larderello, Italy	--[b]	14,300	21
The Geysers, California	24.5	1,850	22

[a] This emission rate has been recalculated.

[b] The hydrogen sulfide concentration associated with the emission rate was not reported.

extraction rates calculated from the temperature-dependent function previously discussed. Table 1 also contains estimates of the uncontrolled emission rates of hydrogen sulfide from power plants at vapor-dominated resources (i.e., The Geysers and Larderello, Italy). To study the uncertainty of the measured concentrations and uncontrolled emission rates, we have prepared a lognormal probability plot of the empirical cumulative

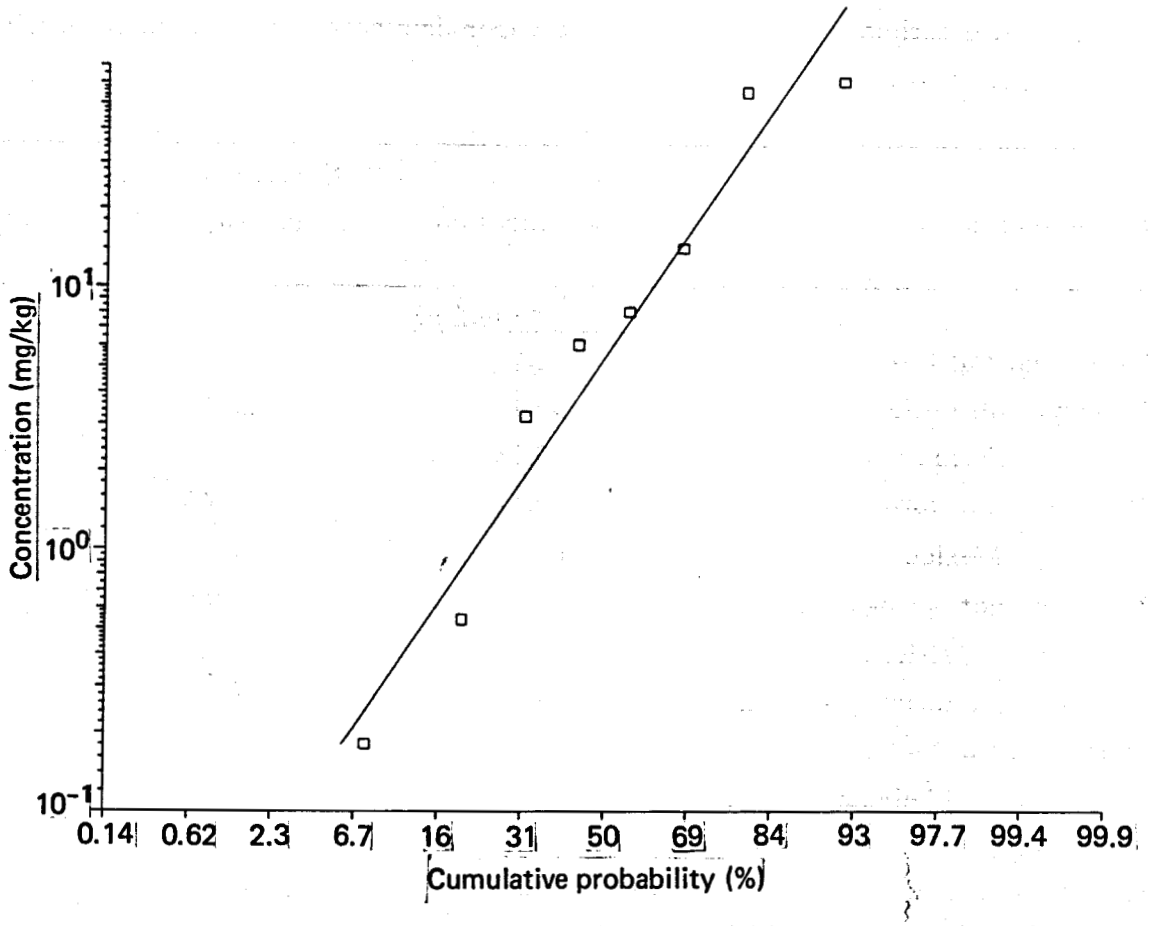

Figure 6. Lognormal probability plot of hydrogen sulfide concentrations in geothermal fluids from eight water-dominated resource areas in the U.S.

distribution of hydrogen sulfide concentrations (see Fig. 6). The geometric mean μ_g of the U.S. data on hydrogen sulfide concentrations is 5.4 mg/kg with a geometric standard deviation σ_g of 7.8. The arithmetic mean value of the untransformed concentration data,* computed from μ_g and σ_g, is 44 mg/kg with a geometric standard error (GSE)** of approximately 3.4. An estimate of the average, uncontrolled emission rate of hydrogen sulfide from geothermal facilities is the product of the weighted mean value (i.e., 19 kg/MW_e • s) for the extraction rates and the mean concentration of hydrogen sulfide (i.e., 44 mg/kg) or 836 mg/MW_e • s. The equivalent emission rate of sulfur is 787 mg/MW_e • s.

---

* The arithmetic mean of a lognormal distribution is equal to $\exp[\ln(\mu_g) + 0.5 \ln^2(\sigma_g)]$.

** The geometric standard error of a lognormal mean is estimated from $\exp[(\ln^2(\sigma_g)/n + 0.5 \ln^4(\sigma_g)/(n+1))^{1/2}]$ where n is the sample size.[23]

Benzene

Benzene is associated with the gas phase of fluids derived from geothermal reservoirs of sedimentary origin. Nonmethane hydrocarbon gases, including benzene, are thought to evolve from the thermal metamorphism of sediments containing organic matter.[24] Table 2 contains data on concentrations of benzene in noncondensing gases for two water-dominated geothermal resource and two vapor-dominated systems. Additional data on benzene are from Des Marais et al. who analyzed samples of dry or noncondensing gases from steam separators at Cerro Prieto, Mexico; steam wells at The Geysers in northern California; and thermal springs and fumaroles at Steamboat Springs in Nevada and at Yellowstone in Wyoming.[29] Their analyses revealed benzene concentrations ranging from 0.1 to 15 ppmv.

Based on the proposed relationship between rock type and occurrence of hydrocarbon gases, we would expect gases from igneous-related geothermal systems to have much smaller levels of benzene or none at all because such systems are depleted in organic matter. Data developed by Nehring and Truesdell[30] support this hypothesis. They collected samples of noncondensing gases from igneous and sedimentary-related geothermal resources and discovered that the gas samples from igneous areas (i.e., Kilauea, Hawaii and Steamboat Springs, Nevada) had much lower quantities of organic gases than the samples from sedimentary and metamorphic rocks at The Geysers and Cerro Prieto. In other supporting work, Des Marais et al. found that the ^{13}C content of hydrocarbon gases from the Cerro Prieto geothermal field was quite comparable to the ^{13}C content of coal found in drill cuttings from wells located in that resource area.[29] Furthermore, pyrolysis of that coal in the laboratory produced methane that had a ^{13}C content similar to that of the methane measured in the noncondensing gases from the geothermal field.

Because the existing data indicate that significant benzene emissions should only be expected from geothermal reservoirs of sedimentary origin, we restricted our analyses to those types of reservoirs. Table A-1 of Appendix A shows that nearly all of the reservoirs are comprised of volcanic rocks. The major exceptions are the reservoirs of the Imperial Valley. To estimate the potential benzene emissions from facilities there, we used concentration data from Ludwick et al. for well G-2 at East Mesa and the Woolsey well at the Salton Sea area.[26] Their measurements showed that benzene was 0.01 mol % of the noncondensing gases from those wells, with noncondensing gases representing 3.5 and 1.7 wt % of the steam, respectively. Assuming that 0.2 kg of steam is produced per kilogram of geothermal fluid and that noncondensing gases are composed almost entirely of carbon dioxide, then the corresponding concentrations of benzene in the geothermal

Table 2. Concentrations of benzene in noncondensing gases from geothermal reservoirs of sedimentary origin.

Resource area	Concentration (ppmv)	Reference
East Mesa, California[a]	85 - 370[b]	25, 26
Salton Sea, California[a]	100	26
The Geysers, California[c]	0 - 45.5	27
Larderello, Italy[c]	0.3 - 38	28

[a] Water-dominated resource.

[b] Concentration was originally reported as a wt% in the geothermal fluid.

[c] Vapor-dominated resource.

fluids are 1×10^{-3} and 6×10^{-4} g/kg, respectively. If we assume that those concentrations are from a lognormal distribution, then the mean value is 8×10^{-4} g/kg with a GSE of 1.3.

Mercury

Mercury is often present in geothermal waters and gases. The most comprehensive studies on mercury emissions from geothermal power plants have been done by Robertson et al.[31,32] Their measurements show that mercury is released from geothermal facilities in liquid and gaseous discharges. For example at the Cerro Prieto power plant, where one set of measurements was made, approximately 90% of the mercury initially dissolved in extracted geothermal fluids was vaporized at the steam separator and entered the power plant with the incoming steam. The principal chemical form of the mercury vapor was elemental mercury (about 90% as Hg^{o}).[33] At the power plant, over half of the mercury condensed with the steam and was subsequently released to the atmosphere via the cooling tower ($\sim$80%); most of the remainder ($\sim$20%) was emitted through the gas ejector that removes noncondensing gases from the condenser. A small percentage of mercury was also released in the waste water discharged from the cooling tower. Measurements of mercury fluxes at electrical generating units at The Geysers (units 3, 7, 8, and 11)

produced somewhat different results. The mass balances for those units also indicated that the cooling tower was the primary atmospheric release point for the mercury, but the remaining mercury was not fully accounted for by either the ejector emissions or discharges of waste water from the cooling tower. However, sludge in the basin of the cooling tower contained 0.02- to 0.2-wt% mercury, and Robertson et al. believe that precipitation of mercury within the basin is an important removal mechanism.[31] Table 3 contains data on elemental mercury concentrations for water-dominated systems. A lognormal probability plot of the concentration data is shown in Fig 7. The μ_g of the concentrations is 0.003 mg/kg and the σ_g is 1.7. The mean of the distribution is 3.5×10^{-6} g/kg with a GSE of 1.3.

Radon

Radon (^{222}Rn), a radioactive gas with a half-life of 3.8 d, is a daughter product of the decay chain of naturally occurring ^{238}U. After radon is formed from the decay of ^{226}Ra in near-surface soils and rocks, it diffuses to the atmosphere at rates that are dependent on ^{226}Ra activity, soil properties, meteorological conditions, and soil moisture.[34] At The Geysers, exhalation rates have been measured that range from 2.6×10^{-6} to 150×10^{-6} $pCi/m^2 \cdot s$.[35] Similar rates have been measured elsewhere in the world.[36] Radon produced deeper in the Earth's crust may never reach the surface because ^{222}Rn can dissolve in groundwater where it decays to its daughter radionuclide ^{218}Po, or the rate of diffusion is so slow with respect to its radioactive decay rate that virtually all of the gas is converted by the time it reaches the near-surface environment.

Table 3. Elemental mercury in geothermal fluids from four water-dominated resource areas.

Resource area	Concentration (g/kg of geofluid)	Reference
Salton Sea, California	1.8×10^{-6}	15
East Mesa, California	6×10^{-6}	15
Puna, Hawaii	3.4×10^{-6}	19
Cerro Prieto, Mexico	2.5×10^{-6}	32

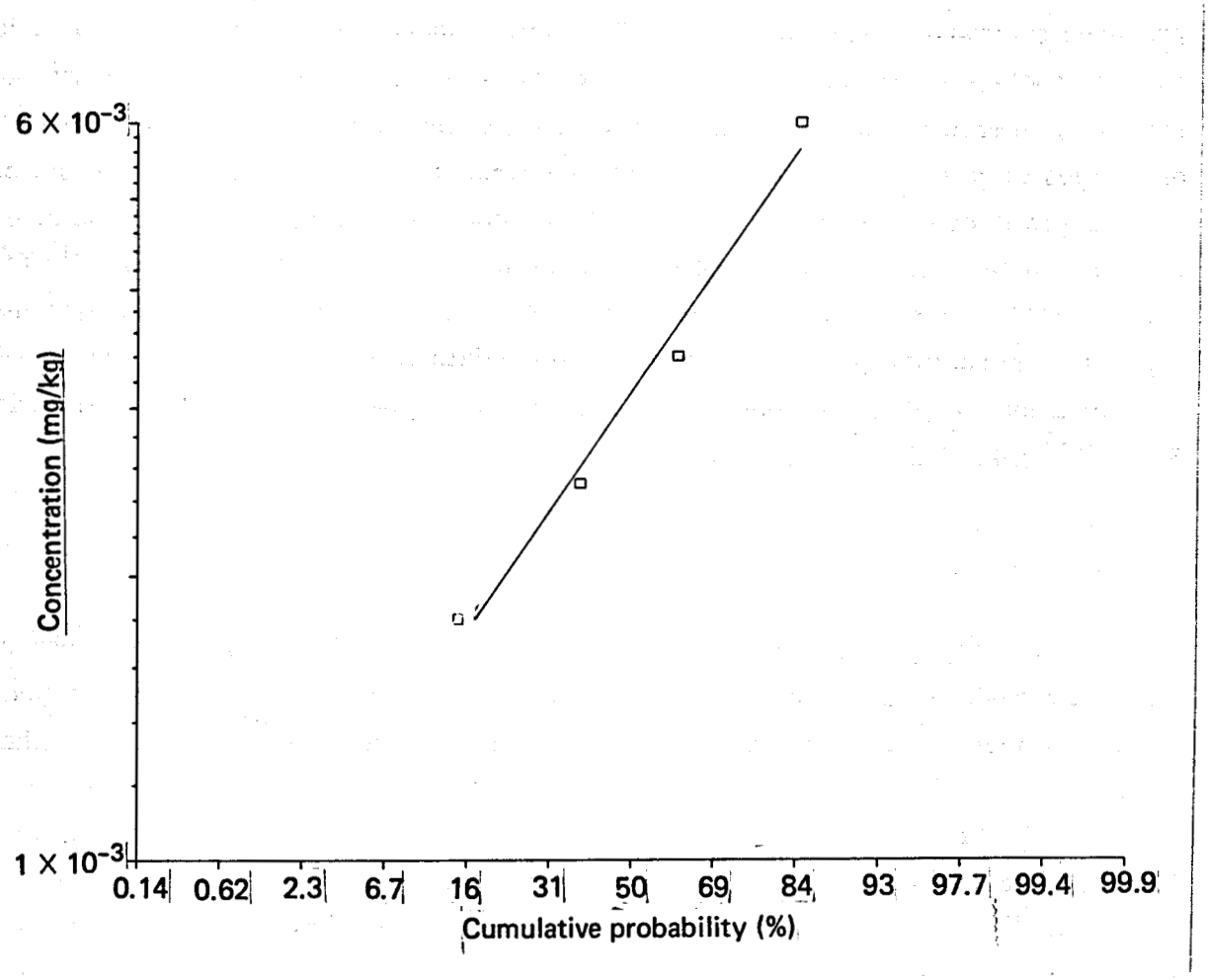

Figure 7. Lognormal probability plot of mercury concentrations in geothermal fluids from four water-dominated resource areas.

The radioactive decay of ^{226}Ra within a geothermal reservoir will produce ^{222}Rn that is dissolved in the geothermal fluids. When those fluids are extracted for power production, the ^{222}Rn will volatilize in a steam separator and the gas will eventually be released to the atmosphere along with the other noncondensing gases. In the Imperial Valley, ^{222}Rn levels range from 480 pCi/kg of geothermal fluid at the East Mesa resource area to 810 pCi/kg at the Salton Sea resource area.[15] These values are consistent with those obtained from a study conducted by O'Connell and Kaufman in which 118 different geothermal waters were sampled for radon.[37] The lognormal probability plot for these data is shown in Fig. 8. The μ_g of the data is 508 pCi/ℓ of geothermal fluid, with a σ_g of 3.7. The arithmetic mean value for the distribution is 1196 pCi/ℓ with a GSE of 1.2.

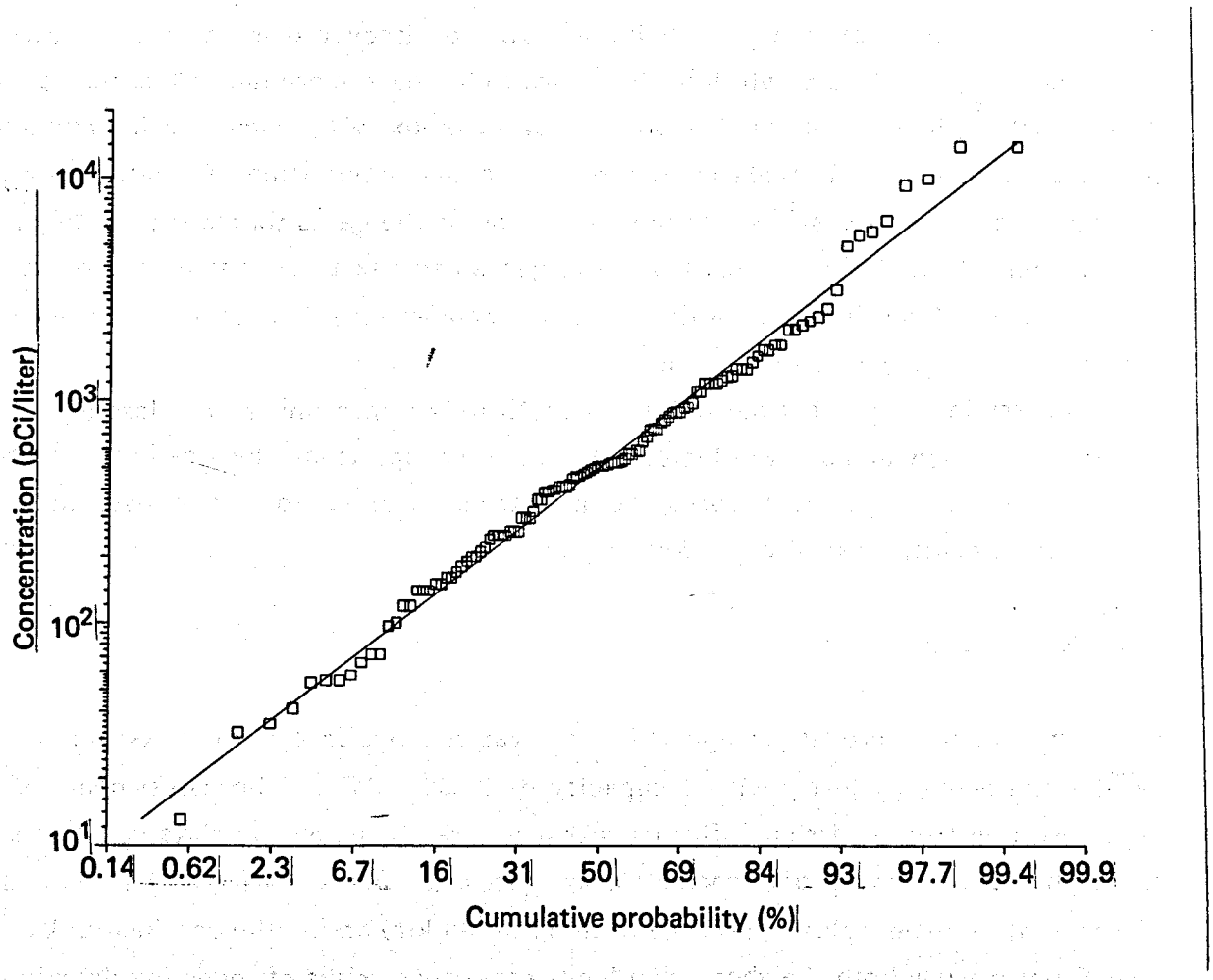

Figure 8. Lognormal probability plot of ^{222}Rn concentrations in 118 different geothermal waters in the western U.S. Data from O'Connell and Kaufman.[37]

HUMAN HEALTH EFFECTS

A mature geothermal power industry will result in health risks both to workers in the industry and to the general public. The primary source of public health risks is the inhalation of toxic gases emitted by geothermal power plants. As noted earlier, the most important gases in this regard are hydrogen sulfide, benzene, mercury, and radon. Hydrogen sulfide emissions can cause noxious odors; sulfur oxides (from the atmospheric

oxidation of hydrogen sulfide) might produce negative health effects including premature death; benzene is leukemogenic; radon is carcinogenic; and mercury can cause neurologic disorders. The ingestion of toxic substances released into the environment is another source of public health risk. Although we are fairly confident that the toxic substances listed above are the only significant ones from a health effects standpoint, we cannot rule out the possibility that some new pollutant will be discovered in the process streams or that a recognized pollutant will later be shown to be much more hazardous than previously recognized.[38] An example of this is benzene. Prior to 1978, when Nehring and Truesdell published results of their analyses of the organic gas composition of noncondensing gases from geothermal systems,[30] benzene was not one of the gases that was routinely assessed in environmental analyses of geothermal projects because there was no reason to expect its presence. Even now, measurements of nonmethane hydrocarbon gases are not available for most geothermal resources.

Workers in the geothermal industry constitute another important class of individuals at risk. We review and analyze historical data on occupational illnesses in the geothermal industry as well as similar, surrogate industries in order to derive estimates of the occupational health risks of expanded development.

PUBLIC HEALTH

Our purpose here is to quantify the various public health risks for a mature geothermal energy industry with a capacity of 21,000 MW_e. The assessments of health risks resulting from emissions of noncondensing gases focus on the risks due to near-field atmospheric dispersion of noncondensing gases (80-km radius around flashed-steam geothermal facilities) plus long-range transport (>80 km) across the continental U.S.

We also study both the short- and long-term cancer risks of ingesting arsenic derived from geothermal operations. We define short-term risks as those that accrue to individuals who were exposed to geothermal pollutants while generating facilities were operating. Long-term risks, in contrast, are those that accrue to future generations. The main source of short-term risks is the emission of arsenic from future flashed-steam power plants located next to croplands in the Imperial Valley of California. Arsenic emitted from cooling towers at these plants will land on crops (we examine lettuce as the target crop), which are later ingested by man. We quantify the transfer of arsenic from geothermal fluids to cooling tower water (i.e., steam condensate) to lettuce and

subsequently to the general population. We then use a dose response function to determine effects. Long-term cancer risks are from the disposal of waste material containing arsenic at surface disposal sites. We employ a method of analysis that allows us to estimate in a crude way the effects that may accumulate over centuries.

Risk Assessment Model and Uncertainty Analysis

An individual's risk of exhibiting a given health effect (e.g., death, cancer, etc.) from exposure to an atmospheric pollutant from a geothermal power plant is a function of personal exposure to that pollutant and the relationship between exposure and the probability of effect. In our assessments of public health risks, we use a multiplicative model with linear terms that has the following mathematical form:

$$R = C \cdot E \cdot \frac{\chi}{Q} \cdot P \ , \qquad (2)$$

where

R = an individual's lifetime risk of an effect resulting from exposure to the pollutant,

C = concentration of pollutant in geothermal fluid,

E = extraction rate of geothermal fluid,

$\frac{\chi}{Q}$ = annual-average ambient concentration of pollutant per unit emission rate, and

P = probability of an effect due to unit pollutant exposure.

Another multiplicative term could be added to the model (i.e., $\chi e/\chi$) that relates the predicted outdoor or ambient concentration χ with an effective concentration χe that represents the composite indoor and outdoor concentration an individual would be exposed to over a year. This term would be especially applicable to a pollutant like sulfur dioxide, which is usually higher in outdoor air than indoor air.[39,40] However, because there are insufficient data on the indoor and outdoor concentrations for the pollutants we consider and on the life styles of residents in rural areas of the western U.S. where most of the geothermal resources are located, we assume by default that χe equals χ.

An accurate prediction of an individual's risk of an adverse health effect resulting from exposure to a pollutant in the environment is often difficult to obtain because of uncertainties regarding estimates of exposure as well as the dose-response function for the pollutant being assessed. Therefore, it is helpful to quantify the uncertainties to gain

a better understanding of how they affect the prediction of health risk. A simple method of incorporating uncertainty into the multiplicative assessment model is to assume that the parameters are lognormally distributed and they are independent.[3,41,42] The uncertainties of the arithmetic means of the individual parameters can then be propagated to obtain an overall estimate of the uncertainty for the average population health risk by

$$\gamma^2(R) = \gamma^2(C) + \gamma^2(E) + \gamma^2(\chi/Q) + \gamma^2(P) \qquad (3)$$

where for example,

$\gamma^2(R)$ = $\ln^2 GSE(R)$ and

GSE(R) = geometric standard error of the arithmetic mean of the lognormal distribution for R

The GSE is calculated from σ_g and the sample size; however, when sufficient data are absent, it must be determined judgmentally.

Effects of Hydrogen Sulfide

Atmospheric releases of hydrogen sulfide represent the most significant public health concern of geothermal energy production. Hydrogen sulfide is a toxic gas[43]; at concentrations above 1000 parts per million by volume (ppmv) it can cause respiratory paralysis and above 200 ppmv this gas is still dangerous and should be recognized as an imminent threat to life. Olfactory paralysis takes place at concentrations of 150 to 250 ppmv and consequently its characteristic odor becomes undetectable at life-threatening levels.[38] The threshold for serious eye damage is between 50 and 100 ppmv.

Absorption of hydrogen sulfide through the lung or the gastrointestinal tract produces toxic effects that are believed to be caused by the reversible inhibition of cellular cytochrome oxidase by the undissociated form of hydrogen sulfide.[43] However, hydrogen sulfide is detoxified in humans and animals by oxidation to benign sulfates. For example, guinea pigs can detoxify 85% of a single lethal dose of sulfide each hour. This gas is considered a noncumulative poison because of the detoxification mechanism and because of its reversible inhibition of enzyme systems. There is no evidence that indicates that hydrogen sulfide in air is carcinogenic, mutagenic, or teratogenic.[44]

From a public health perspective, odor annoyance rather than the acute effects discussed above is the primary consequence of hydrogen sulfide emissions. The more severe effects are unlikely because atmospheric dispersion of the gas after release from a power plant will typically result in nontoxic, ground-level concentrations. Anspaugh and Hahn have reviewed the literature concerning the odor detection threshold of hydrogen sulfide.[5] With one exception, most of the studies they examined agreed fairly well and indicated that the median threshold for odor perception is about 0.005 ppmv. In addition, approximately 20% of the population can smell this gas at a concentration of 0.002 ppmv. There is also some evidence that chronic exposures to low levels of hydrogen sulfide may produce other health effects, primarily of a neurasthenic nature. For example, residents downwind of power units situated at The Geysers resource area have complained of headaches, nausea, sinus congestion, abrupt awakening, etc., when ambient levels were near 0.1 ppmv.

A primary issue therefore of geothermal energy development is the presence of undesirable odors in the vicinity of future generating facilities. In evaluating the potential for odor annoyance, we are basically concerned about the occurrence of short-term (i.e., 1 h or less) concentrations of hydrogen sulfide downwind from one or more power plants. Ermak et al. have shown that in order to avoid violations of the California hourly standard* for hydrogen sulfide (i.e., 0.03 ppmv) from occurring beyond a distance of 1 km from a 100-MW_e geothermal power plant operating in the Imperial Valley, its emission rate would have to be 0.8 g/s (equivalent to 30 $g/MW_e \cdot h$).[45] The California standard, however, is too high to prevent the odor of hydrogen sulfide from being detected by most people. At 0.03 ppmv more than 80% of the population would be able to detect its odor. At this point, a distinction should be made between odor detection and annoyance. It is conceivable that some individuals would not be bothered by slight odors (i.e., at their personal threshold levels) that occur only occasionally-- other individuals, though, may be annoyed by the same infrequent odors. However, it appears that an ambient level of 0.03 ppm (hourly average)-- six times higher than the median, instantaneous threshold value-- would result in odor problems, in part because elevated excursions (10 to 15 min) during an hour could be particularly annoying.

An emission rate of nearly 1 g/s from a single power plant (equivalent to 36 $g/MW_e \cdot h$ from a 100-MW_e facility) would lead to levels that are occasionally

* The California standard was originally set to protect against odor annoyance, but it was based on a study that had anomalously high detection thresholds as compared with other studies (see Ref. 38).

annoying since, according to the calculations of Ermak et al. for such a facility in the Imperial Valley, ambient concentrations of around 0.03 ppmv would be expected at distances of up to a kilometer from the source.[45] For comparison, future power plants at The Geysers, where emissions of hydrogen sulfide are a continuing environmental concern, may have to limit emissions to 0.6 g/s.[46] In summary, it appears that emission rates from generating facilities may have to be kept below 1 g/s to avoid unwanted odors.

To estimate the magnitude of potential odor-related problems of the reference geothermal energy industry, we calculated the emission rates for single power plants in each of the 51 resource areas, based on the assumption that all of the geothermal fluids contain 0.7 mg/kg of hydrogen sulfide. That concentration represents the 16th percentile on the lognormal probability plot of the cumulative distribution of the hydrogen sulfide concentrations previously discussed (see Fig. 6). Even with that low concentration, nearly 60% of the resource areas still would have one or more generating facilities with uncontrolled emission rates exceeding 1 g/s.

Effects of Sulfur Oxides

Hydrogen sulfide released from a geothermal power plant will oxidize in the atmosphere to sulfur dioxide, which is then oxidized to sulfate aerosols. The human health effects of exposure to sulfur oxides have been examined in numerous laboratory and epidemiological studies (see, for example, Ref. 47). Studies dealing with the acute effects of inhalation of sulfur oxides generally indicate that these effects are unlikely at the ambient levels expected to occur as a result of the atmospheric oxidation of hydrogen sulfide. Our interest, therefore, is in the health response to long-term exposure to low concentrations of sulfur oxides--specifically, an individual's risk of premature death. Epidemiological studies such as those carried out by Mendelsohn and Orcutt[48] and Lave and Seskin[49] suggest that the inhalation of particulate sulfates rather than sulfur dioxide is a primary source of health risks associated with long-term, low-level exposure to polluted air. Work done by Amdur showing that sulfate aerosols are a respiratory irritant[50] would seem to support their findings. On the other hand, the epidemiological studies are unable to determine whether sulfate, which could actually be correlated with some other unmeasured, potentially toxic contaminant like respirable particles, is truly the cause of the health effects (i.e., deaths). For this risk analysis, we follow Wilson et al. who suggest that sulfate respresents a reasonable surrogate or substitute measure of the health hazard of exposure to polluted atmospheres containing sulfur oxides and particles until further health effects research is completed.[51]

To assess the risks of the 51 geothermal facilities, we modified equation (2) to

$$R = C \cdot P \cdot \frac{\chi}{Q} \cdot \sum_{i=1}^{51} E_i POP_i \qquad (4)$$

where E_i is the extraction rate of geothermal fluid in the ith resource area and POP_i is the population in the vicinity of the ith resource area. The values of E_i were computed from eq. (1) and temperature estimates in Mariner et al.[52] as shown in Table A-1 of Appendix A. Population values for the 80 km radii around facilities were derived from population data of the 1980 Census.[53] We employed a Gaussian diffusion model developed by Ermak and Nyholm[54] to calculate the annual, ground-level concentrations of sulfate around the reference facility. This analytical model can simulate the conversion of hydrogen sulfide to sulfur dioxide and then to sulfate as well as the deposition of all three species onto the ground. In addition, the model computes the ambient concentration of each of the species. The model was run with meteorological data (i.e., joint probability of wind speed, direction, and atmospheric stability) measured at a location in the central part of the Imperial Valley. A conversion rate of 1.48×10^{-5}/s was used to represent the oxidation of hydrogen sulfide to sulfur dioxide[55] and a rate of 2.78×10^{-6}/s was used to represent the oxidation of sulfur dioxide to sulfate.[56] The deposition velocity of hydrogen sulfide was taken to be 2×10^{-4} m/s after Judeikis and Wren[57]; a value of 1×10^{-2} m/s was used for sulfur dioxide[58]; and finally, the deposition rate of sulfate aerosols was set equal to 1×10^{-3} m/s.[59] Simulation of the atmospheric diffusion, conversion, and deposition out to a radius of 80 km from the plant showed a fairly uniform distribution of sulfate, averaged over 16 wind sectors. The sector-averaged values of χ/Q at 10 km increments ranged from a high of 2.6×10^{-4} $\mu g \cdot s/m^3 \cdot g$ at 10 to 20 km from the source to a low of 1.8×10^{-4} $\mu g \cdot s/m^3 \cdot g$ at 80 km. The weighted average value over the 80 km radius was 2×10^{-4} $\mu g \cdot s/m^3 \cdot g$.

The parameter values used to quantify the health risks of sulfate exposure are contained in Table 4. The near-field population exposures were obtained by multiplying the values for C and χ/Q times the sum of the products of the temperature-dependent fluid extraction rates specific to each of the 51 resource areas and the associated populations at risk (i.e., $\Sigma E_i POP_i$ of eq. (2)). The value of C for hydrogen sulfide (2.2×10^{-3} g/kg of geofluid) is computed for an assumed 95% control of hydrogen sulfide (i.e., 0.044 mg/kg • 0.05). The GSE of $\Sigma E_i POP_i$ was judged to be 1.5, reflecting uncertainties in both the population distributions and fluid extraction rates. The error of

Table 4. Lognormal parameters used in the risk assessment of the near- and far-field exposures to atmospheric sulfate.

Parameter	Units	Arithmetic mean of lognormal parameter	Geometric standard GSE
		Near-field	
C^a	g/kg	2.2×10^{-3}	3.4
$\Sigma E_i POP_i$	kg/s	3.9×10^{10}	1.5
χ/Q^b	$\mu g \cdot s/m^3 \cdot g$	2×10^{-4}	2.5
P	$m^3/\mu g \cdot y$	4.4×10^{-5}	1.7
		Far-field	
LX	$\mu g \cdot persons/m^3$	1×10^{6}	5

[a] Quantity of hydrogen sulfide that would be released to the atmosphere after 95% abatement.

[b] Value for particulate sulfate.

the weighted-mean value for χ/Q was assumed to be a factor of 2.5, based in part on the work of several authors who have studied the performance of Gaussian diffusion models.[60,61,62] The mean value of the near-field exposures is computed at 1.7×10^4 $\mu g \cdot persons/m^3$ with a GSE of 4.86. To calculate the population exposures resulting from the long-range transport of sulfate, we were limited to the use of population exposures (provided by Rowe[63]) derived from a long-range transport code that computes sulfate concentrations as the by-product of sulfur dioxide oxidation. Given this limitation, we made an upper-bound exposure estimate by converting the hydrogen sulfide emission rate to an equivalent emission rate for sulfur dioxide. This equivalent emission rate would increase the downwind concentrations of sulfate because sulfate would then be produced from the direct conversion of sulfur dioxide, rather than as the by-product of hydrogen sulfide to sulfur dioxide decay. The far-field exposure estimate (i.e., 1×10^6 $\mu g \cdot persons/m^3$) was judged to have a standard error of 5, which

incorporates uncertainties of the hydrogen sulfide concentrations fluid extraction rates and the long-range transport model. We estimated the total exposure and its uncertainty by converting the individual lognormal parameters to their normal equivalents, adding those distributions to obtain a composite normal distribution, and then calculating the equivalent lognormal parameters (see Appendix B for a discussion of the methodology). For sulfate, the average total exposure was 1×10^6 $\mu g/m^3$ with a GSE of 5.

The risk factor for sulfate was computed as the mean value of five studies included in the review of Wilson et al.[51] (i.e., 4.4×10^{-5} $m^3/\mu g \cdot y$). Some clarifying comments relating to the value of P should be mentioned here. First, we have implicitly assumed that at low levels of ambient sulfate, the dose-response function is linear with no threshold of effects. If the curve is actually concave at low doses or if it has a threshold, this assumption will lead to over-estimates of health risk. It is interesting to note, however, that the epidemiological studies by Mendelsohn and Orcutt[48] and Lave and Seskin[49] do support the linearity assumption. Nevertheless, inadequacies in the epidemiological studies (e.g., uncontrolled confounding factors such as cigarette smoking, inaccurate air-quality measurements, etc.) could conceivably act together to obscure the nature of the relationship between sulfate exposure and premature death. Indeed, at low concentrations sulfate exposure may not cause negative health effects.

The average population risk becomes 44 premature deaths per year, with a GSE of 5.4. For 30 y of energy production the total number of deaths is 1320 deaths, representing 66 deaths per 10^{18} J. The estimated uncertainty range is from 0 deaths (i.e., predicted concentrations are below an effects threshold) to a total of about 360 deaths/10^{18} J, which was calculated by multiplying the mean by 5.4. The upper-bound estimate is approximately the 84th cumulative percentile of a lognormal distribution, indicating that there is 16% probability that the mean value could be higher. We expect though that the actual probability of exceeding the upper-bound in this particular case is smaller than 16% because of our use of a sulfur dioxide emission rate rather than one for hydrogen sulfide due to the modeling limitations discussed earlier.

Effects of Benzene

Benzene is a hematotoxin that can cause various blood disorders including anemia, leukopenia, and thrombocytopenia. In addition, it has been identified as a leukemogen.

The primary sources of information on the relationship between benzene and leukemia have not been animal studies, but rather epidemiological studies of workers exposed to benzene. Studies by Aksoy et al. involving shoe workers in Turkey[64] and Infante et al. involving workers in the U.S. rubber industry[65] provide strong evidence that the chronic inhalation of benzene can lead to leukemia. The geometric mean of the lifetime risk factor for inhaling benzene is equal to 7.5×10^{-6} $m^3/\mu g$ with $\sigma_g = 2.9$ and is from Hattis and Mendez,[66] who revised an earlier estimate made by Albert[67] that was based on three separate epidemiological studies. The arithmetic mean value is 1.3×10^{-5} $\mu g/m^3$ with a GSE of 2.1. The risk factor was adjusted downward by multiplying it by the ratio of the assumed life of the geothermal industry (i.e., 30 y) to the average life expectancy (i.e., 70 y) to obtain 5.6×10^{-6} $m^3/\mu g$ (see Table 5).

Table 5. Lognormal parameters used in the risk assessment of the near- and far-field exposures to benzene.

Parameter	Units	Arithmetic mean of lognormal parameter	Geometric standard error
		Near-field	
C	g/kg	8×10^{-4}	1.3
$\Sigma E_i POP_i$	kg • persons/s	1.8×10^{10}	1.5
χ/Q	$\mu g \cdot s/m^3 \cdot g$	8.7×10^{-3}	2.5
P	$m^3/\mu g$	5.6×10^{-6}	2.1
		Far-field	
LX	$\mu g \cdot persons/m^3$	3.7×10^{5} [a]	3

[a] Calculated for an emission rate of 88 g/s from geothermal facilities in the Imperial Valley.

Table 5 contains the calculations of the health risks of exposure to benzene. The near-field population exposure to benzene amounted to 1.2×10^5 μg • persons/m^3 with a GSE of 2.8. The far-field exposure to benzene resulting from the emission of 88 g/s from geothermal facilities in the Imperial Valley amounted to 3.7×10^5 μg • persons/m^3 with a GSE equivalent of 3. The far-field exposure value was computed using the normalized exposure tabulations for sources located in each of 243 Air Quality Control Regions (AQCRs) across the U.S. Exposure is calculated for sources releasing respirable particles having a dry deposition velocity of 0.23 cm/s.[68] For a mixing depth of approximately 500 m, the emitted particles will have a residence time in the atmosphere of about 2×10^5 s (with no wet deposition). In comparison, the half-life of benzene due to chemical conversion is estimated at about 5×10^5 s, corresponding to an average residence time of 7×10^5 s.[69] We would therefore expect the predicted population exposure to be low unless the dry deposition velocity of benzene is greater than 0.23 cm/s (assuming that depletion by wet deposition is equal for both pollutants).

Combining the distributions for the two exposures results in an average population exposure of 5.6×10^5 μg • persons/m^3 with a GSE of 2.6. The mean number of leukemias resulting from benzene inhalation is then 3 with a GSE of 3.4. The health risk is then 0.15 leukemias per 10^{18} J of electrical energy produced. The approximate uncertainty bounds are 0 and 0.51 leukemias per 10^{18} J of electrical energy.

Effects of Mercury

The health effects of long-term exposure to airborne, elemental mercury have received far less scrutiny than the effects caused by the ingestion of foods (e.g., fish and seed grains) contaminated with the methylated form of mercury.[70,71] Epidemiological studies of persons exposed to mercury vapors in their work environments have shown that mercury intoxication can manifest itself in several ways; for example, muscle tremors, psychosomatic disturbances, deterioration of intelligence, inflammation of the oral cavity, and lens discoloration. Such symptoms are rarely encountered nowadays because occupational exposures to mercury have been greatly reduced or eliminated by improved industrial hygiene practices. Mercury emissions from geothermal facilities are not likely to cause acute health effects; however, prolonged exposure to atmospheric mercury may cause subtle effects such as psychosomatic disturbances and finger tremors.[72] Muscle tremors are the more reliable indicator of mercury poisoning, primarily because they are

objectively verifiable. Using data from four studies of workers exposed to mercury,[73-76] we developed an estimate of the lifetime probability P of manifesting such tremors due to the prolonged inhalation of ambient mercury.

Three of the studies on which our estimate of P is based (see Table 6) give a breakdown of symptoms claimed or observed; in those instances we used the figures given for muscle tremors as the symptom of mercury intoxication. The fourth study (Kesic and Haeusler) simply reported the incidence of "outspoken symptoms of chronic mercury poisoning" with no breakdown,[75] so we utilized the single figure reported. We conservatively assumed that the dose-response function for mercury is linear without an effects threshold because mercury has no known metabolic function and no human threshold has yet been demonstrated.[77] The risk factor P for each study listed in Table 6 was computed by dividing the incidence of reported effects by the lifetime exposure equivalent. The geometric mean for the risk factors was 9.6×10^{-2} $m^3/\mu g$ with σ_g equal to 2.8. The mean value was 1.6×10^{-1} $m^3/\mu g$ with a GSE of 1.5. When adjusted for the 30 y exposure period, the mean value becomes 6.9×10^{-2} $m^3/\mu g$. This risk value is almost certainly too large. It would suggest for example that a resident of New York City, where ambient mercury is on the order of 0.01 $\mu g/m^3$, faces a risk of 7 in 10,000 of developing mercury-induced tremors over a 30 y exposure. One possible source of error, of course, is that humans may in fact have some dose-response threshold; another source is the body's clearance mechanism. In extrapolating public exposure-response curves from data on occupational or other exposures of limited duration, one must first convert the response to lifetime-exposure equivalents. The most conservative way to do this (and the way used in deriving the value of P above) is to assume response is entirely a function of the cumulative exposure independent of its time distribution. Thus

$$\varepsilon_l = \varepsilon_o \cdot \frac{8\ h}{24\ h} \cdot \frac{240\ d}{365\ d} \cdot \frac{T_o}{A_o} \quad , \tag{5}$$

where

ε_l = equivalent lifetime concentration of mercury to which an individual is exposed,

ε_o = concentration of mercury in the workplace,

T_o = duration of occupational exposure, and

A_o = age of exposed worker.

Table 6. Epidemiological data used in the derivation of the dose-response function for elemental mercury.

Concentration Hg^0 (mg/m^3)		Mean duration of exposure[a]	Sample	Cases of observed	Equivalent lifetime exposure	
Range	Mean[a]	(y)	size	mercurialism	($\mu g/m^3$)	Reference
0.18 - 0.38	0.262	0.2	67	5[b]	0.402	73
		2.53	29	17[b]	4.819	
0.07 - 0.88	0.248	0.2	13	3[b]	0.326	74
		1.22	13	6[b]	1.955	
		5.47	26	23[b]	8.473	
0.25 - 1	0.5	8.61	70	47	24.747	75
0.01 - 0.05	0.022	5.47	276	19[b]	0.682	76
0.06 - 0.1	0.077	5.47	145	12[b]	2.395	
0.11 - 0.14	0.124	5.47	61	6[b]	3.844	
0.24 - 0.27	0.255	5.47	27	14[b]	7.905	

[a] Geometric mean.

[b] Incidence of objective tremor.

[c] Hat factory only.

In fact, however, mercury is cleared from the body at some rate C such that

$$B_t = \frac{D}{C} (1 - e^{-Ct}) , \qquad (6)$$

where

B_t = body burden at time t,

D = dose rate, and

C = clearance rate.

Note that as t increases, B_t approaches D/C; at a sufficiently large t therefore, B_t reaches a virtual equilibrium. Unfortunately, while the clearance rate of elemental mercury is known for several organs, it is not known for the brain, the critical organ for chronic exposures. The available evidence suggests that it remains in the brain far longer than in other organs, with a halftime possibly as long as several years.[78] While it is probable therefore that the cumulative-exposure model overestimates the risk of inhaled mercury, we do not know by how much. However, since the rate of clearance from the brain is evidently much slower than the whole-body rate, we can at least estimate a lower bound for risk by setting the brain clearance rate equal to the body rate. With a value of 50 d for the whole-body halftime,[78] the value of P is roughly an order of magnitude lower than the value based on the cumulative-dose model.

Table 7 contains the parameters used to calculate the public health risks of mercury emitted to the atmosphere. The mean values of the near- and far-field exposures are 950

Table 7. Lognormal parameters used in the risk assessment of the near- and far-field exposures to mercury.

Parameter	Units	Arithmetic mean of lognormal parameters	Geometric standard error
		Near-field	
C	g/kg	2.8×10^{-6}[a]	1.3
$\Sigma E_i POP_i$	kg • persons/s	3.9×10^{10}	1.5
χ/Q	$\mu g \cdot s/m^3 \cdot g$	8.7×10^{-3}	2.5
P	$m^3/\mu g$	6.9×10^{-2}	1.5
		Far-field	
LX	$\mu g \cdot persons/m^3$	2.6×10^{3}[b]	3

[a] The average fluid concentration of 3.5×10^{-6} g/kg was multiplied by 0.81 to estimate the amount of elemental mercury that would actually be released to the atmosphere.

[b] Calculated from 1.3×10^{6} µg/s of mercury emitted from geothermal facilities located in 7 AQCRs in the western U.S.

and 2.6×10^3 μg • persons/m^3, with both error terms equal to 3. The mean of the combined distributions is 4.2×10^3 μg • persons/m^3 with an error term of 2.6. The mean population risk due to mercury emissions is then 290 cases of tremors, or $14/10^{18}$ J of electrical energy. The uncertainty range is from 0 (i.e., predicted mercury concentrations are below a threshold value) to 39 tremors/10^{18} J.

Effects of Radon

Considerable attention has been devoted to deriving risk factors for the induction of lung cancer from exposure to radon and its short-lived daughters. This is because of the documented excess incidence of lung cancer among miners exposed to high levels of radon and its daughters underground. Several such studies have been reviewed recently in the BEIR-III report.[79] They conclude that the risk estimates "now range from about 6 to 47 cases per 10^6 PY per WLM." They further conclude,

> The most likely risk estimates, at exposure of about 1 WL and with characteristic smoking experience, are about 10 cases per 10^6 PY per WLM for the age group 35-49, 20 cases per 10^6 PY per WLM for the age group 50-65, and about 50 cases per 10^6 PY per WLM for those over 65. These values apply to the age at diagnosis and are consistent with available followup data.[78]

In the quotations above, PY is the person-years at risk and is generally calculated by assuming a latent period of 10 y and risk then lasting for life.[79,80] The unit of exposure is the working level (WL) and is equal to 100 pCi/ℓ of ^{222}Rn in equilibrium with its daughters. The unit of integrated exposure is working level month (WLM), where month is equal to 170 h (of occupational exposure).

These risk estimates are based on a linear dose-effect relationship and have been criticized as being at least an order of magnitude too high.[81] If we accept them at face value, assume a lognormal distribution of risks, and assume that 6 and 47 cases per 10^6 PY per WLM are at the 5% and 95% probability levels, then $\mu_g = 20 \times 10^{-6}$ and $\sigma_g = 2$.

Cohen has applied the age-specific risk factors to the U.S. population and has calculated that 21,765 cases of lung cancer per year are predicted based on a calculated exposure to background levels of radon of 0.22 WLM/year.[80] From this we can derive an age- and sex-averaged absolute risk factor of nearly 1×10^{-3} per WLM. Cohen also notes that compared on an equivalent basis, the UNSCEAR derived value[82] is about three times

lower.[83] We have therefore somewhat arbitrarily chosen to use a risk factor of 5×10^{-4} per WLM and further assume that the range is from 0 to 1×10^{-3} per WLM.

We then proceed with the calculation of P as follows :

$$P = \frac{m^3}{10^3 \ell} \cdot \frac{\ell \, WL}{100 \, pCi} \cdot 30 \, y \cdot \frac{24 \, h}{d} \cdot \frac{365 \, d}{y} \cdot \frac{M}{170 \, h} \cdot \frac{5 \times 10^{-4}}{WLM} \quad , \tag{7}$$

$$P = 8 \times 10^{-6} \, m^3/pCi \quad .$$

Table 8 contains the values of the parameters we used in our assessment of the health risks of radon. Adding the distributions for the near- and far-field exposures to ^{222}Rn results in a mean population exposure of 1.7×10^6 pCi • persons/m^3 with a GSE of 2.6. The mean population risk is 0.68 lung cancers per 10^{18} J of electrical energy with an estimated GSE of 2.6. The approximate uncertainty range is from 0 to 1.8 lung cancers per 10^{18} J of electricity.

Table 8. Lognormal parameters used in the risk assessment of the near- and far-field exposures to radon.

Parameter	Units	Arithmetic mean of lognormal parameters	Geometric standard error
		Near-field	
C	pCi/kg	1196	1.2
$\Sigma E_i POP_i$	kg • persons/s	3.9×10^{10}	1.5
χ/Q	pCi • s/m^3 • pCi	8.7×10^{-9}	2.5
P	m^3/pCi	8×10^{-6}	3
		Far-field	
LX	pCi • persons/m^3	1.1×10^6	3

Ingestion Pathway

The two principal mechanisms by which geothermally-derived contaminants can enter human diets are the deposition of cooling tower drift onto agricultural lands supporting food crops in California's Imperial Valley and the long-term migration of toxic substances from waste disposal sites to potable waters.

Drift deposition on croplands in the Imperial Valley. In a flashed-steam facility, fluids produced from wells completed in a geothermal reservoir are depressured at the surface to produce steam that is used to run a turbine. Residual liquids produced after steam separation are subsequently injected back into the reservoir or some other suitable subsurface formation via other wells. Condensed steam is used as the sole source of cooling water for the facility, and consequently, the chemical composition of the water droplets emitted from cooling towers is a function of the composition of the condensate. Existing data indicate that arsenic, a known carcinogen, is likely to be present in condensed steams. Crecelius et al. conducted a sampling program at the Cerro Prieto geothermal power plant in Mexico, and they found that most of the arsenic dissolved in unflashed geothermal fluids stayed with the residual hot water after flashing, however, some arsenic was carried over in the steam.[33] Their data indicate that approximately 4.4 g/h of condensable arsenic were transferred to the steam phase per 2484 g/h arsenic in geothermal fluids, equivalent to a partition coefficient of 1.8×10^{-3}. The emission rate of arsenic from a cooling tower depends on the number of times the condensate is concentrated by evaporation and the rate of drift emission, computed as a percentage of the circulation rate of water in a power plant cooling system. Drift rates can range from 0.01% of circulating flow (poor elimination of drift) to near 0.001%. A drift rate of 0.002% represents a reasonable estimate of state-of-the-art drift control. Table 9 shows the quantities of arsenic emitted from a cooling tower for two drift rates and cycles of evaporative concentration of condensate containing 1.5×10^{-2} mg/ℓ of arsenic. That concentration is the product of a weighted-average value of arsenic concentrations in three geothermal resource areas in the Imperial Valley (i.e., 8.3 mg/ℓ) and a partition coefficient of 1.8×10^{-3}. The deposition of arsenic onto lands out to a distance of 10 km from a mechanical draft cooling tower was calculated by a computerized drift model developed by Dunn et al. (see Appendix C for a discussion of the model and its inputs).[84] The target crop we used for estimating the transfer of arsenic to humans is lettuce, the

Table 9. Emissions of arsenic from a cooling tower operating with a reference 100-MW_e flashed-steam power plant in the Imperial Valley.[a]

Drift rate, % of circulating water flow	Cycles of evaporative concentration	Emission rate, $g/MW_e \cdot h$
0.01	5	0.0027
0.01	10	0.0054
0.001	5	0.00027
0.001	10	0.00054

[a] Circulating flow of water in tower is 3.6×10^7 kg/h and the concentration of arsenic in condensate is 1.5×10^{-2} mg/ℓ before evaporative concentration.

primary leafy vegetable grown in the Valley. Most of the arsenic deposited on lands supporting lettuce will enter that vegetable through foliar deposition, as lettuce accumulates little arsenic through its roots. The following equation, adapted from Hoffman et al. (see Appendix D) accounts for the steady-state or chronic deposition of arsenic onto the plant surface.[85]

$$A_e = D \cdot r \cdot \frac{[1 - \exp - (w \cdot t_c)]}{w} \cdot L_a \qquad (8)$$

where

A_e = annual mass of arsenic transferred to the general population, g;
D = deposition rate, $g/m^2 \cdot d$;
r = ratio of the mass of arsenic intercepted by lettuce to the mass of arsenic deposited, dimensionless,
w = rate parameters for weathering of material deposited on lettuce, d^{-1};
t_c = time of vegetation cover prior to harvesting, d;
L_a = annual land area of lettuce, m^2/y.

Table 10 includes the parameter values we used to calculate annual foliar uptake of arsenic for four emission rates, representing four different operational modes of a mechanical-draft cooling tower, consisting of different combinations of drift rates and cycles of evaporative concentration. The quantities of arsenic added to lettuce during the production of approximately 6.1×10^{18} J of electricity in the Imperial Valley range from 7.6×10^{2} and 1.5×10^{3} g, modes 3 and 4, to 7.6×10^{3} and 1.5×10^{4} g, modes 1 and 2 (see Table 10 for an explanation of the alternative modes). To calculate our best estimate, we use a drift rate of 0.002% and 5 cycles of evaporative concentration, which yield a value of 1.5×10^{3} g of arsenic deposited on lettuce per 6.1×10^{18} J. Exposure to environmental arsenic can result in skin cancer (ingestion) and lung cancer (inhalation). The risk of skin cancer through the ingestion of water containing arsenic has been quantified by the U.S. EPA to be 4×10^{-4} per μg/ℓ,[86] equivalent to a lifetime risk of 0.01/g ingested, assuming a consumption of 2.2 ℓ/d over 50 y. This linear dose-response function predicts between 16,000 to 80,000 skin cancers annually among the U.S. population, based on the daily consumption of 20 and 100 μg of arsenic per person,

Table 10. Parameters used in the risk assessment of arsenic emitted from a reference 100-MW_e flashed-steam power plant.

Parameter	Units	Mode[a]	Value
D[b]	$g/m^2 \cdot d$	1	9.1×10^{-9}
		2	1.8×10^{-8}
		3	9.1×10^{-10}
		4	1.8×10^{-9}
r	dimensionless		0.8
w	d^{-1}		5.7×10^{-2} [c]
t_c	d		75
L_a	m^2/y		3.14×10^{7}

[a] Modes 1 and 2 are for a drift percentage of 0.01% and 5 and 10 cycles of evaporative concentration, respectively. Modes 3 and 4 are for a drift percentage of 0.001% and 5 and 10 cycles of evaporative concentration, respectively.

[b] Weighted-average deposition value over the entire affected area.

[c] From Hoffman et al.[85].

respectively.[87] For comparison, over 300,000 skin cancers are reported annually in the U.S., most of which are thought to be due to sun over-exposure.[88] Although it is plausible that dietary arsenic could cause between 5 and 25 percent of skin cancers, we believe that this is unlikely. First of all, there is evidence that arsenic is an essential element,[89,90] which suggests that at low intake levels an effects threshold may indeed exist. In addition, other studies indicate that mammals have a detoxification mechanism of methylation[86] and that vitamin C can counteract the toxic effects of arsenic ingestion.[91] Further, Valentine et al. report that "arsenic levels in water at concentrations of 100 μg/liter or less seem not to produce an undue body burden."[92] Thus, we conclude that the existing risk factor probably over estimates the actual cancer risk. Skin cancer is not necessarily fatal, and if it is assumed that about 1% of the skin cancers end in death,[88] then the value of the existing dose-response function becomes 1×10^{-4}/g. Using this risk factor, we predict 0.15 fatal skin cancers for 6.1×10^{18} J of development in the Imperial Valley. Upper and lower bound estimates, based on cooling tower operating modes 2 and 3, are 1.5 and 7.6×10^{-2} deaths, respectively. The lower bound, nevertheless, is equal to 0 if there is indeed a threshold for the induction of skin cancer by arsenic ingestion.

The estimates of the quantity of arsenic entering the food chain constitute only 0.17% of the total arsenic emitted under each of the four operational modes addressed. A question then arises as to the extent of health risks for the arsenic deposited on nonagricultural lands. The answer to that question is complex because it involves analyses of the movement of arsenic to man via alternative pathways over large land areas. The same analytical problem is associated with the quantification of risks of toxic substances at waste disposal sites. In essence, the risks of ground deposition and waste disposal occur over long periods of times, further complicating the risk analysis. What is needed then is a method of estimating risks that does not require detailed pathway analyses. Such a method has been developed by Cohen, and we use it in the following section to quantify the risks of arsenic released to the environment by cooling towers and by waste disposal.[93]

Risks of waste disposal and ground deposition. Arsenic contained in soils and rocks near the surface is eventually weathered and carried to the ultimate sink, the world's oceans. However, a portion of the arsenic is transported to man by food and water. Cohen has estimated that the probability of ingesting one atom of arsenic before it enters

the ocean is 0.047.*[93] This so-called transfer probability can then be used to calculate how much of the arsenic released from geothermal operations will enter man, but over a time of scale of at least 100,000 y.

Solid wastes from geothermal operations include solids separated from residual geothermal fluids prior to disposal by subsurface injection and scale periodically removed from pipelines and other components. The production of those solid wastes is controlled primarily by the chemistry of the geothermal fluids processed to produce electrical energy. Unfortunately, there are few published data on waste volumes and composition because the development and operation of geothermal facilities using hot-water resources is in its infancy in the U.S.

Before residual hot-water can be disposed of by subsurface injection, suspended solids in the liquid usually must be removed (or prevented from forming in the cooler waste fluids) in order to prevent the plugging of the well and the target formation that is to receive the waste water. Injectate loaded with suspended material can drastically shorten the life of an injection well, necessitating costly workover and maintenance. In the Salton Sea resource area, where suspended solids reach 400 mg/ℓ, the separation of such material could produce as much as 1×10^5 kg of solids per $MW_e \cdot y$.[7] The geothermal fluids in that resource area contain approximately 11 mg/ℓ of dissolved arsenic.[94] Morris and Stephens[95] measured arsenic at a concentration of 400 µg/g in solids separated from the liquid effluent of an experimental geothermal facility located there, and based on that measurement, we calculate that 40 kg of arsenic would be produced as part of the separated solids per $MW_e \cdot y$ of power plant operation.[95] This particular resource has the highest levels of total dissolved solids (TDS) of all of the identified resource areas, and therefore we would expect that suspended solids would be higher in these fluids than in others-- due in part to the precipitation of sulfides, silica, and carbonate under the reduced temperatures and pressures encountered after steam separation. It is difficult to estimate the quantities of arsenic that would be produced at other geothermal resource areas because of the significant differences in the chemical composition of fluids as well as the use of chemical conditioning (e.g., acidification of waste fluids prior to subsurface injection) to inhibit the formation of undesirable precipitates. The combination of lower salinity fluids at other resource areas and effective chemical controls means that little or no solid wastes and associated

---

* This transfer probability was calculated for a daily ingestion value of 1000 µg. However, a daily consumption of 50 µg is a more reasonable estimate for U.S. diets.[87] The modified transfer probability is 0.002.

contaminants will be produced at many geothermal facilities. A reasonable scenario then is to assume that the Salton Sea area produces virtually all of the waste arsenic from the reference industry. The quantity of arsenic requiring surface disposal is therefore

$$\frac{40 \text{ kg As}}{MW_e \cdot y} \cdot \frac{3400 \ MW_e}{1} \cdot \frac{30 \text{ y}}{1} = 4.1 \times 10^6 \text{ kg} \quad (9)$$

The scale formation rates have been measured at an experimental facility in the Salton Sea resource area.[96] Geothermal brines of different salinities were flowed through an expansion tube and scale deposition measured. Scale deposition rates decreased with decreasing salinity, and ranged from 8.6×10^{-5} of the mass flow rate of dissolved solids (30 wt% TDS in brine) to 3.9×10^{-5} (17.8 wt% TDS in brine). With an arsenic concentration of 150 μg/g in scale,[95] we estimate that 0.2 kg of arsenic would be produced per $MW_e \cdot y$ at the Salton Sea resource area, assuming that scale inhibitors are 75% effective. If we again assume that nearly all of the scale is from that resource area, then the quantity of arsenic becomes

$$\frac{0.2 \text{ kg As}}{MW_e \cdot y} \cdot \frac{3400 \ MW_e}{1} \cdot \frac{30 \text{ y}}{1} = 2 \times 10^4 \text{ kg} \quad (10)$$

The quantity of arsenic released from cooling towers will vary according to the tower operating conditions of the various power plants, but for our purposes here, we calculate arsenic emissions for cooling towers operating with a 0.002% drift rate, 5 cycles of evaporative concentration, and a circulating water flow rate of 3.6×10^5 kg/$MW_e \cdot$ h. The emission rates of arsenic at the Salton Sea area for these reference cooling tower conditions, a partition coefficient of 1.8×10^{-3}, and a dissolved arsenic level of 11 mg/ℓ are 6.2×10^{-3} kg/$MW_e \cdot$ y. The emission rate at other resource areas is 1.4×10^{-3} kg/$MW_e \cdot$ y, based on an average arsenic concentration of 2.5 mg/ℓ. The total quantity of arsenic released to the environment via drift is 1.4×10^3 kg. The cumulative amount of arsenic produced from the reference industry is 4.1×10^6 kg. This quantity constitutes less than 0.1% of the arsenic processed during energy production. The long-term (~100,000 y) population risk in terms of fatal skin cancers is then $(4.1 \times 10^9 \cdot 0.002 \cdot 1 \times 10^{-4})$ 820. This value is equivalent to 41 fatal cancers per 10^{18} J of electricity. The uncertainty range is 0 to 205 deaths/10^{18} J. The upper bound estimate was calculated by multiplying the best estimate by a factor of 5.

Sources of Uncertainty in the Health Risks

The results of our analyses are particularly sensitive to changes in the dose-response functions for the different noncondensing gases. For example, we have assumed that the dose-response function for mercury is linear with no threshold for effects because it has no known metabolic function and no threshold concentration has yet been quantified. We have adopted linear, no-threshold dose-response functions for benzene, radon, and sulfate aerosols as well. Such functions may indeed over estimate effects at low doses--this represents an area for future research. Calculation of the population exposures resulting from long-range transport could be further refined by using improved transport models that explicitly include the chemical transformation of hydrogen sulfide to sulfate and the effects of wind-shear. Regional-level models ($\sim$ 1000 km) more accurately quantifying population exposures near areas of potentially large geothermal development, like the Imperial Valley, might also be of value. Finally, there are some uncertainties about the pollutant source terms. In particular, whether emission controls for hydrogen sulfide will actually reduce the emissions of other noncondensing gases. We have assumed that benzene, mercury, and radon are unaffected by these controls, however, measurements are needed to determine if this is indeed the case.

A primary source of uncertainty related to the calculation of cancer risks from the ingestion pathway is the dose-response function for arsenic. More research is needed on the carcinogenicity of this element. To improve our estimates of the quantity of arsenic entering vegetable crops, additional measurements are needed on the partitioning of arsenic between steam and geothermal liquids. Our estimates of the long-term health risks of arsenic depend a great deal on the transfer factor Cohen has estimated for the entire U.S.[92] The factor is probably different for various regions within the country.

OCCUPATIONAL HEALTH

Today the only large-scale commercial units producing significant quantities of geothermal energy in the U.S. are those steam power plants operating in the vapor-dominated resource of The Geysers, which spans across parts of Lake and Sonoma Counties in northern California. Generating units at The Geysers have operated since 1960 and now have a total capacity of over 1000 MW_e.[2] The reference geothermal industry that we address is assumed to consist almost entirely of flashed-steam power plants that will be operated in liquid-dominated geothermal resource areas.

Consequently, it is not appropriate to project rates of occupational disease or accidental deaths for a mature industry from available data concerning occupational health problems in the relatively young vapor-dominated industry. Instead, we use existing data on The Geysers as an aid to associate the various segments of geothermal activities with surrogate mature industries. We use the occupational mortality, injury, and illness statistics available for these surrogate industries to predict best estimates of accidental death and occupational injury and disease rates for the mature 20×10^{18} J geothermal industry, as well as the lower and upper bounds for these best estimates.

The Geothermal Industry Today

Previous work concerning the occupational health effects related to the geothermal industry have addressed various kinds of occupational hygiene problems, including occupational illnesses, accidental deaths, exposures to hazardous chemicals, etc. Preliminary estimates of potential occupational problems associated with geothermal operations have been discussed by Hahn,[97] Anspaugh and Hahn,[5] and Layton et al.[98] In addition, statistics concerning occupational illnesses associated with geothermal energy in Lake, Sonoma, and Imperial Counties have been compiled for the last half of 1974 through the end of 1977 by Hahn [97] from "Doctors First Report of Occupational Injury or Illness" forms filed with the California State Department of Industrial Relations, Bureau of Labor Statistics and Research. In this section of the report, we combine additional data from "Doctors First Report Forms" from 1978 through 1979 for Lake, Sonoma, and Imperial Counties[99] with that reported by Hahn.[97]

The combined data from "Doctors First Reports" for the latter half of 1974 through the end of 1979 appear in Fig. 9. For each half-year interval (i.e., from June 1974 through December 1979)* we determined the total number of illnesses reported; the illnesses peculiar to the geothermal industry and related directly or indirectly to the presence of hydrogen sulfide in geothermal fluids; the illnesses peculiar to the geothermal industry but unrelated to the presence of hydrogen sulfide in geothermal fluids; and, the illnesses that are not peculiar to the geothermal industry. In addition to the information presented in Fig. 9, we also discovered from analysis of the "Doctors First Reports" that skin disease was responsible for a number of illnesses, and numerous cases of skin disease were attributed either directly or indirectly to hydrogen sulfide.

* This period represents the only time frame, other than the first quarter of 1982, when statistics for "Doctors First Reports of Occupational Injury or Illness" were compiled.

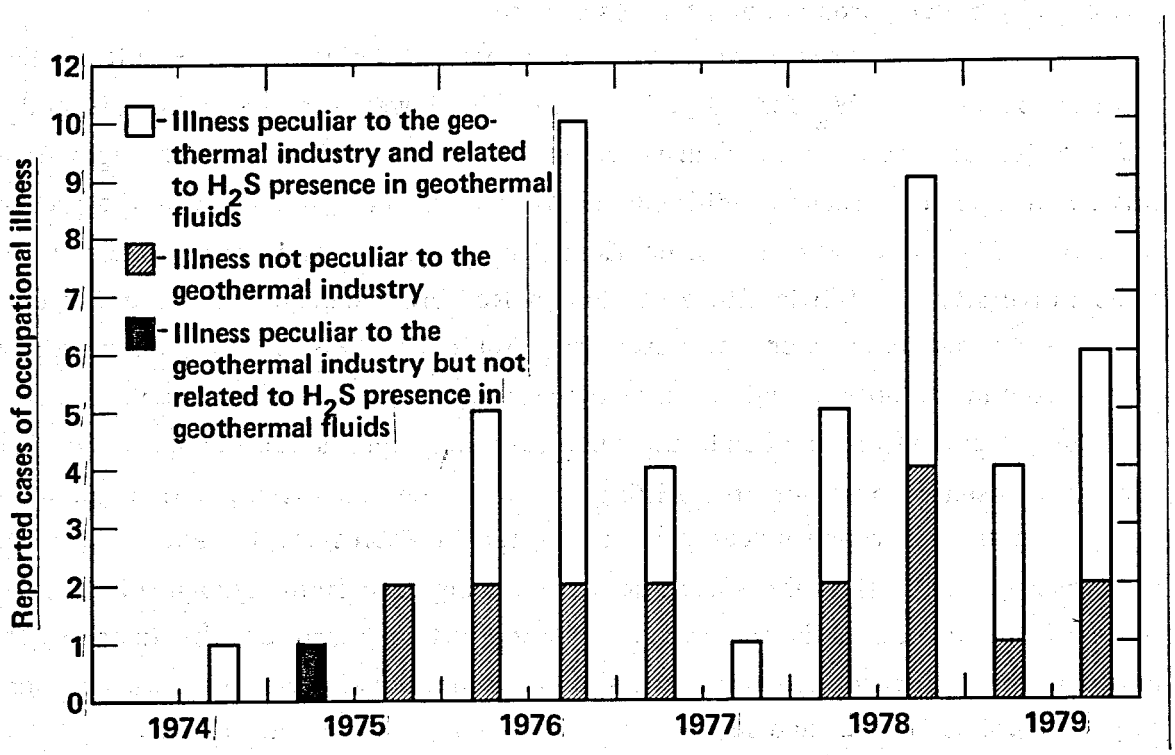

Figure 9. Cases of illness per six-month period for the geothermal industry between June 1974 and December 1979, inclusive. Number of cases were compiled from available Doctors First Reports of Occupational Injury or Illness.[95,97]

Skin diseases are of particular concern because many cases are believed to go unreported[100] and there is even evidence to suggest that most cases will require treatment long after exposure has ceased.[101,102]

Occupational Health Effects

The geothermal industry can be divided into 5 stages: 1) exploration of the resource, 2) well drilling and testing, 3) construction of the power plant, 4) operation and maintenance of the power plant, and 5) decommissioning of the power plant.[98] From the standpoint of potential occupational health problems, segments 2 and 4 are of most concern because these workers in particular will be exposed to large quantities of fluids containing toxic gases and other contaminants that are abrasive and corrosive.[98]

Furthermore, during the operating phase, many workers will be exposed to toxic substances used for hydrogen sulfide abatement. Many of the hazardous substances that may be present at geothermal facilities are listed in Table 11 and include sodium hydroxide, hydrogen peroxide, and ferrous sulfate.[103]

We began our assessment of the occupational health risks resulting from the operation of 21,000 MW_e for 30 y, by estimating lower and upper bounds and a best estimate for the number of man-years of labor required for each segment of the geothermal industry. These predictions are based on employment estimates presented in the 1981 HEED[98] and personnel projections for the geothermal energy industry prepared by the University of Utah Institute of Human Resource Management (see Table 12).[104] According to our manpower estimates (see Table 13) 62% of the manpower will be concentrated in the operational phase of the reference geothermal industry.

Our lower and upper bound, and best estimate figures for occupational mortality, injury, and disease rates for the drilling, construction, operation, and decommissioning segments of the reference industry are presented in Tables 14, 15, and 16, respectively. The rates reported in the tables were computed using data from surrogate industries. The choice of the industries is somewhat arbitrary but is based on the concept that the workers in the surrogate industries face similar occupational risks. In one case there were no appropriate surrogates and so we made estimates on a judgmental basis.

The mortality rate estimates for the drilling segment of the geothermal industry were based on data from drilling in the petroleum industry.[112-114] The lower bound for the construction segment was based on data from the construction of a thermal power plant in Canada[115]; whereas, the best estimate was based on the arithmetic mean fatality rate for the U.S. construction industry between 1969 and 1980 (excluding 1979).[116-126] The upper bound for construction was considered to be similar to the fatality rate for the U.S. construction industry in 1970[117], which was the highest fatality rate reported between 1969 and 1980 (excluding 1979). The total average fatality rate between the

Table 11. Hazardous and toxic chemicals that may be present at geothermal power plants.[103]

Hydrogen sulfide	Anthraquinone disulfonic acid
Inorganic arsenic	Hydrogen peroxide
Boron compounds	Vanadium compounds
Sodium hydroxide	Sulfates

Table 12. Employment data used to estimate lower and upper bounds and best estimates for the number of man-years of labor needed for the reference geothermal industry.

Segment of geothermal industry	Employment data	Estimate	Reference
Drilling[a]	23 worker • mo/well	lower bound	104
	50 worker • mo/well	best	98
	112 worker • mo/well	upper bound	104
Construction[b,c]	2000 worker • mo/110 MW_e	lower bound	98
	4096 worker • mo/100 MW_e	best	104
	8299 worker • mo/100 MW_e	upper bound	104
Operation[b,d]	149 worker • mo/100 MW_e	lower bound	104
	543 worker • mo/100 MW_e	best	104
	1200 worker • mo/100 MW_e	upper bound	98
Decommissioning	250 worker • mo/110 MW_e	lower bound[e]	
	500 worker • mo/110 MW_e	best	98
	750 worker • mo/110 MW_e	upper bound[f]	

[a] 80 wells are considered to be needed for exploration, production, injection, and replacement during the lifetime of a 100 MW_e geothermal power plant.[98]

[b] Employment numbers in the Utah Study correspond to 50 MW_e geothermal power plants.[104] We estimate that only a third more workers will be needed for a 100 MW_e power plant because of economies of scale.

[c] Includes construction of the reservoir feed system and transmission lines.

[d] Includes operation of the reservoir feed system.

[e] We consider the lower bound to be half of the best estimate.

[f] We consider the upper bound to be a factor of 1.5 greater than the best estimate.

Table 13. Lower and upper bounds, and best estimates of the number of man-years of labor needed for the reference geothermal industry (20 x 10^{18} J of electrical energy). All numbers are rounded to two significant figures and expressed as 10^3 worker-years.

Segment of geothermal industry	Estimate		
	Lower bound	Best	Upper bound
Drilling	33	70	160
Construction	32	72	145
Operation	78	285	630
Decommissioning	4	8	12
TOTAL	130	340	910
	Normalized to 10^{18} J of electrical energy		
TOTAL	6.5	17	46

years 1966 and 1975 for an energy production company in Canada called Ontario Hydro was used as the lower bound estimate for the fatality rate from operation,[127] and the fatality rate for the U.S. Transportation and Utilities industry in 1980 was selected for the best estimate of the fatality rate for the operation segment.[126] We selected the arithmetic mean fatality rate for the U.S. construction industry for the period 1969 through 1980 (excluding 1979) as the upper bound for the operation segment.[116-126] Finally, the mortality rates selected for the lower and upper bounds, and best estimate for decommissioning were the values for construction of a thermal power plant by Ontario Hydro in Canada[115]; the arithmetic mean for the U.S. Transportation and Utilities industry for 1969 through 1980 (excluding 1979)[116-126]; and the fatality rate for the U.S. construction industry in 1970,[117] respectively. All of the aforementioned mortality rates are listed in Table 14.

Occupational injury rate estimates for all segments of the geothermal industry were calculated from injury statistics for surrogate industries. The injury statistics were taken from those compiled by the California State Department of Industrial Relations for industries operating in California in 1979,[105] and categorized in this document according

Table 14. Surrogate industry occupational mortality rate data used to estimate upper and lower bounds and best estimates for the mortality risk associated with the reference geothermal industry (20×10^{18} J of electrical energy). Data expressed as number of cases per 10^3 worker-years and rounded to two significant figures.

Segment of geothermal industry	Mortality rate	Estimate	Surrogate industry	Reference
Drilling	0.18	Lower bound	Drilling in the petroleum industry in 1981	112
	0.39	Best	Drilling in the petroleum industry in 1979	113
	0.98	Upper bound	Drilling in the petroleum industry in 1980	114
Construction	0.23	Lower bound	Construction of a thermal power plant	115
	0.63	Best	Arithmetic mean fatality rate for the U.S. construction industry for the period 1969 through 1980 (excluding 1979)[a]	116-126
	0.72	Upper bound	Fatality rate for U.S. construction industry in 1970	117
Operation	0.20	Lower bound	Total average fatality rate for Ontario Hydro for the period of 1966 through 1975	127
	0.28	Best	Fatality rate for U.S. transportation and utilities industry in 1980.	126
	0.33	Upper bound	Arithmetic mean fatality rate for the U.S. transportation and public utilities industry for the period 1969 through 1980 (excluding 1979)[a]	116-126
Decommissioning	0.23	Lower bound	Construction of a thermal power plant	115
	0.63	Best	Arithmetic mean fatality rate for the U.S. construction industry for the period 1969 through 1980 (excluding 1979)[a]	116-126
	0.72	Upper bound	Fatality rate for U.S. construction industry in 1970	117

[a] 1979 data were not readily available.

Table 15. Surrogate industry occupational injury rate data used to estimate upper and lower bounds and best estimates for the injury risk associated with the reference geothermal industry (20×10^{18} J of electrical energy). Data expressed as number of cases per 10^3 worker-years.

Segment of geothermal industry	Injury rate	Estimate	Surrogate industry[a]
Drilling	61	Lower bound	Crude petroleum and natural gas workers (SIC 131) in California
	148	Best	Oil and gas extraction industry (SIC 13) in California
	242	Upper bound	Oil and gas field services (SIC 138) in California
Construction	107	Lower bound	Heavy construction workers, except highway, (SIC 162) in California
	207	Best	Nonresidential building construction (SIC 154) in California
	284	Upper bound	Roofing and sheet metal workers (SIC 176) in California
Operation	113	Lower bound	California Transportation and Public Utilities category
	146	Best	California private sector electric, gas and sanitary services (SIC 49)
	183	Upper bound	California public sector electric, gas, and sanitary services (SIC 49)
Decommissioning	107	Lower bound	Heavy construction workers, except highway, (SIC 162) in California
	218	Best	Miscellaneous special trade contractors including wrecking and demolition work (SIC 179) in California
	284	Upper bound	Roofing and sheet metal workers (SIC 176) in California

[a] Data from Ref. 105 and Standard Industrial Classification (SIC) code details supported by information contained in Ref. 106.

Table 16. Surrogate industry occupational disease rate data used to estimate upper and lower bounds and best estimates for the disease risk associated with the reference geothermal industry (20×10^{18} J of electrical energy). Data expressed as number of cases per 10^3 worker-years and rounded to two significant figures.

Segment of geothermal industry	Disease rate	Estimate	Surrogate industry[a]
Drilling	5.1	Lower bound	Mineral extraction and mining
	12	Best	Primary metal industry
	20	Upper bound	Rubber and miscellaneous plastic products production
Construction	4.8	Lower bound	All California industries
	6.1	Best	Construction industry
	15	Upper bound[b]	
Operation	6.6	Lower bound	Private utility industry and electric, gas, and sanitation service workers
	16	Best	Petroleum production industry
	41	Upper bound	Chemical and allied products production
Decommissioning	4.8	Lower bound	All California industries
	6.1	Best	Construction industry
	41	Upper bound	Chemical and allied products production

[a] All surrogate industry category figures are arithmetic mean disease rates for the period 1973 through 1977.[107-111]

[b] To obtain an upper-bound estimate we multiplied the best estimate by a factor of 2.5

to the Standard Industrial Classification (SIC).[106] In the case of the drilling segment of the geothermal industry, occupational injury rates representing lower and upper bounds, and a best estimate value were chosen to be equivalent to those for crude petroleum and natural gas extraction (SIC 131), oil and gas extraction (SIC 13), and oil and gas field services (SIC 138), respectively. The values selected to represent lower and upper bounds, and a best estimate for occupational injuries associated with construction are those for heavy construction, except highway work (SIC 162), nonresidential building construction (SIC 154), and roofing and sheet metal work (SIC 176), respectively. The lower bound estimate for occupational injuries related to operation of geothermal power plants is based on the figure computed by the State of California for the entire Transportation and Public Utilities category. The best estimate for occupational injuries associated with the operating segment is equivalent to the injury rate reported for private sector electric, gas, and sanitary services (SIC 49-private sector). The occupational injury rate for the public sector electric, gas, and sanitary services category was considered applicable as the upper bound value for the operating segment of the geothermal industry (SIC 49-public sector). Finally, the lower and upper bounds for occupational injuries related to decommissioning are considered to be the same as those derived for the upper and lower bounds for the construction segment. However, the best estimate value was chosen to be the rate reported by the State of California for miscellaneous special trade contractors (SIC 179), which includes a subcategory for wrecking and demolition work contractors.[106] Table 15 contains the previously discussed injury rate data.

The occupational disease rates for the surrogate industries correponding to segments of the geothermal industry were estimated from statistics compiled for California industries operating between 1973 and 1977 by the State of California Department of Industrial Relations, Bureau of Labor Statistics.[107-111] The occupational disease rates presented in Table 16 are all arithmetic means computed for each surrogate industry or industries based on the statistics reported for the years 1973 through 1977. The lower and upper bound, and best estimate occupational disease rates for the drilling segment of the geothermal industry are based on surrogate industries in which workers may be exposed to high temperature fluids and/or potentially toxic substances. The lower bound for the drilling phase is based on the mineral extraction industry. The best estimate is considered to be equivalent to the disease rate for workers producing primary metals. The upper bound for the drilling segment is based on the disease rate for workers manufacturing

rubber and miscellaneous plastic products. For the construction segment we chose the value for all California industries to represent the lower bound, and for the best estimate we chose the value for the construction industry. We could not find any reasonable surrogate industry for an upper bound estimate, so we multiplied the best estimate by a factor of 2.5.

For operation and maintenance workers we used as our best estimate of the disease rate the value given for production workers in the manufacture of petroleum products. The lower bound is the rate given for private utilities and electric, gas, and sanitation service workers. The upper bound is the rate for production workers involved in the manufacture of chemicals and allied products. The best estimate and upper bound surrogate industries were chosen because of the unique problems associated with chemical exposure at geothermal power plants. For instance, hydrogen sulfide is an occupational hazard at geothermal power plants today, and is also a problem in the oil and gas industry. Other chemicals needed for hydrogen sulfide control are also present in the manufacturing of chemicals and allied products.

For the decommissioning segment, we used as our best estimate the disease rate for the construction industry in California. The lower bound we used is the disease rate for all California industries, and the upper bound is the disease rate for the production workers of chemicals and allied products. This upper bound was selected because there is no experience with decommissioning, and workers disassembling a power plant and related structures may be exposed to highly toxic chemicals that have accumulated over 30 y of operation. All of the previously described disease rates are summarized in Table 16.

Table 7 contains the product of the multiplication of lower and upper bound, and best estimates of worker-years of labor (see Table 13); and lower and upper bound, and best estimates of accidental death, occupational injury, and occupational disease risks (see Tables 14, 15, and 16), respectively. To facilitate comparison with other industries, we have normalized the predicted number of man-years of labor (see Table 13), and estimated cases of accidental deaths, occupational injury, and occupational disease (see Table 17) to the production of 10^{18} J of energy. From the information presented in Table 17 we conclude that the developers of the nascent geothermal industry of today need to pay careful attention to the kinds of occupational health problems that will be encountered during development in order to minimize the numbers of accidental deaths and occupational injuries and illnesses.

The most critical uncertainty incorporated into these calculations is the number of illness cases that go unreported. For skin disease alone, the under reporting is believed to be a factor of 2 to 50 times the number of cases actually recorded.[100] To reduce the

Table 17. Estimated number of accidental deaths, occupational injuries and illnesses associated with production of 21,000 MW_e for 30 y (20×10^{18} J). All numbers have been rounded.

Segment of geothermal industry	Accidental deaths			Occupational injuries			Occupational diseases		
	Lower bound	Best estimate	Upper bound	Lower bound	Best estimate	Upper bound	Lower bound	Best estimate	Upper bound
Drilling	5.9	27	160	2.0×10^3	10×10^3	39×10^3	170	840	3200
Construction	7.4	45	100	3.4×10^3	15×10^3	41×10^3	150	440	2200
Operation	16	80	210	8.8×10^3	42×10^3	120×10^3	520	4600	26,000
Decommissioning	0.92	5.0	8.6	0.43×10^3	1.7×10^3	3.4×10^3	19	49	490
TOTAL	30	160	480	15×10^3	69×10^3	200×10^3	860	5,900	32,000
	Normalized to 10^{18} J of electrical energy production								
TOTAL	1.5	8.0	24	0.7×10^3	3.4×10^3	10×10^3	43	300	1600

uncertainty expressed by our bounding estimates for occupational illness, research efforts must focus on more accurate statistics concerning the number of cases of occupational illnesses at existing geothermal facilities. This will permit a better analysis of the etiology and epidemiology of occupational illnesses of concern today (e.g., hydrogen sulfide-induced illness and skin disease) and provide information about the effectiveness of industrial hygiene programs. Such data will also help to identify potential occupational health problems confronting the geothermal industry that may be unrecognized but need attention.

ECOSYSTEM EFFECTS

Three potential sources of ecological effects related to the operation of geothermal power plants are releases of noncondensing gases, accidental spills of geothermal fluids, and cooling tower emissions of drift containing toxic substances. Releases of noncondensing gases are only a problem with flashed-steam power plants since binary-fluid plants should not have gaseous emissions so long as geothermal fluids remain under pressure. Of all the noncondensing gases, hydrogen sulfide and carbon dioxide are the only ones that are expected to affect natural vegetation and crops in the vicinity of power plants. Because of the large quantities of geothermal fluids that must be extracted, processed, and disposed of, another potential source of ecological effects is the accidental release of geothermal fluids. Although the effects of a spill would be local in nature, the cumulative effects at the reference level of power production (i.e., 21,000 MW_e) may be important. Drift from cooling towers is the other concern. At The Geysers, boron contained in drift is probably the cause of foliar damage to native trees near some of the power plants.[128] Boron emissions from cooling towers at geothermal plants located elsewhere could also produce phytotoxic effects. A primary example is the Imperial Valley where boron emissions could cause damage to crops on lands adjacent to power plants.

EMISSIONS OF HYDROGEN SULFIDE AND CARBON DIOXIDE

Most of the recent work on the phytotoxicity of hydrogen sulfide has been conducted by Thompson and Kats[129] and Thompson et al.[130] For the experiments described in the first paper they subjected alfalfa, Thompson seedless grapes, lettuce, sugar beets, California buckeye, ponderosa pine, and Douglas fir to continuous fumigations of 30 ppbv (42 $\mu g/m^3$), 300 ppbv (420 $\mu g/m^3$), and 3000 ppbv (4200 $\mu g/m^3$) of hydrogen sulfide. At

the 300-ppbv and 3000-ppbv treatments, most of the plants exhibited stress (i.e., foliar damage or suppressed yield) when compared with the control plants. At 30 ppbv the forest plants did not show any noticeable effects. However, the growth of alfalfa, grapes, sugar beets, and lettuce was actually stimulated at the lower exposure level. In the second paper they reported the results of treating plants with 50-ppmv carbon dioxide and 300-ppbv hydrogen sulfide. Interestingly enough, they found that the addition of 50-ppmv carbon dioxide generally counteracted the negative effects of hydrogen sulfide alone at the 300-ppbv exposure level, and in the cases of cotton and alfalfa, the treatments of hydrogen sulfide plus carbon dioxide actually caused more growth in the fumigated plants than in the controls.

Ambient concentrations of hydrogen sulfide in the vicinity of a reference, 100-MW_e flashed-steam geothermal facility processing fluids containing 5.4 mg/kg of hydrogen sulfide would range from about 2 $\mu g/m^3$ at a distance of 5 km to 0.7 $\mu g/m^3$ at 10 km, assuming no emission controls. If the fluids contained ten times as much hydrogen sulfide, the concentration range would be 7 to 19 $\mu g/m^3$. So even without abatement of hydrogen sulfide, ambient levels are not expected to have deleterious effects on plants, and in fact, the low concentrations may have a minor fertilizing effect.

The potential phytotoxic effects of hydrogen sulfide and carbon dioxide emissions from 3000 MW_e of geothermal development in the Imperial Valley have been analyzed by Kercher.[131] In his study, he used a computer model to simulate the growth of sugar beets, an important cash-crop in the Valley, exposed to ambient concentrations of hydrogen sulfide as well as carbon dioxide emitted from geothermal facilities. Results of that analysis were then used to assess the possible effects on other crops. Without hydrogen sulfide controls and with no emissions of carbon dioxide, the model predicts that the growth of sugar beets would be enhanced throughout the valley, with beets at some places displaying increases of 10% over the control case. Emissions of hydrogen sulfide from all power plants would have to be over 100 t/d before the growth of sugar beets would be reduced.[131] Unabated emissions from all power plants making up the 3000-MW_e scenario, by comparison, are 40 t/d. When carbon dioxide emissions were included in the model simulations along with the hydrogen sulfide emissions, only increased yields were predicted. The results of the sugar beet simulations were then used to estimate the effects on other crops by using comparative data on the sensitivities of sugar beets and other crops to hydrogen sulfide. In this regard, lettuce and alfalfa are 1.6 and 3.4 times more susceptible to hydrogen sulfide phytotoxicity, and consequently, emission rates

of approximately 70 and 30 t/d from all power plants would result in potential injury. However, the compensating influence of carbon dixoide would probably mitigate those effects.

In conclusion, emissions of both hydrogen sulfide and carbon dioxide from geothermal facilities in the reference industry will not result in negative effects on crops and native vegetation. Indeed, growth enhancement is more likely than retardation. Even smaller effects (no significant enhancement) will occur if hydrogen sulfide is abated.

ACCIDENTAL SPILLS

Geothermal power plants must rely on large quantities of geothermal fluids to produce electricity. A 100-MW_e facility, for example, would process between 3.5×10^3 to 1.85×10^4 m^3/h of fluids, based on requirements of 35 $m^3/MW_e \cdot h$ (275°C resource temperature) and 185 $m^3/MW_e \cdot h$ (150°C resource temperature). A potential danger during the extraction, transportation, processing, and disposal of geothermal fluids is the inadvertent release of those hot fluids to adjacent lands. Such a spill would damage vegetation on the affected lands and contaminate soils. To assess the risks of accidental releases, we must determine how much land area would be covered by fluids after a spill occurs and we must also estimate the probability of events that result in spills.

The surface area affected by spills per $MW_e \cdot y$ of energy production is calculated from

$$A_r = \frac{F \cdot T \cdot S_p}{D}, \qquad (11)$$

where

A_r = area affected by a spill in $m^2/MW_e \cdot y$,
F = flowrate of geothermal fluids in m^3/h,
T = duration of spill in h,
D = depth of spill in m, and
S_p = probability of a release per unit of energy production in fraction/$MW_e \cdot y$.

The critical parameter in this analysis is the probability of a release per unit of energy production S_p. It is quite difficult to accurately quantify the probability of a spill event without data on the frequency of spills at actual geothermal power plants. Nevertheless, release probabilities can be estimated with failure-rate data on individual

components (e.g., valves, pumps, piping, etc.) in a power plant. Sung et al. have used such data to estimate the probabilities of two types of geothermal fluid releases: (1) critical, which they define as "a single-point rupture that can be controlled only by closing the wellhead valves" and (2) major, which they define as "a single-point rupture that is controllable by valves other than the wellhead valves."[132] They estimate a probability of 3.7×10^{-5} for a critical release during the 40-y design life of a 50-MW_e flashed-steam facility, or $1.85 \times 10^{-8}/MW_e \cdot y$, and 1.8×10^{-3} for a major release ($9. \times 10^{-7}/MW_e \cdot y$). The reference plant is assumed to have dual pipes carrying fluids from a well field to central steam separators, and hence half of the total flow from a well field would be released if a critical failure occurs. Major releases, though, would be considerably smaller because of the availability of more valves to control the release.

To analyze the amount of land affected by both critical and major releases, we used a computer code termed MACROI[133] to combine the parameter distributions shown in Table 18. The maximum value of F in a critical release is assumed to be half of the flow of a 50-MW_e power plant requiring 100 $m^3/MW_e \cdot h$ of geothermal fluids, our maximum estimate of flow for a reference geothermal facility. The minimum flow associated with a critical release was arbitrarily assumed to be a tenth of the maximum flow. The

Table 18. Parameter distributions and values used in the analysis of the consequences of accidental releases of geothermal fluids.

Parameter	Units	Distribution	Distribution values	
			Critical release	Major release
			(minimum/maximum)[a]	(minimum/maximum)[a]
F	m^3/h	Triangle	250/2500	25/250
T	h	Triangle	0.166/1	0.166/1
D	m	Uniform	0.013/0.152	0.013/0.152
			(μ_g/σ_g)	(μ_g/σ_g)
S_p	fraction/$MW_e \cdot y$	Lognormal	$1.85 \times 10^{-8}/5$	$9 \times 10^{-7}/5$

[a] The minimum and maximum values of the triangle and uniform distributions used to calculate the median values.

maximum flow during a major release was set equal to the minimum discharge during a critical release. The median values of A_r for critical and major releases were calculated to be 1.6×10^{-4} and 8.2×10^{-4} $m^2/MW_e \cdot y$. At the reference level of geothermal energy production (i.e., 21,000 MW_e for 30 y), $6.3 \times 10^5 MW_e \cdot y$ of electricity are generated. Thus the areas of land affected for the reference industry are 101 m^2 and 517 m^2, for a total of just over 600 m^2. At the 99th percentile of the cumulative distributions for A_r, a total of 5×10^4 m^2 (5 ha) would be affected by both types of spills.

If we assume that 12 ha of land are required for a typical 100-MW_e geothermal power plant, 2.5×10^3 ha of land would be required for facilities making up the reference industry. So in a comparative sense, the potential effect of spills on habitats adjacent to geothermal facilities is minor compared with the disruption of habitats caused by land requirements of power plants and well fields (additional site-specific impacts on habitats will of course be caused by roads, transmission line corridors, etc.).

Accidental releases of fluids can be contained by earthen berms and sumps. In addition, pressure-activated sensors can be used to detect inadvertent spills so that remedial action can be taken. Preventive maintenance of equipment will further reduce the likelihood of large spills. To improve the probabilistic analysis of spills, the value of S_p needs to be improved. Sung et al.[132] based their estimates of S_p on failure rate data for equipment in other industries and for power plant designs that may not prove to be representative. Moreover, the estimate of S_p does not include human errors, and that deficiency could significantly change the results. Additional data on the frequency of spills and causes will have to be collected as the geothermal power industry expands in order to improve our estimates of the spill risk. Also, studies are needed to examine the potential for blowouts of geothermal wells. Such events could constitute a more significant threat to habitats.

EFFECTS OF BORON EMISSIONS FROM COOLING TOWERS

Phytotoxic effects from the deposition of cooling tower drift have been reported in native vegetation near all but 2 of the 15 geothermal power units operating in 1979 at The Geysers area of northern California.[128,134] Chemical analyses of both cooling tower water (the source of drift) and damaged plant tissue (leaves) implicate boron as the principal causal agent.[134] Flashed-steam power plants will also emit boron in the form of cooling tower drift, and consequently, phytotoxic effects could also be manifested around

these facilities. Such effects would be of particular concern in the Imperial Valley where flashed-steam geothermal power plants will be operated adjacent to crop lands. Any yield reduction of commercial vegetation in this area will translate into an economic as well as ecological impact. Here we analyze the potential impact on commercial crops from the deposition of boron contained in cooling tower drift emitted from a reference 6400-MW_e geothermal industry located in the Imperial Valley.

Phytotoxicity of Boron

Boron is an element that is known to be both essential for plants and phytotoxic.[135-138] However, only recently has it been identified as a phytotoxic air pollutant.[128,134,137] Formerly, the adverse effects of boron deficiency and toxicity were documented in only two types of studies. The first examined relationships between crop yields and boron concentrations in soils and irrigation water.[137,139] The other addressed the relationship between crop yields and the foliar application of boron, which is a popular technique used for preventing boron deficiency problems caused by insufficient soil boron levels.[140,141] Collectively, all of these studies show that boron tends to accumulate in the leaves of plants, and boron toxicity is expressed as a foliar injury that is characterized by necrosis and yellowing of the leaf.[137,139,142]

The difference between the boron concentration that is critical for preventing boron deficiency and the concentration that represents the threshold for boron toxicity is depicted as the tolerance plateau in Fig. 10. The length of the plateau is presumed to be

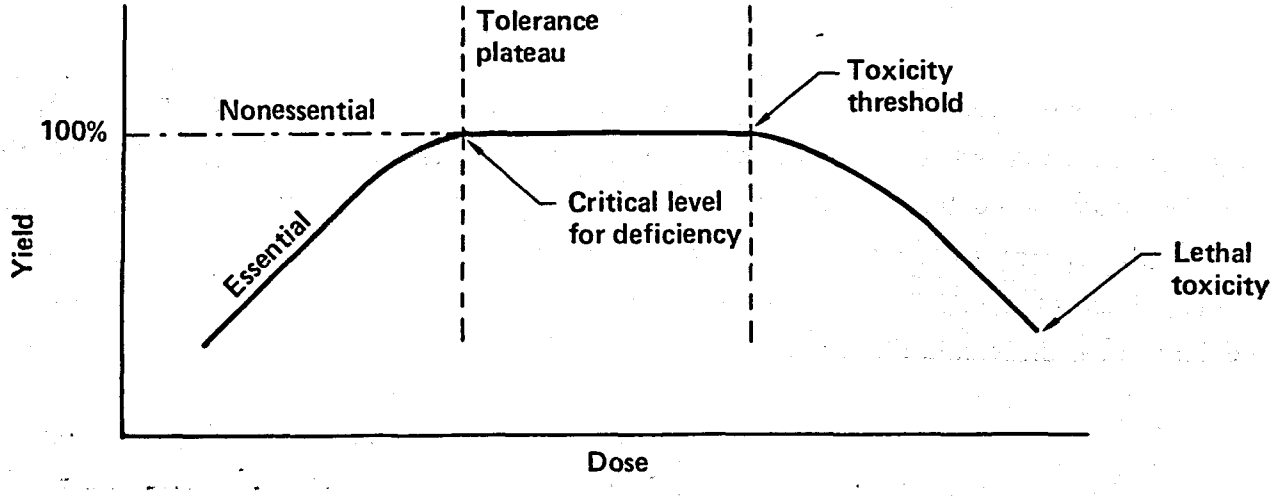

Figure 10. A generalized dose response curve for essential and nonessential elements adapted from Berry and Wallace.[143]

species specific. Thus, the threshold for toxicity will differ depending on the plant species, if all other factors remain constant. For our analysis we assume that for an individual toxic element such as boron, the slope of the line after the threshold has been surpassed (i.e., the yield decrease per additional unit of an individual toxic element) will be the same for all commercial crops.

The exact physiological mechanisms of the plant that are affected by boron deficiency, adequacy, and toxicity are not understood completely.[135] Nevertheless, several functions for boron in plant cells have been postulated[144]:

- It participates in the activity of enzyme systems.
- It is involved in the translocation of sugars.
- It is a micronutrient that is essential for cellular differentiation and development.
- It is utilized in the fertilization process.
- It is needed for the metabolism of nitrogen, carbohydrates, hormones, fats, and phosphorus, as well as for active salt absorption, water movement, and photosynthesis.
- Intercellular boron concentrations interact in an inverse relationship with extracellular calcium concentrations.

There is experimental evidence that indicates that an inverse relationship may exist between boron and the chlorophyll content (a pigment essential for the utilization of light energy during photosynthesis) in a leaf where the disappearance of chlorophyll as a result of excess boron in the leaf could be the result of harmful effects from chains of reactions initiated by boron acting at several different sites.[145] This reduction in chlorophyll would reduce photosynthetic activity in the leaves considerably, which eventually would cause plant mortality and corresponding yield reductions. Data in more recent reports, which address the redistribution of boron in plants after foliar application, reveal that the greatest proportion of the boron absorbed through the leaf remains in the leaf.[140,146] In the leaf, boron is probably present as borate polysaccharide complexes, which are believed to be responsible for preventing any substantial translocation of the element from the leaf.[146]

Deposition of Cooling Tower Drift Containing Boron

The boron contained in the drift resides in the geothermal fluids. During the flashing process it is partitioned between the steam and the residual fluid. After the

steam is condensed, the boron that is present enters the cooling tower where some of it escapes as drift.* The boron fraction in the steam is described by its partitioning coefficient. Our analysis of data[147,148] involving the partitioning of boron between steam and residual geothermal wastewaters indicates that the average partitioning coefficient is approximately 0.03 with a GSE of 1.12. The weighted mean boron concentration for geothermal fluids in the Imperial Valley is about 240 mg/ℓ, based on concentration data of Pimentel et al.[94] and on the geothermal resource potentials of individual resource areas in the Valley. Consequently, by multiplying the partitioning coefficient by the proportion of boron in the geothermal fluid and then multiplying that figure by the number of cycles of evaporative concentration, we obtain an estimate of the boron concentration in the circulating water of the cooling tower.

Our analysis of the effects on commercial crops resulting from the deposition of boron contained in cooling tower drift emitted from a single 100-MW_e flashed-steam facility is based on a cooling tower operating under state-of-the-art conditions of drift elimination and only five cycles of evaporative concentration. The salt concentration of the cooling water was considered to be 4000 mg/ℓ,** and the droplet size distribution of the drift corresponds to that measured by Laulainen et al.[150]

The rate of drift deposition for boron was estimated using the drift model developed for the Electric Power Research Institute by Dunn et al.[84] The rate was calculated for sequential concentric areas of 100-m width from the cooling tower. The first area of 100-m radius (3.1×10^4 m^2) is considered to be an exclusion zone and will not contain commercial crops. Therefore, the distance from 100 to 200 m, a concentric area of 9.4×10^4 m^2, is the first area considered. The deposition rates of boron (D) onto the concentric areas for a distance from 100 to 1000 m from the cooling tower are used in our assessment model and presented in Table 19.

The vegetation exposed to drift deposited around the cooling tower consists of the nine crops composing 90% of the planted acreage in the Imperial Valley. These crops, the percentage of land around the cooling tower that we have determined they could occupy, as well as the estimated yield of each crop in the absence of geothermal energy production are listed in Table 20.

---

* For the purposes of our assessment of crop effects we assume that boron is removed from a tower via drift or wastewater discharges. Volatile forms of boron are neglected.

** We assumed a salt concentration of 4000 mg/ℓ because the concentration of total dissolved solids in waste waters from cooling towers is limited to this value.[149]

Table 19. Boron deposition onto 100-m wide successive concentric areas around the cooling tower of a 100-MW_e geothermal power plant. Figures are based on state-of-the-art cooling tower drift elimination (0.002% drift rate) and five cycles of evaporative concentration.

Distance from cooling tower (m)	Concentric area (m^2)	Boron deposition rate ($\mu g/m^2 \cdot h$)
100 to 200	9.4×10^4	64
200 to 300	1.6×10^5	6.2
300 to 400	2.2×10^5	1.7
400 to 500	2.8×10^5	1.2
500 to 600	3.5×10^5	0.90
600 to 700	4.1×10^5	0.56
700 to 800	4.7×10^5	0.44
800 to 900	5.3×10^5	0.38
900 to 1000	6.0×10^5	0.15

Assessment Model for Crop Effects

The principal concern regarding deposition of boron contained in drift is a yield reduction in adjacent commercial crops or native plant species. Our assessment focuses on predicting the potential yield reduction in commercial crops that could accompany operation of individual 100-MW_e facilities in the Imperial Valley of southern California. The Imperial Valley contains nearly one third of the resource base of the reference geothermal energy industry, and it also is one of the more intensively cultivated areas in the U.S.

Our quantitative assessment of vegetation damage employs a crop dose model and probit analysis. The dose model is used to estimate the concentration of boron in the leaves of crops as a result of both foliar and root uptake of boron. Probit analysis is used to predict any corresponding yield reduction in the individual crops when the concentration of boron in the leaf exceeds the toxicity threshold.

Table 20. Percentages of land area and economic yields for nine commercial crops grown in the Imperial Valley.

Commercial crop[a]	Percent of land area[b]	Economic yield at harvest[c] (kg/m^2)
Alfalfa	30	1.8
Wheat	16	0.59
Sudan grass	13	1.1
Sugar beets	13	5.6
Cotton	12	0.11
Lettuce	9	3.2
Sorghum	3	6.7
Cantaloupe	1	1.4
Rye grass	1	0.22[d]

[a] From data on planted acreage.[151]

[b] Values have been adjusted to account for crop season and periods of fallow land, and therefore their sum does not equal 100%.

[c] Based on yields of ton/acre reported for Imperial County agriculture.[152-157]

[d] An estimate based on the dollars per ton, total value of the entire crop, and estimated acreage planted.[151-157]

Crop Dose Model. The quantity of boron that enters a commercial crop is basically a function of the amount of drift intercepted and absorbed by leaves and the amount of boron taken up by roots. The model we used to calculate the concentration of boron in leaves is adapted from Hoffman et al.[85] (see Appendix D) and has the following mathematical form:

$$C_B = D[I + R], \tag{12}$$

where

C_B = the concentration of boron in plant leaves, μg/g leaf dry weight;

D = the deposition rate of the boron, $\mu g/(m^2 \cdot h)$;

I = coefficient of foliar interception and absorption, $(m^2 \cdot h)$/g leaf dry weight; and

R = coefficient of root uptake, $(m^2 \cdot h)$/g leaf dry weight.

Incorporated into the variables, I and R are the time period that the crop is exposed to drift and the proportion of boron that actually enters the crop by absorption through the leaf or by root uptake from the soil.

The period that a commercial crop is exposed to the deposition of cooling tower drift (t_c) can be expressed mathematically as the time between the point when half of the ground is covered by the crop's foliage ($t_{1/2fc}$) to that when harvesting takes place (t_h). This time frame is geometrically equivalent to the area under the curve in Fig. 11 from the time of emergence (t_e) to the time of harvest. The time of exposure is then incorporated into a formula that accounts for the weathering of material from the surface of vegetation. For root uptake, the period corresponds to the lifetime of the geothermal power plant (t_b) because soil accumulation will be greatest in the final year of operation and therefore the growing season in the final year will be the one most significantly affected. This time period is incorporated into a formula which accounts for the migration of the substance out of the root zone (see Appendix D).

The proportion of boron absorbed into the leaves of commercial crops was considered to be the same as that measured directly for radishes (i.e., 74%).[146] Although this value has a great deal of uncertainty associated with it for crops other than radishes, the ratio of absorption to deposition of boron has been measured directly only in this instance and for our purposes we assume that this value is the most representative. The concentration of boron in the leaves of crops as a result of root uptake was calculated for each crop. The ratio of dry matter appearing as biological yield to leaf dry weight was also calculated for each crop from the reported economic yield based on information in the literature.[139,158] This relationship is important because boron accumulates in the leaves and toxicity thresholds are reported in terms of μg of boron per g of leaf dry weight.

Probit Analysis. As previously mentioned, we presume that all species of vegetation will exhibit the same dose-response relationship once the toxicity threshold for an individual toxic agent has been exceeded. Toxicity thresholds for boron accumulation in the leaves of the nine commercial crops of interest are presented in Table 21. The dose-response

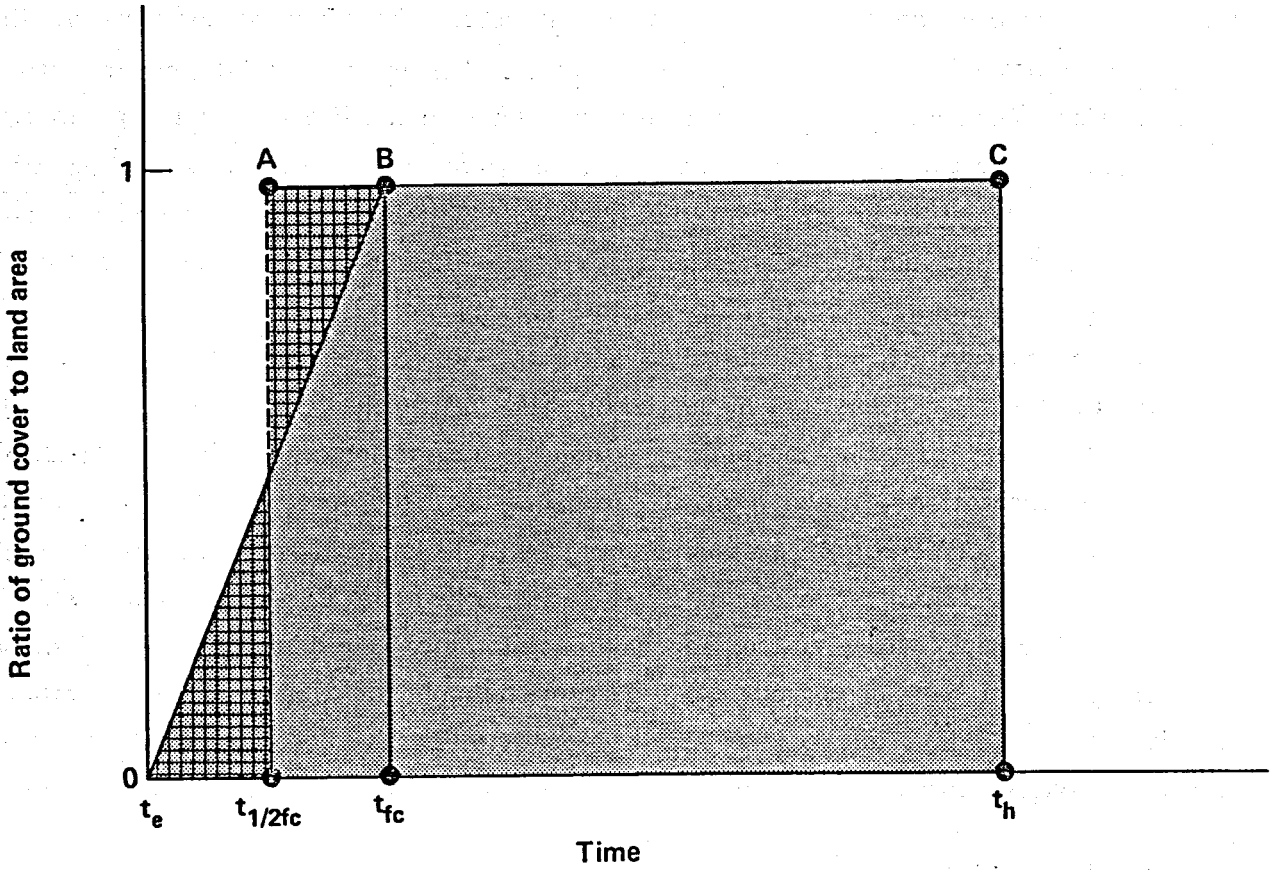

Figure 11. Relationship between the exposure of vegetation to drift and time of exposure. The time of exposure is mathematically expressed as $t_h - t_{1/2fc}$, or the area of the rectangle $t_{1/2fc}$, A, C, t_h, which is geometrically equivalent to the area under the curve t_e, B, C, t_h, where t_e equals time of plant emergence, $t_{1/2fc}$ equals time of one-half full cover, t_{fc} equals time of full cover, and t_h equals time of harvest.

Table 21. Toxicity thresholds based on the leaf boron concentration (μg/g leaf dry wt) for commercial crops historically planted in the Imperial Valley of southern California.[a]

Commercial crop	Range[b]	Geometric mean	Geometric standard deviation
Alfalfa	516 to 996	720	1.28
Wheat (barley)[c]	288 to 1462	650	1.87
Sudan grass (sorghum)[d]	625 to 2009	1100	1.59
Sugar beets	495 to 1008	710	1.31
Cotton	522 to 1625	920	1.55
Lettuce	70 to 817	240	2.57
Sorghum	625 to 2009	1100	1.59
Cantaloupe (muskmelon)[e]	923 to 3875	1900	1.73
Rye grass (perennial)	9540[f]	9500	1.69[g]

[a] From Bradford.[160]

[b] Range derived from Eaton.[139]

[c] Barley used as surrogate for wheat based on Wilcox and Durum.[161]

[d] Sorghum used as surrogate for sudan grass.

[e] Cantaloupe is a type of muskmelon.

[f] Range not available, but specific value indicated by Oertli et al.[162]

[g] Average of all geometric standard deviation values for the other eight crops.

relationship between percentage yield and concentration of toxic agent, once the toxicity threshold is exceeded, can be described with probit analysis.[159] As discussed by Finney,

> Probit analysis is a technique for assessing the dose-response relationship between toxic agents and biological systems, which respond in a quantal (i.e., all-or-nothing) fashion. The methodology consists of transforming the units of the data, concentration of toxic agent and corresponding percentages or proportions of organisms killed, into natural logarithms and probits,* respectively, and plotting the transformed values on linear scales so that a straight line relationship can be obtained.[159]

* A statistical unit of measurement of probability that is calculated on the basis of deviations from the mean of a normal frequency distribution.

We insert the absolute value for the slope of the linear relationship between probits and natural logarithms of boron concentrations into the following mathematical expression:

$$P(U\%) = P(100\%) + S[\ln(C_B)_t - \ln(C_B)_m], \quad (13)$$

where

$P(U\%)$ = the unknown probit value, which can be transformed back to units of percentage yield;

$P(100\%)$ = transformed probit value corresponding to the yield that is equivalent to the one reported by Eaton[139] at the boron toxicity threshold;

$\ln(C_B)_t$ = the natural logarithm of the toxicity threshold value predicted for individual crops (Table 21);

$\ln(C_B)_m$ = the natural logarithm of the leaf boron concentration; and

S = the absolute value of the slope of the line describing the relationship between probit of the percent yield and the natural logarithm of the leaf boron concentration in crops.

By transforming the unknown probit value P(U%) back into the units of the data (i.e., percentage yield) and substracting from 100%, we determine the percentage crop loss for each of the nine Imperial Valley commercial crops.

We determined the slope of the line, which describes the relationship between probits of percent yield and the natural logarithms of boron concentrations in the leaves of crops grown in the Imperial Valley, using the following methodology. First, we transformed the most comprehensive dose-response data available for boron toxicity in both entire plants and in the leaves of plants[139] into probits and corresponding natural logarithms of the concentration of boron. Then we performed regression analyses on each resulting slope, which revealed r^2 values that commonly exceeded 0.8, indicating that the variance in the probit domain is explained for the most part entirely by the natural logarithms of the boron concentration. The next step was to determine the distribution of all of the slope values so that a mean value could be calculated for the slope of the ratio between probit and the natural log of the boron concentration in plant leaves $\ln(C_B)$. Figure 12 contains the lognormal and arithmetic probability plots of the slope values for both entire plant and leaf accumulation of boron. The lognormal probability plot provides a superior fit to the slope values. We used the geometric mean value of the slopes as the one value that best describes the relationship between probit of percent yield and the

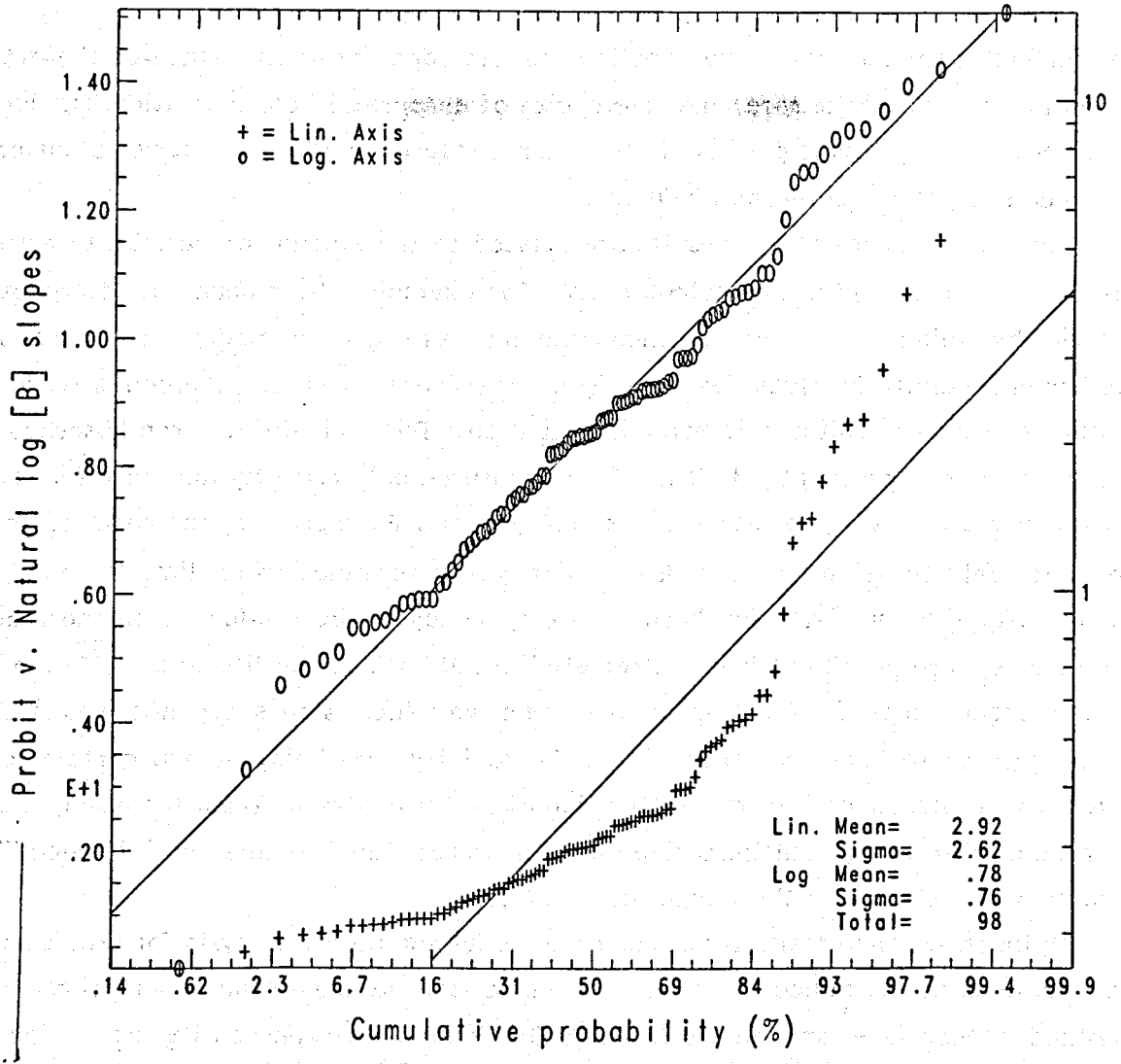

Figure 12. Lognormal and normal (linear) probability plots of slopes describing the relationship between probits of percent yield and the natural log of the boron concentration in the leaves of nine commercial crops historically planted in the Imperial Valley.

natural logarithm of boron concentration in the leaves of crops. Thus, this geometric mean value of 2.2 becomes the S term in the formula for calculating P(U%).

Estimated Crop Losses

We employed the dose model and probit analysis to estimate the total crop loss over 30 y for two different scenarios of electric power production:

- a reference 100-MW_e geothermal power plant operating in the Imperial Valley and
- a reference 6400-MW_e geothermal industry operating in the Imperial Valley.

We further assumed that the cooling towers operate with state-of-the-art drift elimination (0.002% drift rate) and five cycles of evaporative concentration. Under these conditions, no crop loss is predicted for either a reference 100-MW_e power plant or for a reference 6400-MW_e geothermal industry.

The uncertainties in our results are related to the amount of variability associated with each number used in our calculations. For example, the amount of interception of material by foliage has only been measured for pasture crops under certain conditions. Another uncertainty involves the time from emergence to harvest, which will vary as a function of climate, soil conditions, and irrigation. The quantity of boron absorbed into a leaf after being deposited by drift has been measured only recently and only for radishes, and this value may vary for other crops considerably. Furthermore, the ratio of grams of economic yield to grams of leaf dry weight was determined using limited data. Most importantly, the threshold for boron toxicity needs to be evaluated further, because current levels are predicted from extremely limited data in the literature.[139] Moreover, if commercial crops do not respond the same way (i.e., slopes are not equal) or in a quantal fashion to levels of boron above the toxicity threshold, then a certain level of variability is introduced into the application of probit analysis. Thus, the absence of crop loss predicted from our multiplicative model and probit analysis may be influenced by the variability in the value of these input parameters.

To illustrate the sensitivity of our dose model and probit analysis for predicting crop loss from boron contained in cooling tower drift, we make the assumption that the threshold values are at the 10th and 90th cumulative percentile of a lognormal distribution. At the 90th cumulative percentile threshold value there are no significant crop losses. There are however, two additional facts that must be considered when interpreting the magnitude of any of our results. First, we used annual, sector-averaged values for drift deposition rates. Therefore, drift deposition is considered to be uniformly distributed around the cooling tower, even though sectors along the path of prevailing winds will be receiving the greatest amount of deposition. Consequently, crop losses may be conspicuous in some of the sectors, especially if cooling towers are not operating at optimal efficiency. However, even if cooling towers are operating at a drift rate of 0.01% and five cycles of evaporative concentration, we estimate an upper bound crop yield reduction of only 0.05 metric tonne, and this would be for lettuce only (the most sensitive crop of the nine considered). Second, boron concentrations in the condensed steam may increase with time. This phenomenon has occurred at The Geysers in northern

California,[134] and may be due to the practice of injecting residual condensate containing an elevated boron concentration back into the geothermal reservoir. While this phenomenon is currently showing signs of stabilization at The Geysers, the concentration in the drift from most cooling towers more than tripled in less than 10 years.[134]

To further assess the sensitivity of the probit analysis, we doubled the slope value (from 2.20 to 4.40) and reduced the threshold levels for phytotoxic effects for each crop to minimum levels, but used the drift deposition figures corresponding to five cycles of concentration and a 0.002% drift rate. The result of the above analysis was that none of the crops of interest manifested a significant reduction in productivity. Lettuce is effected very minimally (0.0002% reduction over a distance of 100 to 200 m from the cooling tower).

SALINE DRIFT EMISSIONS FROM COOLING TOWERS

Future binary-fluid power plants located in the Imperial Valley will have to rely on external sources of cooling water, because unlike flashed-steam power plants, they do not generate steam condensate. However, some flashed-steam facilities may also have to use external cooling water supplies due to local policies requiring that all extracted geothermal fluid be injected in order to minimize land subsidence. In any event, the primary source of cooling water is agricultural waste water containing about 4000 mg/ℓ TDS. When concentrated five times by cooling tower evaporation, drift emitted from towers contains 20,000 mg/ℓ salt. Deposition of the salts onto agricultural lands could add to the salt stresses that already affect crop yields in the Valley. Accordingly, in this analysis we study the potential effects on crops of depositing additional salt on soils in the vicinity of cooling towers.

Irrigation water in the Imperial Valley contains about 1000 mg/ℓ TDS. A normal application of 1.6 m of water onto irrigated lands produces a salt loading of 1.6 kg/m^2. Because of the high evapotranspiration rate in the Valley, the salts become concentrated in soil waters, exerting a toxic effect on many of the crops. To combat this problem, most of the fields have subsurface drainage systems to remove excess salts that are leached through the soil column by extra water applications. Approximately 2.6×10^6 metric tonne of salt are added to agricultural lands each year and drainage systems remove essentially the same amount. However, some soils do not drain easily, with the result that salts are ineffectively leached and crop stresses occur.

A cooling tower operating with a 100-MW_e geothermal facility will emit 126 metric tonnes/y of salt assuming a drift rate of 0.002% of a circulating flow of 3.6×10^7 kg/h of water. Only about half that emitted will fall on agricultural lands. Some salt will fall on the plants and another significant portion will be dispersed away from cultivated lands as dry particles. So, for 6400 MW_e of development in the Valley we estimate that 4×10^3 metric tonnes of salt will actually fall on agricultural lands each year. This represents a 0.15% increase in salt loading. To bound that estimate, drift rates of 0.01 and 0.001% would result in 0.75 and 0.075% increases. Lands immediately adjacent to towers (100 to 200 m) could receive up to 0.38 kg/m^2 of salt annually (0.002% drift rate), representing a 24% increase. An upper bound estimate of salt deposition at a 0.01% drift rate is 1.9 kg/m^3. That deposition value, although unlikely, would probably result in some crop losses. The deposition value for our best estimate would not necessarily result in significant yield reductions because additional leaching could be used to offset any salt increases. Alternatively, fewer cycles of evaporative concentration could be used to reduce salt emissions at the expense, however, of increased discharges of saline waste water that would have to be disposed of--probably by subsurface injection.

To reduce the amount of uncertainty in our quantification of ecosystem effects from the boron and salt contained in cooling tower drift, we recommend the following research efforts.

- For specific commercial crops and native vegetation, measurements need to be made to determine the ratio of boron concentration in the leaves to the amount of boron both on the leaves and in the soil.
- Further experiments such as those conducted by Eaton[139] are required for better estimates of boron toxicity thresholds for both commercial crops and native vegetation.
- A dose-response model needs to be developed for the effects of boron and salt on native vegetation.

NONPOLLUTANT EFFECTS

The two primary nonpollutant effects that are associated with geothermal power production are land subsidence and induced seismicity. The magnitude of these effects is highly site-specific. For example, the amount of land subsidence caused by geothermal operations is a function of the pressure changes that occur in aquifers as hot fluids are

extracted; the compaction of the aquifer material in response to the pressure changes; and ultimately, the propagation of the subsurface compaction through overburden material (e.g., caprock, alluvial material, etc.) to the surface. The fraction of subsurface compaction that is manifested at the surface in the form of land settlement is affected by site-specific characteristics such as the depth of the reservoir, the radial extent of the reservoir, and the thickness of the compressible beds. Pressure changes are directly related to the fluid extraction rates as well as the geohydrologic properties of the aquifer or aquifers making up the reservoir. Increased seismic activity is another possible consequence of extracting and injecting the large volumes of hot water necessary to sustain a geothermal facility. Enhanced seismic activity at The Geysers geothermal resource area has been linked to changes in the temperatures and pressures within the reservoir resulting from steam extraction.[163] Injection of residual geothermal fluids along a stressed fault zone could also induce seismic events.[164] Again, such seismic activity would depend on the unique features of individual reservoirs. The appropriate level of analysis, given the site-specific nature of subsidence and seismicity, is to bound both effects based on what is known about the general characteristics of geothermal reservoirs and the mechanisms by which both effects are caused.

BOUNDING ANALYSIS FOR LAND SUBSIDENCE

The total downward stress on an arbitrary point within a porous rock is counterbalanced by fluid pressure and the rock matrix. In mathematical terms,

$$T_S = E_S + P \quad , \tag{14}$$

where

T_S = total stress,
E_S = effective stress, and
P = fluid pressure.

Effective stress E_S is that portion of total stress T_S that is not carried by the fluid pressure P. When T_S (i.e., the weight of a column of rock and water above the reference point) is constant, $\Delta E_S = -\Delta P$. The extraction of hot water from a geothermal reservoir will reduce the P contained in the pore spaces and fractures of the rock, causing a

corresponding increase in the E_S. An increase in the E_S within the skeletal matrix of a reservoir rock will result in the volumetric compression of the rock. The compression is either recoverable (i.e., elastic) or unrecoverable (i.e., inelastic). Of primary interest in predicting land subsidence is the inelastic response of the matrix of the reservoir rock to changes in E_S and the subsequent response of the overburden to that deformation. The following analysis of those processes relies in part on field-based computational techniques proposed by Helm.[165]

One measure of the inelastic response of reservoir rock to changes in E_S is the coefficient of volume compressibility m_v. This coefficient is defined as

$$m_v = (-\Delta V/V) / \Delta E_S \ , \qquad (15)$$

where

m_v = coefficient of volume compressibility, m^2/N;
ΔV = change in rock or soil volume, m^3;
V = total volume of compressible material, m^3; and
ΔE_S = change in effective stress, N/m^2.

The compaction of compressible reservoir rock for changes in P is calculated as the product of the thickness of the beds b and m_v and ΔP. For vertical settling of the land surface to occur above a compacting reservoir, the subsurface compaction must propagate through overburden to the surface. Helm has defined a variable, the coning factor E, which is the ratio of vertical land subsidence to reservoir compaction directly above the center of a disk-shaped reservoir that exhibits a uniform drop in P.[165] It is a function of reservoir depth, the radius of the cylindrical reservoir, and the thickness of the compressible beds. Land subsidence caused by reductions in P in a geothermal reservoir can then be calculated as

$$S_L = E \cdot b \cdot m_v \cdot \Delta P \ , \qquad (16)$$

where

S_L = ultimate amount of vertical land settling (m),
E = coning factor (fraction),
b = thickness of compressing beds (m),
m_v = coefficient of volume compressibility (m^2/N), and
ΔP = change in reservoir fluid pressure (N/m^2).

To study the potential magnitudes of land subsidence, we calculated the values of the ultimate amount of vertical land settling S_L for each of the 51 geothermal resource areas and then computed a weighted-average value S_{LW} as the sum of the products of the site-specific estimates of S_L and the ratios of the energy potentials of the individual resource area to the total energy potential for the reference industry. Background data on the geometries and lithologies of the geothermal reservoirs (i.e., depths, bed thicknesses, and areas) were obtained from Mariner et al.[52] and are presented in Appendix A. The m_v for each reservoir depends heavily on the types of rock present. More specifically, porous sedimentary rocks composed of clays, shales, sandstones, etc. will not compact the same as metamorphic or igneous rocks. Generally, sedimentary rocks are more compressible than solid rocks with fracture-controlled permeabilities. We explored the sensitivity of S_L to m_v by using values of m_v that are applicable to the two types of rocks.

Approximately 30% of the energy potential of the reference industry is derived from reservoirs composed of sedimentary rocks. The compressibility of these rocks can be determined in the laboratory by subjecting a sample to a uniform stress and measuring the change in volume. This method, though, does not necessarily duplicate the inelastic response of rock to in situ stresses. An alternative approach is to derive values of m_v from field data relating decreases in porosity to increases in depth. Porosities of sedimentary rocks decrease with depth in response to the increases in E_S that correspond to the weight of overlying sediments. The compression of the porous rock with depth represents long-term, steady-state responses to depth-dependent stresses, and as such, values of m_v computed from such porosity-stress relationships should be considered upper bound estimates of rock compressibility.[166] Helm developed two expressions relating rock compressibility with changes in rock porosity with depth[165]: one is based on an exponential relationship of porosity and depth and the second uses a logarithmic relationship. We used depth-dependent relationships to calculate m_v for sedimentary reservoirs. The reservoirs representing the remaining 60% of the reference industry are composed primarily of igneous rocks (e.g., basalts, volcanics, etc.) and metamorphic rocks, both intermixed on occassion by sedimentary rock units. We used ranges of compressibility to reflect the varied lithologies of those reservoirs. Table 22 shows the values of land subsidence per 100 m drop in hydrostatic head (equivalent to 9.8×10^5 N/m^2).

For case 1 the value of S_{LW} ranges from 0.16 to 0.48 m, based on whether the rock compresses horizontally and vertically (i.e., isotropic response) or just vertically. Vertical

Table 22. Weighted-average values of ultimate land subsidence for various values of m_v, with ΔP equal to 9.8×10^5 N/m^2.

Case number	Ultimate land subsidence (m)		Compressibility values (m^2/N)	
	Isotropic volume compression	Vertical volume compression	Sedimentary reservoirs[a]	Igneous/metamorphic reservoirs
1	0.16	0.48	2×10^{-9}	1×10^{-11}
2	0.44	1.34	2×10^{-9}	1×10^{-9}
3	0.32	0.96	5×10^{-9}	1×10^{-11}
4	0.6	1.81	5×10^{-9}	1×10^{-9}

[a] The average compressibilities for cases 1 and 2 are calculated from an exponential relationship between m_v and depth. The average compressibilities for cases 3 and 4 are calculated from a logarithmic relationship of m_v with depth.

compression is three times greater than isotropic compression. As expected, the greatest values of vertical land settling occur at sedimentary reservoirs, and under case 1 reach a maximum of 4.4 m per 100 m decline in hydrostratic head at one reservoir. By increasing the value of m_v for the igneous/metamorphic reservoirs to 1×10^{-9} m^2/N, the individual values of S_L for the various reservoirs become comparable to those of the sedimentary reservoirs and the S_{LW} reaches 1.34 m. Similar results are found in cases 3 and 4. It is interesting to note that the logarithmic relationship for m_v and depth gives values of m_v that are a factor of 2.5 greater than the exponential relationship, which means that subsurface compaction would be correspondingly higher at the depths of interest.

The actual effects of land subsidence related to geothermal operations will vary according to the amount of subsidence that occurs and the sensitivity of surface land uses to changes in elevation. Geothermal sites are mainly in rural areas where land settling would not be a problem. Moreover, there are mitigation measures that can alleviate subsidence effects.[167] The calculations prepared here lead to upper-bound estimates, and they do not reflect such things as time lags of compaction and related subsidence or the drainage and compression of overburden. What the calculations do show

is that sedimentary reservoirs are capable of exhibiting subsidence in response to long-term pressure declines. To reduce the uncertainties associated with predictions of land subsidence, more data are needed on the actual in situ responses of reservoir material and overburden to changes in E_S at reservoirs with different geometries and geohydrological characteristics. Such data would be of great use in developing and verifying models.

INDUCED SEISMICITY

Bufe et al.,[163] in a review of the seismicity at The Geysers geothermal resource, have noted that earthquakes there have occurred more frequently over time. They link that increase to pressure and temperature changes that occur in the reservoir as a result of steam extraction and condensate injection. The enhanced seismicity is spatially correlated with geothermal well fields in the resource area. Moreover, the earthquakes related to the geothermal operations occur constantly (compared with the episodic nature of natural seismic events in the region), but at levels under a magnitude of 4 on the Richter scale.[163]

Another possible mechanism for inducing earthquakes is the injection of fluids into fault zones. This has been demonstrated by Raleigh et al.[164] in an injection experiment in Rangely, Colorado, where earthquakes were induced by increasing fluid pressures within a fault zone, which lowered the frictional resistance along fault surfaces. Injection of residual fluids at geothermal resource areas could also pose a risk of enhanced seismicity.

The magnitude of the seismic risks of geothermal operations, needless to say, is highly site-specific. Previous experience with geothermal operations in the U.S. and elsewhere suggests that the enhanced seismicity is not necessarily harmful since the Richter magnitude of the induced events has not been high enough to cause damage. Moreover, the considerable experience associated with injection of waste brines at oil fields has not shown a significant risk of destructive earthquakes.[164] This should not imply that induced seismicity is inconsequential. Geophysical techniques should be developed to screen resource areas with respect to their seismic potential. In this regard, the work of Raleigh et al.[164] could prove helpful. For the long-term, the development of predictive tools to assess seismic problems is also needed.

CONCLUSIONS

The analyses in this HEED provide some valuable insights into the manageability of health and environmental risks of geothermal power production, the relative importance of different effects, and the need for future research to reduce the uncertainties of the risk analyses. In our analysis of hydrogen sulfide, for example, we showed that emissions of that gas from geothermal facilities would probably have to be kept below 1 g/s to avoid the occurrence of unwanted odors in the vicinity of power plants. We further estimated that nearly 60% of the resource areas would have at least one power plant with emissions greater than 1 g/s, assuming that no controls are implemented and that geothermal fluids contain 0.7 mg/kg of hydrogen sulfide. The use of hydrogen sulfide abatement equipment to minimize potential odor problems has a second-order benefit--the reduction of health risks from exposure to particulate sulfate, the oxidation by-product of hydrogen sulfide in the atmosphere. The chemical treatment of noncondensing gases to remove hydrogen sulfide may also lower emissions of mercury, benzene, and radon. However, the degree of control in that particular situation is not known at this time. Interestingly enough, efforts to abate hydrogen sulfide have led to a secondary health problem, occupational exposure to toxic substances used in the control systems (e.g., sodium hydroxide). Thus, the management of one health risk can actually lead to another unless precautions are taken.

The public health risks of geothermal development could be greatly reduced by implementing binary-fluid power plants, which are not expected to release noncondensing gases so long as geothermal fluids are under pressure. Again, the occupational risks of the newer, binary-fluid technologies could be greater than flashed-steam systems--this should be the subject of future research. One drawback of the binary-fluid plants is their need for external sources of cooling water. In the arid West, the siting of those facilities may be a real problem and consequently their use may be severly restricted.

We used occupational data from similar industries to calculate the occupational risks, and unfortunately there is no way of knowing the direction of bias caused by using the surrogate data until more data become available on operating geothermal facilities. Furthermore, until more is known about the sources of occupational illnesses and deaths, it is not possible to determine how effective industrial hygiene practices will be in reducing risks.

During our analyses of the health and environmental risks of producing geothermal energy, several avenues of future research became apparent that should help to reduce uncertainties in our risk estimates.

- In general, more data are needed on the chemistry of geothermal fluids. A program of sampling and analyses of fluids from more geothermal resources would be a cost-effective way of reducing one source of uncertainty in our analyses. This is especially true for benzene, an organic gas that has only recently been discovered in noncondensing gases. Additional data on hydrogen sulfide and mercury would also be helpful.

- Improved models for calculating the population exposures resulting from the long-range transport of noncondensing gases are needed. For example, none of the existing models we reviewed could simulate the chemical conversion of hydrogen sulfide to sulfate.

- A major source of uncertainty involves the dose-response relationships of the substances we have assessed. It is clear that more laboratory and epidemiological studies are needed to increase our understanding of the toxicology of the different gases. Additional information would be particularly helpful on the dose-response function for sulfate aerosols. Our analysis of the health risk of mercury would be improved if we knew more about the clearance rate of mercury from the brain. More research is needed on the homeostatic function of arsenic.

- Data should be collected on the frequency of occupational illnesses associated with the geothermal industry. These data would be instrumental in developing industrial hygiene programs to manage potential risks.

APPENDIX A

BACKGROUND DATA ON GEOTHERMAL RESOURCE AREAS

The following table contains geophysical data (e.g., energy potential, fluid temperature, reservoir depth and radius) that we used in our analyses of the 51 geothermal resource areas comprising the reference industry. These data are from Mariner et al.[52] In addition, we have included data on the population densities around each of the resource areas.

Table A-1. Background data on the 51 geothermal resource areas in the western U.S. that comprise the reference geothermal industry.[52,53]

Geothermal Resource Area, State and County	Energy potential MWe • 30 y	Temp. (deg.C)	Population density (people/mi^2)	Reservoir depth (km)	Reservoir area (km^2)	Thick-ness (km)	Rock types
ALASKA							
Hot Springs Cove, Aleutian Is.	27	164	0.5	1.7	2	1.7	Andesite, argillite keratophyre, diabase
Geyser Bight, Aleutian Is.	136	208	0.5	1.5	6.3	1.7	Andesite
Bailey Bay, Ketchikan	26	162	8	1.5	2	1.7	Granite
ARIZONA							
Power Ranches, Pinal	23	165	17	2	3.3	0.8	Alluvium over andesite or granite
CALIFORNIA							
Surprise Valley, Modoc	1490	152	2	1.5	128.3	1.7	Alluvium over rhyolite
Morgan Springs, Lassen	116	217	5	1.5	5	1.7	Dacite, andesite
Sulphur Bank, Colousa	75	194	11	1.5	4	1.7	Basalt flows over Franciscan rks
Clear Lake, Lake	900	190	29	1.5	50	1.7	Rhyolite, dacite, basalt
Long Valley, Mono	2100	227	3	1.5	81.7	1.7	Rhyolite tuffs, flows, domes
Coso, Inyo	650	220	2	0.5	27.3	1.7	Rhyol. & basalt over granitic & metamorphic rks
Randsburg, San Bernardino	84	172	44	1	5.7	1.7	Andesite overlying quartz
Salton Sea, Imperial	3400	260	22	0.5	60.3	1.9	Deltaic sediments
Westmorland, Imperial	1710	217	22	1.1	80	1.5	Deltaic sediments
Brawley, Imperial	640	253	22	1.9	25.7	1.3	Sandy deltaic sediments
East Mesa, Imperial	360	182	22	1.8	32	1.1	Sandy deltaic sediments
Border, Imperial	31	160	22	1.8	3.5	1.1	Sandy deltaic sediments
Heber, Imperial	650	182	22	1.5	41.7	1.7	Sandy deltaic sediments
COLORADO							
Paradise Hot Spring, Dolores	24	154	2	1.5	2	1.7	Sandstone, shales, siltstone
HAWAII							
Kamaili, Hawaii	210	273	20	1	7.3	1.3	Basalt
Kapoho, Hawaii	41	275	20	2.2	2	0.9	Basalt
IDAHO							
Crane Creek, Washington	340	171	6	1.5	23.3	1.7	Basalt & fluvial deposits
Big Creek, Lemhi	26	162	2	1.5	2	1.7	Granite

Table A-1. (continued)

Geothermal Resource Area, State and County	Energy potential MWe • 30 y	Temp. (deg.C)	Population density (people/mi²)	Reservoir depth (km)	Reservoir area (km²)	Thickness (km)	Rock types
NEVADA							
Baltazor, Humboldt	46	158	1	1.5	3.7	1.7	Alluvium, volcanics, granodiorite
Pinto, Humboldt	90	173	1	1.5	6	1.7	Granodiorite
Great Boiling, Washoe	32	178	31	1.5	2	1.7	Alluvium, lake sediments, granodiorite
San Emedio, Washoe	28	166	31	1.5	2	1.7	Alluv. over basalt, andesite, tuffaceous sed.
Steamboat, Washoe	350	200	31	0.3	11.7	2.5	Volcanics, granite, metamorphics
Lee Hot Spring, Churchill	28	166	3	1.5	2	1.7	Volcanics
Soda Lake, Churchill	146	157	3	1	11.3	1.7	Lake deposits, basaltic tuff
Stillwater, Churchill	450	159	3	1	35.3	1.7	Alluvium & basalt
Fernley, Churchill	33	182	3	1.5	2	1.7	Alluv. over basalt, andesite, tuffaceous sed.
Brady, Churchill	157	155	3	1	13	1.7	Basalt/alluvium
Desert Peak, Churchill	750	221	3	1.5	30	1.7	Andesite, basalt, tuffs, metavol.
Humboldt, House, Pershing	47	217	0.6	1.5	2	1.7	Playa deposits over carbonates
Kyle Hot Springs, Pershing	97	159	0.6	1.5	7.7	1.7	Alluvium metamorphic rocks
Leach Hot Springs, Pershing	77	162	0.6	1.5	5.8	1.7	Alluvium, sed. rocks, basalt
Beowawe, Eureka	127	229	0.3	1.1	5.3	1.5	Alluvium, basalt, andesite
Hot Sulphur, Elko	27	165	1	1.5	2	1.7	Lacustrine rocks
Sulphur Hot Springs, Elko	74	178	1	1.5	4.7	1.7	Alluvium, granite, metamorphics
NEW MEXICO							
Valles Caldera, Sandoval/Rio Ar	2700	273	7	1	75	1.7	Rhyol. flows & tuffs, andes. over(?) sandstones
OREGON							
Newberry Caldera, Deschutes	740	230	21	1.5	28.3	1.7	Andesite, basalt
Crump's Hot Spring, Lake	61	167	0.9	1	4.3	1.7	Basalt overlain by alluvium
Mickey Hot Springs, Harney	160	205	0.8	1.5	7.7	1.7	Andesitic tuff-breccia, basalts, andesite
Alvord Hot Spring, Harney	49	181	0.8	1.5	3	1.7	Rhyodacite, basalt & andesite
Hot Lake, Harney	91	191	0.8	1.5	5	1.7	Alluvium & playa deposits, basalts
Trout Creek, Harney	24	154	0.8	1.5	2	1.7	Basalt, andesite, rhyolite
Neal Hot Springs, Malheur	36	188	3	1.5	2	1.7	Basalts
Vale Hot Springs, Malheur	870	157	3	1.5	70	1.7	Lacustrine deposits over basalt & rhyolite
UTAH							
Cove Fort, Beaver	330	167	2	1.5	24.6	1.6	Latite & andesite over paleozoic sedim. rks
Roosevelt, Beaver	970	265	2	0.8	23.7	2	Granite intruded to gneiss
WASHINGTON							
Gamma Hot Springs, Snohomish	27	165	161	1.5	20	1.7	Dacite & rhyolite tuffs

APPENDIX B

METHODOLOGY FOR ADDING THE LOGNORMAL DISTRIBUTIONS ASSOCIATED WITH EXPOSURES TO EMITTED GASES

The uncertainties in the parameters defining the multiplicative equation we use to quantify the health risks of atmospheric emissions (i.e., eq. (3)) are propagated by summing the logarithmic variances. This procedure, however, cannot be used when lognormally distributed parameters are added, for example, when the near- and far-field exposure distributions are combined. To estimate the mean and GSE of the composite distribution for the sum of the population exposures, we use the following methodology. First, we convert the lognormal parameters for both exposures to the equivalent normal means and variances. Those values are then added to obtain values for a composite normal distribution, which are subsequently converted to lognormal parameters.

In mathematical terms, we define β as

$$\beta = \ln(\mu_g) + 0.5 \ln^2 (\sigma_g) \qquad \text{(B-1)}$$

and assume, as Land[23] does, that it is normally distributed. The arithmetic mean of the lognormal distribution defined by μ_g and σ_g is $\exp(\beta)$, denoted M. The approximate variance of β for a sample size of n is

$$\gamma^2 = \ln^2(\sigma_g)/n + 0.5 \ln^4(\sigma_g)/(n+1) \qquad \text{(B-2)}$$

The arithmetic variance is expressed as

$$S_N^2 = \exp(2\beta + \gamma^2) (\exp(\gamma^2)-1) \qquad \text{(B-3)}$$

and the arithmetic mean equivalent is

$$X_N = \exp(\beta + 0.5 \gamma^2) \qquad \text{(B-4)}$$

The arithmetic mean and variances of the near- and far-field exposures are computed using equations B-3 and B-4 and then added to obtain the values of the composite normal

distribution. Those values are converted to the lognormal equivalents by the following expressions

$$M = X_N (1 + (S_N/X_N)^2)^{-1/2} \quad \text{(B-5)}$$

$$\gamma^2 = \ln (1 + (S_N/X_N)^2) \quad \text{(B-6)}$$

The GSE is computed as $\exp(\gamma)$.

We will now illustrate this procedure using the estimates of the near- and far-field exposures for sulfate. The mean values of the near- and far-field sulfate exposures were 1.7×10^4 and 1×10^6 μg • persons/m^3, respectively, with GSE's of 4.86 and 5. The corresponding arithmetic variances computed from Eq. (B-3) were 3.9×10^{10} and 1.6×10^{14}. The equivalent means, computed from Eq. (B-4), were 5.9×10^4 μg • persons/m^3 for the near-field exposures and 3.6×10^6 μg • persons/m^3 for the far-field exposures. We added the variances and means to obtain values of the composite normal distribution. We then converted those values to the lognormal values, using Eqs. B-5 and B-6, or

$$M = 3.7 \times 10^6 (1 + (1.3 \times 10^7/3.7 \times 10^6)^2)^{-1/2}$$
$$M = 1 \times 10^6 \text{ μg • persons/m}^3 \quad \text{(B-7)}$$

$$\gamma^2 = \ln (1 + (1.3 \times 10^7/3.7 \times 10^6)^2) \ ,$$
$$\gamma^2 = 2.59 \quad \text{(B-8)}$$

and the GSE is computed as $\exp(2.59^{1/2})$, which is equal to 5. In this particular example the uncertainty of the near-field exposure contributed little to the overall estimate of uncertainty because of the magnitude of the far-field exposure.

APPENDIX C
ATMOSPHERIC EMISSIONS FROM COOLING TOWERS

A portion of the water circulating through the cooling system of a flashed-steam geothermal power plant is emitted to the atmosphere as water droplets that are entrained in the air exhausted from its mechanical-draft cooling water. The emitted water, known as drift, contains the dissolved substances present in the circulating water. Condensed steam is the primary source of cooling water for flashed-steam facilities, and consequently, the water circulating through the tower can contain soluble substances derived from the steam (e.g., boron and arsenic). The rate by which a dissolved contaminant is discharged from a tower in the form of drift depends on the contaminant's concentration in steam, the number of times the source water (i.e., condensate) is concentrated by tower evaporation, and the drift rate.

The drift rate is calculated as a percentage of the mass or volumetric flow rate of water circulating through a cooling system, which in turn is governed by the amount of heat that must be transferred or rejected from the condenser. For example, a 1 MW_e power plant operating with a thermal efficiency of 10% will reject approximately 9 MW_t and require some 5.6×10^5 kg/h of water circulating through the cooling system with a 13.8°C temperature change across the condenser. With an increase in thermal efficiency to 15%, the ratio of heat rejected to energy produced and the water circulation rate become 5.7 MW_t/MW_e and 3.4×10^5 kg/h, respectively. Drift rate percentages range from about 0.01 to 0.001% of the circulating water flows through mechanical-draft towers. Drift elminators are used to reduce the entrainment of water droplets in exiting air. Without such eliminators or if they are poorly designed or maintained, percentages can range from 0.1 (no elimination) to 0.01% (poor elimination) of circulating flow. The concentrating effect of evaporation on the levels of dissolved solids in the circulating water is controlled by discharging a portion of that water as waste (known as blowdown). If 20% of the condensed water produced is discharged as blowdown and the remainder evaporated, the dissolved solids are concentrated four times.

Deposition of drift on the ground around a cooling tower is governed by the meteorology of the site, properties of the emitted drift (i.e., droplet size distribution and salinity), and the physical characteristics of the cooling tower. A model of the drift transport must address the rise of the vapor plume from the tower, the points at which droplets break away from the plume, the subsequent evaporation of droplets, and the settling velocities associated with the changing droplet sizes. For assessments of the

health and environmental effects of drift we used a model developed by Dunn et al.[84] that incorporates these important features. The model has been validated, in part, against field data, and it predicts drift deposition generally within a factor of 3. Input to the simulation includes characteristics of a cooling tower and the emitted drift together with seasonal or annual meteorological data.

Table C-1 includes the physical parameters of the reference cooling tower used in our calculations of drift deposition. The droplet spectrum we used in the drift model is from Laulainen[150] (see Table C-2), who measured the diameters and corresponding mass fractions of droplets emitted from a mechanical-draft cooling tower operating at a power plant in California. A significant portion of droplets ($\sim$ 45 wt%) have diameters greater than 600 μm, which means that more drift deposition is to be expected near towers rather than far away ($\sim$ 1 km). This is in general agreement with previous studies of vegetative effects of cooling tower emissions that have shown plant stress adjacent to towers (<200 m).[134,168]

Another factor influencing the deposition of drift is the salinity of the water droplets. With higher salinity, evaporation from droplets is suppressed, larger droplet sizes are maintained, and thus deposition is higher nearer the tower. Figure C-1 shows how the predicted salt deposition decreases with distance for cooling waters of 4000 and 20,000 mg/ℓ TDS but with the same drift droplet size distribution. Within 300 m of the tower, the deposition values for the 20,000 mg/ℓ TDS water are more than a factor of 5 higher than for the 4000 mg/ℓ TDS water.

Table C-1. Parameters used to define the mechanical-draft cooling tower used in the simulations of cooling tower drift.

Parameter	Value
Number of cells	10
Diameter of cells	9.6 m
Tower height	18.3 m
Tower width	12 m
Tower length	122 m
Heat rejected	450 MW_t
Water: air mass ratio	1.6

Table C-2. Distribution of droplet diameters by wt %.[150]

Droplet diameters (μm)	Wt%
10 to 60	24.3
60 to 150	10.3
150 to 300	6.8
300 to 600	13.1
600 to 1200	14.9
1200 to 2200	19
2200 to 3400	11.3
TOTAL	99.7

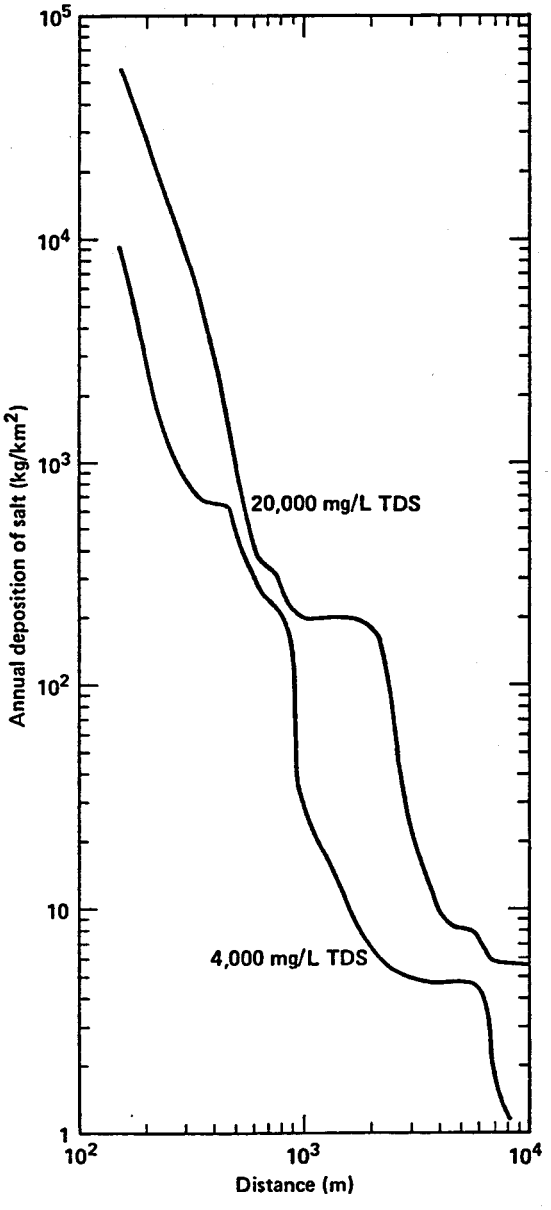

Figure C-1. Annual, sector-averaged salt deposition for a mechanical-draft cooling tower operating with cooling waters of two different salinities. Variations in the two curves are due in part to the salinity-controlled evaporation rates of the droplets. Droplets of saline water do not evaporate as quickly as fresh droplets, and consequently the saline droplets will fall to the ground more rapidly.

APPENDIX D

Calculation of Crop Losses

We adapted the model given by Hoffman et al.[84] to estimate the concentration of a substance in a crop after foliar and root uptake. Their model has the basic form

$$C = D[G + Q], \tag{D-1}$$

where

$$G = \frac{r}{y_b} \quad \frac{1 - \exp(-w \cdot t_c)}{w} \tag{D-2}$$

$$Q = \frac{1}{p} \quad \frac{1 - \exp(-\lambda \cdot t_b)}{\lambda} \tag{D-3}$$

and

- C = the concentration of the deposited substance in the vegetation, μg/g;
- D = the deposition rate of the substance of interest, $\mu g/m^2 \cdot h$ (see Table D-1);
- r = the proportion of the deposited substance that is intercepted by the standing vegetation, dimensionless;
- y_b = the biological yield in dry weight of the standing crop, g/m^2;
- w = the rate constant for the environmental removal of material deposited on the surface of vegetation (i.e., weathering term), h^{-1};
- t_c = the amount of time that the vegetation is exposed to deposition prior to the time of harvest, $t_h - t_{1/2fc}$ (see Fig. 11);

Table D-1. Drift deposition at 100 m increments from the cooling tower.

Distance from tower m	D^a ($\mu g/m^2 \cdot h$)
100 to 200	64
200 to 300	6.2
300 to 400	1.7
400 to 500	1.2
500 to 600	0.90
600 to 700	0.56
700 to 800	0.44
800 to 900	0.38
900 to 1000	0.15

[a] Deposition rate for a 100-MW_e geothermal power plant with a cooling tower operating at 0.002% drift rate and 5 cycles of evaporative concentration.

B = the ratio of the amount of substance in the dry weight of the vegetation, μg/g, to the amount of substance in the soil, μg/g; presumed to be 0.29 based on boron measurements in crops and soil in the Imperial Valley of California[169];

p = the effective surface density of the soil, based on a 15-cm depth for the root zone, g/m^2;

Ω = the rate constant that describes the downward migration of the deposited substance out of the 15-cm root zone, h^{-1}; and

t_b = the operating lifetime of the geothermal power plant, h.

The coefficient of foliar interception and absorption (I) in Eq. (12) is obtained by multiplying G in Eq. (D-2) by the proportion of the substance absorbed into the leaves of the crop after deposition η (see Table D-2) and by a conversion factor K (see Table D-2), which represents the ratio between biological dry weight and leaf dry weight. The coefficient of root uptake (R) in Eq. (12) is obtained by multiplying Q in Eq. (D-3) by the conversion factor K (see Table D-2). We assume that all boron from root uptake is translocated into the leaves. The y_b terms and conversion factors for the crops in Table D-2 were derived from relationships between economic yield, biological yield, crop

dry weight, and leaf dry weight reported for each crop in the literature.[139,158,170,188] The y_b terms and conversion factors are necessary because boron accumulates in the leaves of crops and toxicity thresholds are reported in terms of μg of boron per g of leaf dry weight; however, only economic yields are usually reported for commercial crops. The value for p (see Table D-2) is the figure given by Hoffman et al.[84] The value for Ω was calculated according to the equation and parameters described by Baes.[167]

$$\lambda = V\,(d\,[1 + \frac{\rho}{\theta}\,k_d])^{-1} \qquad \text{(D-4)}$$

where

V = the vertical percolation rate of water, assumed to be 74 cm/y*;

d = the depth of the soil root zone, assumed to be 15 cm;

ρ/θ = the ratio of the bulk density of the soil to its water content, g/mℓ;

k_d = the equilibrium distribution coefficient for boron between soil and water; considered to be 0 for our purposes (i.e., all of the boron is readily solubilized in water and therefore does not absorb onto the soil but instead is present in the water occupying the interstitial soil spaces).

* The median value for this parameter based on statistical analyses presented in Ref. 170.

Table D-2. Parameters used in the dose model for calculating leaf concentration of boron in commercial crops.

	CROPS								
	Alfalfa	Wheat	Sudan grass	Sugar beets	Lettuce	Cotton	Sorghum	Cantaloupe	Rye grass
r[a] (dimensionless)	0.77	0.95	0.65	1.0	0.80	0.92	1.00	0.80	0.15
y_b (g/m^2)	500	1000	350	2400	6200[b]	830	2600	1400[b]	54
w (h^{-1})	0.0024	0.0024	0.0024	0.0024	0.0024	0.0024	0.0024	0.0014	0.0024
t_c (h)	450	1900	380	2400	1800	2200	1600	1400	4300
η[c] (dimensionless)	0.74	0.74	0.74	0.74	0.74	0.74	0.74	0.74	0.74
p (g/m^2)	213,000	213,000	213,000	213,000	213,000	213,000	213,000	213,000	213,000
Ω(h^{-1})	0.00056	0.00056	0.00056	0.00056	0.00056	0.00056	0.00056	0.00056	0.00056
t_b (h)	260,000	260,000	260,000	260,000	260,000	260,000	260,000	260,000	260,000
K	2.6	1.3	3.7	4.2	1.5	4.2	3.7	1.9	1.0

[a] $r = 1-\exp-(\mu y_b)$, where $\mu = 3.0\ m^2/kg$[158] and y_b = crop specific yield, kg/m^2.

[b] Wet weight, as specified by Hoffman et al.[85]

[c] Based on absorption of boron into radish leaves.[146]

REFERENCES

1. L. Rybach, "Geothermal Systems, Conductive Heat Flow, Geothermal Anomalies," in Geothermal Systems: Principles and Case Histories, L. Rybach and L.J.P. Muffler, Eds. (John Wiley and Sons, Ltd., New York, 1981), p. 3.

2. California Energy Commission, "Geysers Promise 3,000 MW of Power as World's Largest Goethermal Plant Complex," Calif. Energy Comm. News Comment 11, 4 (1983).

3. D. W. Layton and L. R. Anspaugh, Health Impacts of Geothermal Energy, International Symposium on Health Impacts of Different Sources of Energy, Nashville, TN, June 22-26, 1981.

4. G. Heiken, H. Murphy, G. Nunz, R. Potter, and C. Grigsby, "Hot Dry Rock Geothermal Energy," Am. Sci. 69, 400 (1981).

5. L. R. Anspaugh and J. L. Hahn, "Human Health Implications of Geothermal Energy," in Health Implications of New Energy Technologies, W. N. Rom and V. E. Archer, Eds. (Ann Arbor Science Publishers, Inc., Ann Arbor, MI, 1980), p. 565.

6. D. L. Ermak and P. L. Phelps, An Environmental Overview of Geothermal Development: The Geysers-Calistoga KGRA, Volume 1. Issues and Recommendations, Lawrence Livermore Laboratory, Livermore, CA, UCRL-52496, vol. 1 (1978).

7. D. W. Layton and W. F. Morris, "Geothermal Power: Accidental Fluid Releases and Waste Disposal," Chem. Eng. Prog. 77(4), 62 (1981).

8. L. J. P. Muffler, Ed., Assessment of Geothermal Resources of the United States--1978, U.S. Geological Survey, Arlington, VA, Circular 790 (1979).

9. D. W. Layton, An Assessment of Geothermal Development in the Imperial Valley of California; Environment, Health, Socioeconomics, and Environmental Control Technology, Executive Summary, U.S. Department of Energy, Washington, DC, DOE/TIC-11308 (1980).

10. R. C. Robertson A. D. Sheperd, C. S. Rosemarin, and M. W. Mayfield, Water-Related Constraints to the Development of Geothermal Electric Generating Stations, Oak Ridge National Laboratory, Oak Ridge, TN, ORNL/TM-7718 (1981).

11. J. H. Anderson, "The Vapor-Turbine Cycle for Geothermal Power Generation," in Geothermal Energy: Resources, Production, Stimulation, P. Kruger and C. Otte, Eds. (Stanford University Press, Stanford, CA, (1973), p. 163.

12. W. L. Pope, P. A. Doyle, H. S. Pines, R. L. Fulton, L. F. Silvester, and J. M. Angevine, "Conceptual Design Optimization," in Sourcebook on the Production of Electricity from Geothermal Energy, J. Kestin, R. DiPippo, H. E. Khalifa, and D. J. Ryley, Eds. (Brown University, Providence, RI, 1980), p. 729.

13. C. A. Brook, "Variability and Sources of Hydrogen Sulfide and Other Gases in Steam at The Geysers," in Research in The Geysers-Clear Lake Geothermal Area, Northern California, R. J. McLaughlin and J. M. Donnelly-Nolon, Eds., U.S. Geological Survey, Washington DC, Professional Paper 1141 (1981), p. 193.

14. E. F. Wahl, Geothermal Energy Utilization (John Wiley and Sons, New York, 1977).

15. D. L. Ermak, R. A. Nyholm, and P. H. Gudiksen, Imperial Valley Environmental Project: Air Quality Assessment, Lawrence Livermore National Laboratory, Livermore, CA, UCRL-52699 (1979).

16. F. B. Stephens, J. H. Hill, and P. L. Phelps, Jr., State-of-the-Art Hydrogen Sulfide Control for Geothermal Energy Systems: 1979, U.S. Department of Energy, Washington, DC, DOE/EV-0068 (1980).

17. K. L. White, A. C. Hill, and W. O. Ursenbach, Environmental Overview Report on Utah Geothermal Resource Areas, University of Utah Research Institute, Salt Lake City, UT, UCRL-13955, vols. 1 and 2 (1978).

18. P. F. Ellis and M. F. Conover, Materials Selection Guidelines for Geothermal Energy Utilization Systems, U.S. Department of Energy, Washington, DC, DOE/RA/27026-1 (1981).

19. S. R. Cosner and J. A. Apps, A Compilation of Data on Fluids from Geothermal Resources in the United States, Lawrence Berkeley Laboratory, Berkeley, CA, LBL-5936 (1978).

20. R. C. Axtmann, "Emission Control of Gas Effluents from Geothermal Power Plants," Environ. Lett. 8, 135 (1975).

21. R. DiPippo, Geothermal Energy as a Source of Electricity, U.S. Department of Energy, Washington, DC, DOE/RA/28320-1 (1980).

22. Pacific Gas and Electric Co. (PG&E), Notice of Intention, Geysers Unit 17, PG&E, San Francisco, CA (1978).

23. C. E. Land "An Evaluation of Approximate Confidence Interval Estimation Methods for Lognormal Means," Technometrics 14, 145 (1972).

24. N. L. Nehring and J. J. Fausto, "Gases in Steam from Cerro Prieto Geothermal Wells with a Discussion of Steam/Gas Ratio Measurements," Geotherm. 8, 253 (1979).

25. D. W. Layton, D. J. Powers, P. Leitner, N. B. Crow, P. H. Gudiksen, and Y. E. Ricker, Environmental Summary Document for the Republic Geothermal, Inc., Application for a Geothermal Loan Guaranty Project; 64 MW Well Field and 48 MW(Net) Geothermal Power Plant, Lawrence Livermore National Laboratory, Livermore, CA, UCID-18095 (1979).

26. J. D. Ludwick, D. E. Robertson, J. S. Fruchter, and C. L. Wilkerson, "Analysis of Well Gases from Areas of Geothermal Power Potential," Atmos. Environ. 16, 1053 (1982).

27. N. L. Nehring, "Gases from Springs and Wells in The Geysers-Clear Lake Area," in Research in The Geysers-Clear Lake Geothermal Area, Northern California, R. J. McLaughlin and J. M. Donnelly-Nolan, Eds., U.S. Geological Survey, Washington, DC, Professional Paper 1141 (1981), p. 205.

28. A. H. Truesdell and N. L. Nehring, "Gases and Water Isotopes in a Geochemical Section Across the Larderello, Italy, Geothermal Field," Pageoph 117, 276 (1978/79).

29. D. J. Des Marais, J. H. Donchin, N. L. Nehring, and A. H. Truesdell, "Molecular Carbon Isotopic Evidence for the Origin of Geothermal Hydrocarbons," Nature 292, 826 (1981).

30. N. L. Nehring and A. H. Truesdell, "Hydrocarbon Gases in Some Volcanic and Geothermal Systems," Geotherm. Resour. Counc. Trans. 2, 483 (1978).

31. D. W. Robertson, E. A. Crecelius, J. S. Fruchter, and J. D. Ludwick, "Mercury Emissions from Geothermal Power Plants," Science 196, 1094 (1977).

32. D. W. Robertson, J. S. Fruchter, J. D. Ludwick, C. L. Wilkerson, E. A. Crecelius, and J. C. Evans, "Chemical Characterization of Gases and Volatile Heavy Metals in Geothermal Effluents," Geotherm. Resour. Counc. Trans. 2, 579 (1978).

33. E. A. Crecelius, D. E. Robertson, J. S. Fruchter, and J. D. Ludwick, "Chemical Forms of Mercury and Arsenic Emitted by a Geothermal Power Plant," in Trace Substances in Environmental Health--X, D. D. Hemphill, Ed. (University of Missouri, Columbia, MO, 1976), p. 287.

34. H. L. Beck, "Gamma Radiation from Radon Daughters in the Atmosphere," J. Geophys. Res. 79, 2215 (1974).

35. L. R. Anspaugh, Final Report on the Investigation of the Impact of the Release of 222-Rn, its Daughters, and Precursors at The Geysers Geothermal Field and Surrounding Area, Lawrence Livermore National Laboratory, Livermore, CA, Environmental Sciences Division Report (1978).

36. M. H. Wilkening, W. E. Clements, and D. Stanley, "Radon 222 Flux Measurements in Widely Separated Areas," in The Natural Radiation Environment II, J. A. S. Adams, W. M. Lowder, and T. F. Gesell, Eds. (NTIS, Springfield, VA, CONF-720805-P2, 1972), p. 717.

37. M. F. O'Connell and R. F. Kaufman, Radioactivity Associated with Geothermal Waters--the Western United States. Basic Data, U.S. Environmental Protection Agency, Office of Radiation Programs, Las Vegas, NV, ORP/LV-75-8A (1976).

38. L. R. Anspaugh and P. Leitner, "Health and Safety Concerns," in An Assessment of Geothermal Development in the Imperial Valley of California, Volume 1. Environment, Health, and Socioeconomics, D. W. Layton, Ed., U.S. Department of Energy, Washington, DC, DOE/EV-0092, vol. 1 (1980).

39. J. D. Spengler, "Comments," J. Air Pollut. Control Assoc. 29, 929 (1979).

40. D. J. Moschandreas, J. Zabransky, and D. J. Pelton, Comparison of Indoor and Outdoor Air Quality, Electric Power Research Institute, Palo Alto, CA, EPRI EA-1733 (1981).

41. E. Crouch and R. Wilson, "Regulation of Carcinogens," Risk Anal. 1, 47 (1981).

42. D. L. Shaeffer and F. O. Hoffman, "Uncertainties in Radiological Assessments--A Statistical Analysis of Radioiodine Transport via the Pasture-Cow-Milk Pathway," Nuclear Tech. 45 (1), 99 (1979).

43. U. S. National Research Council, Hydrogen Sulfide (University Park Press, Baltimore, MD, 1979).

44. U. S. National Institute for Occupational Safety and Health (NIOSH), Criteria for a Recommended Standard...Occupational Exposure to Hydrogen Sulfide, NIOSH, Washington, DC, 77-158 (1977).

45. D. L. Ermak, R. A. Nyholm, and P. H. Gudiksen, "Potential Air Quality Impacts of Large-Scale Geothermal Energy Development in the Imperial Valley," Atmos. Environ. 14, 1321 (1980).

46. W. F. Morris and F. B. Stephens, Strategies for Steam Handling and Hydrogen Sulfide Abatement at Geothermal Power Plants in The Geysers Area of Northern California, Lawrence Livermore National Laboratory, Livermore, CA, UCRL-53137 (1981).

47. B. G. Ferris, "Health Effects of Exposure to Low Levels of Regulated Air Pollutants. A Critical Review," J. Air Pollut. Control Assoc. 28, 482 (1978).

48. R. Mendelsohn and G. Orcutt, "An Empirical Analysis of Air Pollution Dose-Response Curves," J. Environ. Econ. Manage. 6, 85 (1979).

49. L. B. Lave and E. P. Seskin, Air Pollution and Public Health (The Johns Hopkins University Press, Baltimore, MD, 1977).

50. M. O. Amdur, "Toxicological Appraisal of Particulate Matter, Oxides of Sulfur, and Sulfuric Acid," J. Air Pollut. Control Assoc. 9, 638 (1969).

51. R. Wilson, S. D. Colome, J. D. Spengler, and D. G. Wilson, Health Effects of Fossil Fuel Burning. Assessment and Mitigation (Ballinger Publishing Company, Cambridge, MA, 1980).

52. R. H. Mariner, C. A. Brook, J. R. Swanson, and D. R. Mahey, Selected Data for Hydrothermal Convection Systems in the United States with Estimated Temperatures > 90°C, U. S. Geological Survey, Washington, DC, Open-File Report 78-858 (1978).

53. Bureau of the Census, 1980 Census of Population and Housing, Preliminary Data, U.S. Bureau of the Census, Washington, DC (1981).

54. D. L. Ermak and R. A. Nyholm, Multiple Source Dispersion Model, Lawrence Livermore National Laboratory, Livermore, CA, UCRL-52592 (1978).

55. J. L. Sprung, "Tropospheric Oxidation H_2S," in Advances in Environmental Science and Technology (John Wiley and Sons, New York, 1977), p. 263.

56. L. Newman, "Atmospheric Oxidation of Sulfur Dioxide," in Atmospheric Sulfur Deposition. Environmental Impact and Health Effects (Ann Arbor Science Publishers, Inc., Ann Arbor, MI, 1979), p. 131.

57. H. S. Judeikis and A. G. Wren, "Deposition of H_2S and Dimethyl Sulfide on Selected Soil Materials," Atmos. Environ. 11, 1221 (1977).

58. J. N. de Wys, A. C. Hill, and E. Robinson, "Assessment of the Fate of Sulfur Dioxide from a Point Source," Atmos. Environ. 12, 633 (1978).

59. J. A. Garland, "Dry and Wet Removal of Sulfur from the Atmosphere," Atmos. Environ. 12, 349 (1978).

60. R. R. Draxler, "An Improved Gaussian Model for Long-Term Average Air Concentration Estimates," Atmos. Environ. 14, 597 (1980).

61. K. Telegadas, G. J. Ferber, J. L. Heffter, and R. R. Draxler, "Calculated and Observed Seasonal and Annual Krypton-85 Concentrations at 30-150 km from a Point Source," Atoms. Environ. 12, 1769 (1978).

62. C. V. Gogolak, H. L. Beck, and M. M. Pendergast, "Calculated and Observed ^{85}Kr Concentrations within 10 km of the Savannah River Plant Chemical Separation Facilities," Atmos. Environ. 15, 497 (1981).

63. M. D. Rowe, Brookhaven National Laboratory, Upton, NY, private communication (1982).

64. M. Aksoy, S. Erdem, and G. Dincol, "Leukemia in Shoe-Workers Exposed Chronically to Benzene," Blood 44, 837 (1974).

65. P. F. Infante, J. K. Wagoner, R. A. Rinsky, and R. F. Young, "Leukaemia in Benzene Workers," Lancet 2, 76 (1977).

66. D. Hattis and W. Mendez, Discussion and Critique of the Carcinogenicity Assessment Group's Report on Population Risk Due to Atmospheric Exposure to Benzene, Massachusetts Institute of Technology, Center for Policy Alternatives, Cambridge, MA, CPA-80-1 (1980).

67. R. E. Albert, Carcinogen Assessment Group's Final Report on Population Risk to Ambient Benzene Exposure, U. S. Environmental Protection Agency, Research Triangle Park, NC, EPA-450/5-80-004 (1979).

68. M. D. Rowe, Human Exposure to Particulate Emissions from Power Plants, Brookhaven National Laboratory, Upton, Long Island, NY, BNL-51305 (1981).

69. W. L. Dilling, "Atmospheric Environment," Environmental Risk Analysis for Chemicals, R. A. Conway, Ed. (Van Nostrand Reinhold Company, New York, 1982), pp. 154-197.

70. J. V. Ordonez, J. A. Carillo, M. Miranda, and J. L. Gale, "Estudio Epidemiologico de una Enfermedad Considerada como Encefalitis en la Region de los Altos de Guatemala," Bol. Of. Sanit. Panam. 60, 18 (1966).

71. F. Bakir, S. F. Damluji, L. Amin-Zaki, M. Murtadha, A. Khalidi, N. Y. Al-Rawi, S. Tikriti, H. I. Dhahir, T. W. Clarkson, J. C. Smith, and R. A. Doherty, "Methylmercury Poisoning in Iraq," Science 181, 230 (1973).

72. H. B. Gerstner and J. E. Huff, "Clinical Toxicology of Mercury," J. Toxicol. Environ. Health 2, 491 (1977).

73. D. Benning, "Outbreak of Mercury Poisoning in Ohio," Ind. Med. Surg. 27, 354 (1958).

74. Y. M. El-Sadik and A-A. El-Dakhakhny, "Effects of Exposure of Workers to Mercury at a Sodium Hydroxide Producing Plant," Am. Ind. Hyg. Assoc. J. 31, 705 (1970).

75. B. Kesic and V. Haeusler, "Hematological Investigation of Workers Exposed to Mercury Vapors," Ind. Med. Surg. 20, 485 (1951).

76. R. G. Smith, A. J. Vorwald, L. S. Patil, and T. F. Mooney, "Effects of Exposure to Mercury in the Manufacture of Chlorine," Am. Ind. Hyg. Assoc. J. 31, 687 (1970).

77. R. C. Harriss and C. Hohenemser, "Mercury--Measuring and Managing the Risk," Environment 20(9), 25 (1978).

78. T. Suzuki, "Dose-Effect and Dose-Response Relationships of Mercury and its Derivatives," in The Biogeochemistry of Mercury in the Environment, J.O. Nriagu, Ed. (Elsevier-North Holland Biomedical Press, New York, 1979), p. 399.

79. E. P. Radford, Chairman, Committee on the Biological Effects of Ionizing Radiation (BEIR), The Effects on Populations of Exposure to Low Levels of Ionizing Radiation: 1980 (National Academy Press, Washington, DC, 1980).

80. B. L. Cohen, "Health Effects of Radon from Insulation of Buildings," Health Phys. 39, 937 (1980).

81. A. F. Cohen and B. L. Cohen, "Tests of the Linearity Assumption in the Dose-Effect Relationship for Radiation-Induced Cancer," Health Phys. 38, 53 (1980).

82. United Nations Scientific Committee on the Effects of Atomic Radiation (UNSCEAR), Sources and Effects of Ionizing Radiation (United Nations, New York, 1977).

83. B. L. Cohen, "Proposals on Use of the BEIR-III Report in Environmental Assessments," Health Phys. 41, 769 (1981).

84. W. E. Dunn, P. Gavin, B. Boughton, A. J. Policastro, and J. Ziebarth, Studies on Mathematical Models for Characterizing Plume and Drift Behavior from Cooling Towers, Volume 3: Mathematical Model for Single-Source (Single-Tower) Cooling Tower Drift Dispersion, Electric Power Research Institute, Palo Alto, CA, EPRI-CS-1683, Vol. 3 (1981).

85. F. O. Hoffman, R. H. Gardner, and K. F. Eckerman, Variability in Dose Estimates Associated with the Food Chain Transport and Ingestion of Selected Radionuclides, Oak Ridge National Laboratory, Oak Ridge, TN, ORNL/TM-8099 (1982).

86. U. S. Environmental Protection Agency, Ambient Water Quality Criteria for Arsenic, U. S. Environmental Protection Agency, Washington, DC, PB81-117327 (1980).

87. C. F. Jelinek and P. E. Corneliussen, "Levels of Arsenic in the United States Food Supply," Environ. Health Perspect. 19, 83 (1977).

88. American Cancer Society, Inc., Cancer Facts and Figures 1979 (American Cancer Society, Inc., New York, 1978), p. 18.

89. F. J. Nielson, S. H. Givand, and D. R. Myron, "Evidence of a Possible Requirement for Arsenic by the Rat," Fed. Proc. 34, 923 (1975).

90. M. Anke, M. Grun, and M. Partschefeld, "The Essentiality of Arsenic for Animals," in Trace Substances in Environmental Health-X, D. D. Hemphill, Ed. (University of Missouri, Columbia, MO, 1976), p. 403.

91. E. J. Calabrese, Pollutants and High-Risk Groups (John Wiley and Sons, New York, 1978).

92. J. L. Valentine, H. K. Kanz, and G. Spivey, "Arsenic Levels in Human Blood, Urine, and Hair in Response to Exposure via Drinking Water," Environ. Res. 20, 24 (1979).

93. B. L. Cohen, "Long-Term Consequences of the Linear-No-Threshold Dose-Response Relationship for Chemical Carcinogens," Risk Anal. 1, 267 (1981).

94. K. D. Pimentel, R. R. Ireland, and G. A. Tompkins, "Chemical Finger-Prints to Assess the Effects of Geothermal Development on Water Quality in Imperial Valley," Geotherm. Resour. Counc. Trans. 2, 527 (1978).

95. W. F. Morris and F. B. Stephens, Characterization of Geothermal Solid Wastes, Lawrence Livermore National Laboratory, Livermore, CA, UCID-19201 (1981).

96. A. L. Austin, A. W. Lundberg, L. B. Owen, and G. E. Tardiff, The LLL Geothermal Energy Program Status Report, January 1976 - January 1977, Lawrence Livermore National Laboratory, Livermore, CA, UCRL-50046-76 (1977).

97. J. L. Hahn, "Occupational Hazards Associated with Geothermal Energy," Geotherm. Resour. Counc. Trans. 3, 283 (1979).

98. D. W. Layton, L. R. Anspaugh, and K. D. O'Banion, Health and Environmental Effects Document on Geothermal Energy--1981, Lawrence Livermore National Laboratory, Livermore, CA, UCRL-53232 (1981).

99. Division of Labor Statistics and Research, Doctor's First Report of Occupational Injury or Illness 1978-1979, (unpublished) California Department of Industrial Relations, San Francisco, CA (1982).

100. E. Baginsky, Occupational Skin Disease in California, California Department of Industrial Relations, Division of Labor Statistics and Research, San Francisco, CA (1982).

101. S. Fregert, "Occupational Dermatitis in a 10-year Material," Contact Dermatitis 1, 96 (1975).

102. D. Burrows, "Prognosis in Industrial Dermatitis," Br. J. Dermatol. 87, 145 (1972).

103. California Energy Commission, Pacific Gas & Electric Company Geysers Unit 18 Geothermal Power Plant Sonoma County, CA Draft Environmental Impact Report, California Energy Commission, Sacramento, CA, P700-79-015 (1979), Appendix B.

104. University of Utah Institute of Human Resource Management, Geothermal Energy Employment and Requirements 1977-1990, US Department of Energy, Washington, DC, DOE/IR/70004-1 (1981), pp. 66-69.

105. Occupational Injuries and Illnesses Statistics Section Occupational Injuries and Illnesses Survey California, 1979, California Department of Industrial Relations, Division of Labor Statistics and Research, San Francisco, CA (1981), pp. 18-23.

106. Statistical Policy Division, Standard Industrial Classification Manual 1972 Executive Office of the President, Office of Management and Budget, Washington, DC, U. S. Gov't. Printing Office Stock No. 041-001-00066-6 (1972).

107. E. Baginsky, Occupational Disease in California 1973, California Department of Health, Occupational Health Section and Center for Health Statistics, Berkeley, CA.

108. E. Baginsky, Occupational Disease in California 1974, California Department of Health, Occupational Health Branch, Berkeley, CA.

109. E. Baginsky, Occupational Disease in California, 1975, California Department of Health, Occupational Health Branch, Berkeley, CA.

110. E. Baginsky, Occupational Disease in California 1976, California Department of Industrial Relations, Division of Labor Statistics and Research, San Francisco, CA (1979).

111. E. Baginsky, Occupational Disease in California 1977, California Department of Industrial Relations, Division of Labor Statistics and Research, San Francisco, CA (1981).

112. American Petroleum Institute Statistics Department, Summary of Occupational Injuries and Illnesses in the Petroleum Industry, American Petroleum Institute, Washington, DC (1982).

113. American Petroleum Institute Statistics Department, Summary of Occupational Injuries and Illnesses in the Petroleum Industry, American Petroleum Institute, Washington, DC (1980).

114. American Petroleum Institute Statistics Department, Summary of Occupational Injuries and Illnesses in the Petroleum Industry, American Petroleum Institute, Washington, DC (1981).

115. T. R. Hamilton and R. Wilson, "Comparative Risks of Hydraulic, Thermal, and Nuclear Work in a Large Electrical Utility," in Proc. Int. Symp. on Health Impacts of Different Sources of Energy, Nashville, 1981 (International Atomic Energy Agency, Vienna, 1982), pp. 23-31.

116. National Safety Council, Accident Facts 1970 Edition (National Safety Council, Chicago, 1970), p. 23.

117. National Safety Council, Accident Facts 1971 Edition (National Safety Council, Chicago, 1971), p. 23.

118. National Safety Council, Accident Facts 1972 Edition (National Safety Council, Chicago, 1972), p. 23.

119. National Safety Council, Accident Facts 1973 Edition (National Safety Council, Chicago, 1973), p. 23.

120. National Safety Council, Accident Facts 1974 Edition (National Safety Council, Chicago, 1974), p. 23.

121. National Safety Council, Accident Facts 1975 Edition (National Safety Council, Chicago, 1975), p. 23.

122. National Safety Council, Accident Facts 1976 Edition (National Safety Council, Chicago, 1976), p. 23.

123. National Safety Council, Accident Facts 1977 Edition (National Safety Council, Chicago, 1977), p. 23.

124. National Safety Council, Accident Facts 1978 Edition (National Safety Council, Chicago, 1978), p. 23.

125. National Safety Council, Accident Facts 1979 Edition (National Safety Council, Chicago, 1979), p. 23.

126. National Safety Council, Accident Facts 1981 Edition (National Safety Council, Chicago, 1981), p. 23.

127. R. Wilson and W.J. Chase, "Problems in the Intercomparison of Risks of Industries and Technoogies," Chalk River Conf. Health Effects of Energy Production (1979), pp. 221-236.

128. B. L. Malloch, M. K. Eaton, and N. L. Crane, Assessment of Vegetation Stress and Damage Near The Geysers Power Plant Units, Department of Engineering Research, Pacific Gas & Electric Co., San Ramon, CA, 420-79-3 (1979).

129. C. R. Thompson and G. Kats, "Effects of Continuous H_2S Fumigation on Crop and Forest Plants," Environ. Sci. Technol. 12, 550 (1978).

130. C. R. Thompson, G. Kats, and R. W. Lennox, "Effects of Fumigating Crops with Hydrogen Sulfide or Sulfur Dioxide," Calif. Agric. 33 (3), 9 (1979).

131. J. R. Kercher, "An Assessment of the Impact on Crops of Effluent Gases from Geothermal Energy Development in the Imperial Valley, California," J. Environ. Manage. (in press).

132. R. Sung, W. Murphy, J. Reitzel, L. Leventhal, W. Goodwin, and L. Friedman, Surface Containment for Geothermal Brines, TRW Inc., Redondo Beach, CA, T-5003 (1979).

133. L. L. Edwards, MACROI: A Code to Test a Methodology for Analyzing Nuclear-Waste Management Systems, Lawrence Livermore Laboratory, Livermore, CA, UCRL-52736 (1979).

134. J. J. Koranda, Interim Report: Studies of Boron Deposition Near Geothermal Power Plants, Lawrence Livermore National Laboratory, Livermore, CA, UCID-18606 (1980).

135. W. D. James, C. C. Graham, M. D. Glascock, and A. S. G. Hanna, "Water-Leachable Boron from Coal Ashes," Environ. Sci. Technol. 16, 195 (1982).

136. A. A. Elseewi, S. R. Grimm, A. L. Page, and I. R. Straughan, "Boron Enrichment of Plants and Soils Treated with Coal Ash," in Trace Element Stress in Plants: Effects and Methodology, A. Wallace and W. L. Berry, Eds. (Special Symposium Issue of J. Plant Nutr. 3, Marcel Dekker, Inc., New York, 1981), pp. 409-427.

137. P. J. Temple and S. N. Linzon, "Boron as a Phytotoxic Air Pollutant," J. Air Pollut. Control Assoc. 26, 498 (1976).

138. H. J. M. Bowen, "The Biogeochemistry of the Elements," Trace Elements in Biochemistry (Academic Press, New York, 1966), pp. 173-210.

139. F. M. Eaton, "Deficiency, Toxicity and Accumulation of Boron in Plants," J. Agric. Res. 69, 239 (1944).

140. F. Martini and M. Thellier, "Study, with Help of the $^{10}_{5}B(^{1}_{0}n,^{4}_{2}\alpha)^{7}_{3}Li$ Nuclear Reaction, on the Redistribution of Boron in White Clover After Foliar Application," Newsl. Appl. Nucl. Methods Biol. Agric. 4, 26 (1975).

141. J. F. Sutcliffe, "Trace Elements in Plants--Uptake and Translocation," Trace Elements in Soils and Crops, Proceedings of a Conference Organized by the Soil Scientists of the National Agricultural Advisory Service, February 8-9, 1966 (Ministry of Agriculture, Fisheries, and Food, Technical Bulletin 21, London, 1966), pp. 35-40.

142. H. C. Kohl, Jr., and J. J. Oertli, "Distribution of Boron in Leaves," Plant Physiol. 36, 420 (1961).

143. W. L. Berry and A. Wallace, "Toxicity: The Concept and Relationship to the Dose Response Curve," Trace Element Stress in Plants: Effects and Methodology, A. Wallace and W. L. Berry, Eds. (Special Symposium Issue of J. Plant Nutr. 3, Marcel Dekker, Inc., New York, 1981), pp. 13-19.

144. A. Nason and W. D. McElroy, "Modes of Action of the Essential Mineral Elements," Plant Physiology--A Treatise, Vol. III Inorganic Nutrition of Plants, F. C. Steward, Ed. (Academic Press, New York, 1963), pp. 451-536.

145. J. J. Oertli, "The Distribution of Normal and Toxic Amounts of Boron in Leaves of Rough Lemon," Agron. J. 52, 530 (1960).

146. A. R. Chamel, A. M. Andreani, and J. F. Eloy, "Distribution of Foliar-Applied Boron Measured by Spark-Source Mass Spectrometry and Laser-Probe Mass Spectrography," Plant Physiol. 67, 457 (1981).

147. J. S. Wilson, "Environmental Aspects of the Multi-Purpose Development of Geothermal Resources," AIChE Symp. Ser. 70, 782 (1974).

148. G. Anastas, W. S. Bischoff, H. K. Bishop, J. L. Featherstone, C. H. Haas, W. H. Hanenburg, G. J. Hoaglin, W. O. Jacobson, J. P. Kozic, D. K. Mulliner, D. G. Newell, R. J. Peirce, and R. Quong, SDG&E - DOE Geothermal Loop Experimental Facility Quarterly Report for the Period January - March, 1979, San Diego Gas & Electric Company, San Diego, CA, SAN/1137-14 (1979).

149. D. W. Layton, Water for Long-Term Geothermal Energy Production in the Imperial Valley, Lawrence Livermore National Laboratory, Livermore, CA, UCRL-52576 (1978).

150. N. S. Laulainen, R. O. Webb, K. R. Wilber, and S. L. Ulanski, Comprehensive Study of Drift from Mechanical Draft Cooling Towers, Final Report, Pacific Northwest Laboratory, Richland, WA, PNL-3083 (1979).

151. J. M. Sheldon, Imperial Irrigation District Water Report 1975, Imperial County Irrigation District, Imperial, CA (1975), p. 100.

152. C. M. Finnell, Imperial County Agriculture 1976, Imperial County Agricultural Commissioner, El Centro, CA (1977).

153. C. M. Finnell, Imperial County Agriculture 1977, Imperial County Agricultural Commissioner, El Centro, CA (1978).

154. C. M. Finnell, Imperial County Agriculture 1978, Imperial County Agricultural Commissioner, El Centro, CA (1979).

155. C. M. Finnell, Imperial County Agriculture 1979, Imperial County Agricultural Commissioner, El Centro, CA (1980).

156. C. M. Finnell, Imperial County Agriculture 1980, Imperial County Agricultural Commissioner, El Centro, CA (1981).

157. C. M. Finnell, Imperial County Agriculture 1981, Imperial County Agricultural Commissioner, El Centro, CA (1982).

158. Y. C. Ng, W. A. Phillips, Y. E. Ricker, and R. K. Tandy, Methodology for Assessing Dose Commitment to Individuals and to the Population from Ingestion of Terrestrial Foods Contaminated by Emissions from a Nuclear Fuel Reprocessing Plant at the Savannah River Plant, Lawrence Livermore National Laboratory, Livermore, CA, UCID-17743 (1978).

159. D. J. Finney, Probit Analysis: A Statistical Treatment of the Sigmoid Response Curve (The Syndics of the Cambridge University Press, New York, 1952), 2nd ed., pp. 1-64.

160. G. R. Bradford, "Boron," Diagnostic Criteria for Plants and Soils, H. D. Chapman, Ed. (University of California, Division of Agricultural Sciences, Riverside, CA, 1966), pp. 33-61 and Appendix pp. 572-752.

161. L. V. Wilcox and H. V. Durum, "Quality of Irrigation Water," in Irrigation of Agricultural Lands, R. M. Hagan, H. R. Haise, and T. W. Edminster, Eds. (The American Society of Agronomy, Inc., Madison, WI, 1967), (Number 11 in the Series Agronomy) pp. 104-122.

162. J. J. Oertli, O. R. Lunt, and V. B. Youngner, "Boron Toxicity in Several Turfgrass Species," Agron. J. 53, 262 (1961).

163. C. G. Bufe, S. M. Marks, F. W. Lester, R. S. Ludwin, and M. C. Stickney, "Seismicity of The Geysers-Clear Lake Region," in Research in The Geysers-Clear Lake Geothermal Area, Northern California,, R. J. McLaughlin and J. M. Donnelly-Nolan, Eds. (Geological Survey, Professional Paper 1141, Washington, DC, 1981), pp. 129-137.

164. D. B. Raleigh, J. H. Healy, and J. D. Bredehoeft, "An Experiment in Earthquake Control at Rangely, Colorado," Science 191, 1230 (1975).

165. D. C. Helm, Field-Based Computational Techniques for Predicting Subsidence Due to Fluid Withdrawal, Lawrence Livermore National Laboratory, Livermore, CA, UCRL-84398 (1982).

166. J. F. Schatz, P. W. Kasameyer, and J. A. Cheney, Method of Using in situ Porosity Measurements on Geothermal Reservoir Compaction, Lawrence Livermore National Laboratory, Livermore, CA, UCRL-81506 (1979).

167. D. W. Layton and N. B. Crow, "Subsidence and Seismicity," An Assessment of Geothermal Development in the Imperial Valley of California, Vol. 1. Environment, Health, and Socioeconomics, D. W. Layton, Ed., U.S. Department of Energy, Washington, DC, DOC/EV-0092 (1980), vol. 1, sec. 8.

168. J. J. Rochow, "Measurements and Vegetational Impact of Chemical Drift from Mechanical Draft Cooling Towers," Environ. Sci. Technol. 12, 1379 (1978).

169. J. G. Boerngen and H. T. Shacklette, Chemical Analyses of Fruits, Vegetables, and Their Associated Soils from Areas of Commercial Production in the Conterminous United States, U. S. Department of the Interior Geological Survey, Washington, DC, Open-File Report 80-84 (1980).

170. C. F. Baes III, "The Soil Loss Constant $\lambda_{s\ell}$ Due to Leaching from Soils," in A Statistical Analysis of Selected Parameters for Predicting Food Chain Transport and Internal Dose of Radionuclides, F. O. Hoffman and C. F. Baes III, Eds. Oak Ridge National Laboratory, Oak Ridge, TN, ORNL/NUREG/TM-282 (1979), pp. 85-92.

171. D. W. Cudney, R. W. Hagemann, D. G. Kontaxis, K. S. Mayberry, R. K. Sharma, and A. F. Van Maren, Guidelines to Production Costs and Practices 1976-1977 Imperial County Crops, Cooperative Agricultural Extension, University of California, El Centro, CA, Circular 104 (1976).

172. M. E. Jensen and H. R. Haise, "Estimating Evapotranspiration from Solar Radiation," J. Irrig. Drain. Div. Proc. Am. Soc. Civ. Eng. 89 (IR4), 15 (1963).

173. V. E. Hansen, "Unique Consumptive Use Curve Related to Irrigation Practice," J. Irrig. Drain. Div. Proc. Am. Soc. Civ. Eng. 89 (IR1), 43 (1963).

174. T. Hodges and E. T. Kanemasu, "Modeling Daily Dry Matter Production of Winter Wheat," Agron. J. 69, 974 (1977).

175. C. Ehlig, U. S. Department of Agriculture, Riverside, CA, private communication (1982).

176. D. J. Watson, "Comparative Physiological Studies on the Growth of Field Crops," Ann. Bot. 11 (41), 41 (1947).

177. J. E. Adams and G. F. Arkin, "A Light Interception Method for Measuring Row Crop and Ground Cover," Soil Sci. Soc. Am. J. 41, 789 (1977).

178. D. A. Rijks, "Water Use by Irrigated Cotton in Sudan, I. Reflections of Short-Wave Radiation," J. Appl. Ecol. 4, 561 (1967).

179. R. W. Brougham, "Interception of Light by the Foliage of Pure and Mixed Stands of Pasture Plants," Aust. J. Agric. Res. 9, 39 (1958).

180. A. J. Richardson, C. L. Wiegand, G. F. Arkin, P. R. Nixon, and A. H. Gerbermann, "Remotely-Sensed Spectral Indicators of Sorghum Development and Their Use in Growth Modeling," Agric. Meteorol. 26, 11 (1982).

181. B. L. Sharma and R. De, "Pattern of Dry Matter Accumulation and Nutrient Yield in Tall and Dwarf Varieties of Wheat in Relation to Nitrogen and Phosphorus Fertilization," Proc. Indian Nat. Sci. Acad. Part B Biol. Sci. 39, 718 (1974).

182. R. W. Rickman, R. E. Ramig, and R. R. Allmaras, "Modeling Dry Matter Accumulation in Dryland Winter Wheat," Agron. J. 67, 283 (1975).

183. P. J. Gregory, D. V. Crawford, and M. McGowan, "Nutrient Relations of Winter Wheat: 1. Accumulation and Distribution of Na, K, Ca, Mg, P, S and N," J. Agric. Sci. Camb. 93, 485 (1979).

184. A. J. MacKenzie, K. R. Stockinger, and B. A. Krantz, "Growth and Nutrient Uptake of Sugar Beets in the Imperial Valley, California," J. Am. Soc. Sugar Beet Technol. 9, 400 (1957).

185. F. W. Zink and M. Yamaguchi, "Studies on the Growth Rate and Nutrient Absorption of Head Lettuce," Hilgardia 32, 471 (1962).

186. D. M. Bassett, W. D. Anderson, and C. H. E. Werkhoven, "Dry Matter Production and Nutrient Uptake in Irrigated Cotton (Gossypium hirsutum)," Agron. J. 62, 299 (1970).

187. E. W. Crampton and L. E. Harris, "Appendix 3: Table of Feed Composition," Applied Animal Nutrition: The Use of Feedstuffs in the Formulation of Livestock Rations (W. H. Freeman and Company, San Francisco, CA, 1969), 2nd ed., pp. 478-749.

188. B. K. Watt and A. L. Merrill, Composition of Foods, U. S. Department of Agriculture, Washington, DC, Agriculture Handbook No. 8 (1963), pp. 6-66.

Work performed under the auspices of the U.S. Department of Energy by Lawrence Livermore National Laboratory under Contract W-7405-Eng-48.